

# Microscale HPLC Enables a New Paradigm for Commercialization of Complex Chiral Stationary Phases

CHRISTOPHER J. WELCH,<sup>1\*</sup> MYUNG HO HYUN,<sup>2</sup> TAKATERU KUBOTA,<sup>1</sup> WES SCHAFER,<sup>1</sup>  
FRANK BERNARDONI,<sup>1</sup> HEE JUNG CHOI,<sup>2</sup> NAIJUN WU,<sup>1</sup> XIAOYI GONG,<sup>1</sup> AND BRUCE LIPSHUTZ<sup>3</sup>

<sup>1</sup>*Separation and Purification Center of Excellence, Merck & Co., Inc., Rahway, New Jersey*

<sup>2</sup>*Department of Chemistry, Pusan National University, Busan, South Korea*

<sup>3</sup>*Department of Chemistry and Biochemistry, University of California, Santa Barbara, California*

**ABSTRACT** The small column size (0.3 mm i.d.  $\times$  15 cm) used in microscale HPLC contains only a small fraction (<1%) of the chromatographic packing material of a typical analytical HPLC column. Consequently, chromatographic stationary phases that are prohibitively expensive in conventional HPLC, owing either to synthetic complexity or costly starting materials, may become commercially viable in the microscale format. To illustrate this point, a previously described, synthetically complex, crown ether chiral stationary phase was prepared and evaluated in the microscale format, showing excellent separation of the enantiomers of underivatized amine analytes. *Chirality* 20:815–819, 2008. © 2008 Wiley-Liss, Inc.

**KEY WORDS:** microscale HPLC; chiral stationary phase; crown ether; CSP

## INTRODUCTION

The acceptable selling price for an analytical HPLC column places limits on the production costs of any potential new product offering in this area. The cost of the chromatographic stationary phase generally dominates HPLC column production costs, owing to the large amount of specialized organic selector needed for preparation of the stationary phase (as much as 1 g for a typical 4.6 mm i.d.  $\times$  25 cm analytical HPLC column).<sup>1–3</sup> As a result of these limitations, HPLC stationary phases are typically prepared from relatively inexpensive starting materials using only a few synthetic steps. Seeming exceptions to this rule, e.g. the Chirobitic R chiral stationary phase (CSP)<sup>4,5</sup> prepared from the relatively expensive antibiotic, ristocetin (~\$1,600/g), and the Whelko CSP<sup>6–8</sup> prepared in 10 synthetic steps from relatively inexpensive starting materials, serve to emphasize the point—the commercial viability of both of these products only being possible following substantial efforts at process improvement. Not surprisingly, stationary phases with even greater raw material costs or synthetic complexity are often so expensive as to prohibit commercialization, and consequently may remain little more than laboratory curiosities. This situation is especially regrettable owing to the fact that in recent years it has become clear that increased selectivity and performance can often be obtained by introducing significant complexity into stationary phase design.<sup>9–12</sup> Clearly, the introduction of complexity into stationary phase design does not by itself assure improved performance, but greater selectivity can often be afforded when the available palette of design choices is expanded to include costly starting materials and multistep chemical synthesis. In this article we explore the advantages and implications of using microcolumn HPLC, which requires less than 0.5% of the stationary

phase of a conventional analytical HPLC column. This greatly reduced stationary phase requirement can potentially make HPLC columns based on more complex and costly stationary phases commercially viable. We illustrate this point with the preparation and evaluation of microcolumns (300  $\mu$  i.d.) containing a previously described synthetically complex crown ether CSP, and discuss the potential generality and benefits of this approach.

## EXPERIMENTAL SECTION

Acetonitrile, sulfuric acid, and ammonium acetate were purchased from Sigma-Aldrich (Milwaukee, WI). Analytes were available from previous studies. Chromatographic studies were carried out Express 100 microflow HPLC instrument (Eksigent Technologies, Dublin, CA). CSP 1 (see Fig. 1) was prepared using a previously described method.<sup>13</sup> Column packing was carried out using a home-built device with a pneumatic amplifier pump (Haskel, Burbank, CA). Slurries were made by mixing particles (25–30 mg) into 0.5 ml methanol, which was then transferred to the packing reservoir. Nitrogen from a compressed cylinder was used to drive the particle slurry into the capillary column with methanol. The pressure was increased quickly to 10,000 psi to maintain a constant packing rate for around 60 min. The column was then left to depressurize to ambient in 45 min. The columns were

\*Correspondence to: Christopher J. Welch, Separation and Purification Center of Excellence, Merck & Co., Inc., Rahway, NJ 07065.

E-mail: christopher\_welch@merck.com

Received for publication 20 October 2007; Accepted 10 January 2008

DOI: 10.1002/chir.20548

Published online 21 February 2008 in Wiley InterScience (www.interscience.wiley.com).

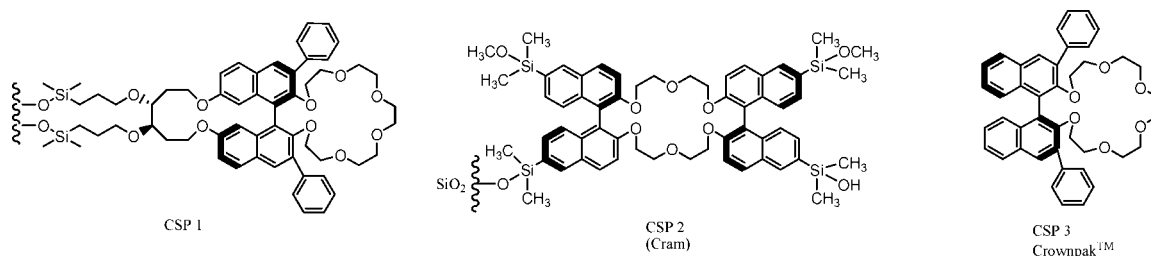


Fig. 1. Crown ether chiral stationary phases for chromatographic separation of amine enantiomers.

conditioned for 10–20 min using the working mobile phase before use.

## RESULTS AND DISCUSSION

Although microscale HPLC has been known for nearly as long as HPLC itself,<sup>14,15</sup> the technique has largely been overshadowed by conventional HPLC using 4.6 mm i.d. columns. We have recently become involved in the use of multiparallel microflow HPLC, primarily as a consequence of trying to fit eight independent HPLC devices within a laboratory instrument of a reasonable size for the purpose of high-throughput analysis<sup>16,17</sup> or multiparallel method development.<sup>18</sup> With increased usage in the past few years, we have become very impressed with the substantial solvent savings and outstanding performance that can be realized with this equipment and with microflow HPLC in general.<sup>19,20</sup> We now describe an additional significant advantage of the technique—the ability to prepare a column using only a small fraction (~1% or less) of the stationary phase required in conventional HPLC, and the flexibility that this affords in the utilization of stationary phases that would be otherwise too expensive to produce commercially.

The advantage of reduced stationary phase requirement for microcolumn HPLC has been noted in the past.<sup>15</sup> However, having been involved in the difficult process of commercializing new chromatographic stationary phases, and having seen a number of excellent HPLC phases fail because of unacceptably high stationary phase costs, we felt that a communication emphasizing this economic advantage of microflow HPLC stationary phase requirements would be warranted.

To illustrate this principle we chose CSP 1, a previously described,<sup>13</sup> synthetically complex crown ether CSP (see Fig. 1). The separation of the enantiomers of primary amines using crown ether CSPs has a long and rich history. Cram and coworkers developed the first crown ether CSP (CSP 2, Fig. 1) in the 1970s as an illustration of the principles of molecular design and preorganization to effect chiral recognition.<sup>21</sup> Given the synthetic complexity of this stationary phase, commercialization was never considered practical, although the performance of the CSP was quite good, even by today's standards. Later, a similar stationary phase was commercialized by Chiral Technologies, Inc. as the Crownpak<sup>TM</sup> CSP (CSP 3, Fig. 1).<sup>22,23</sup> This stationary phase possesses the flanking phenyl substituents on the naphthyl rings shown by Cram to enhance

enantioselectivity, however, the selector possesses no point of attachment, but is instead coated onto the chromatographic support to afford the CSP. Consequently, the selector can be washed from the column by strong organic solvents such as THF and dichloromethane, a significant disadvantage.

The synthetic challenge of creating a covalent analog of the Crownpak CSP is considerable, with introduction of a tether on either the crown ether or the binaphthyl system breaking the symmetry of the molecule and leading to significant synthetic complexity. When we became aware of the elegant approach for the modular synthesis of highly functionalized enantioenriched 3,3'-disubstituted 1,1'-binaphthol derivatives by Lipshutz et al.,<sup>24</sup> we recognized the opportunity for a collaborative preparation of a tethered crown ether CSP.<sup>13</sup> Preliminary evaluations of the resulting CSP showed outstanding performance, far surpassing any other crown ether CSP on the market. However, at 20 synthetic steps (15 steps in the longest linear sequence), the CSP was clearly too expensive for commercialization (see Fig. 2).

With our recent interest in microscale HPLC, we set out to investigate the performance of CSP 1 in microscale HPLC format. CSP 1 was prepared from intermediate 13 as previously described,<sup>13</sup> and was packed into 0.3 mm × 150 mm columns for evaluation. The stationary phase thus obtained was evaluated using microflow HPLC, with the objective of determining if this CSP could possibly be useful in carrying out high-throughput analysis in support of high-throughput pharmaceutical process research investigations.

Initial evaluations reproduced the previously reported performance of the column for a number of primary amine racemates, as illustrated in Figure 3. The previously reported preferred eluent of 15:85 10 mM H<sub>2</sub>SO<sub>4</sub> (aq) and 1 mM CH<sub>3</sub>COONH<sub>4</sub> (aq)/acetonitrile was used at a flow rate of 2 µl/min, which corresponds to the 0.5 ml/min used with the conventional 4.6 mm i.d. columns. The separations were found to be generally comparable with our previous work in this area, demonstrating the feasibility of carrying out microcolumn separations with this CSP. Some of the peak shapes appear a little unusual, with fronting being observed with some peaks, and tailing with others. Some interesting effects of injection solvent on peak shape were observed, with the best results being seen when injection solvent closely matched eluent composition. While we were pleased with the quality of these enantioseparations, the observed analysis times of 30–40 min are much longer than what is generally preferred for

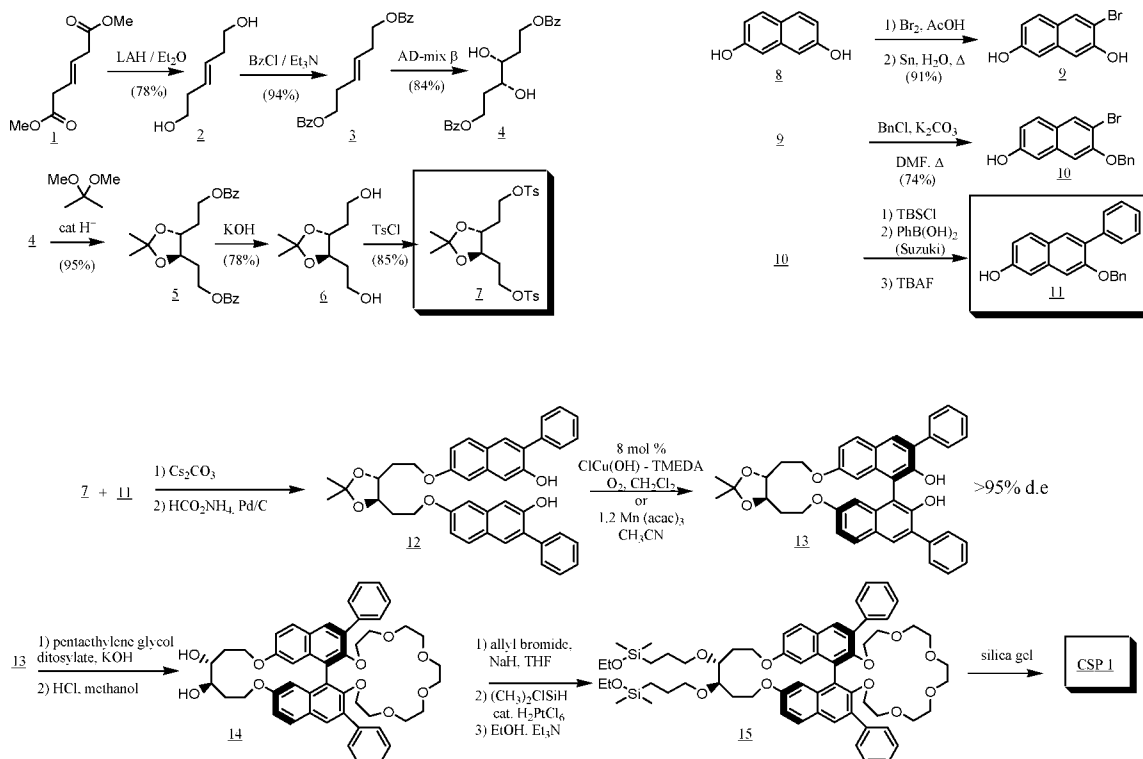


**Fig. 2.** Synthetic procedure used in the preparation of CSP 1. At 20 synthetic steps (15 steps in the longest linear sequence), the preparation of this CSP was too expensive for commercialization.

fast chromatography to support high-throughput analysis, leading us to investigate the potential for speeding up enantioseparations on CSP 1.

We were initially somewhat skeptical about the possibility of carrying out separations with CSP 1 at faster flow rates. Chiral HPLC with crown ether CSPs has historically

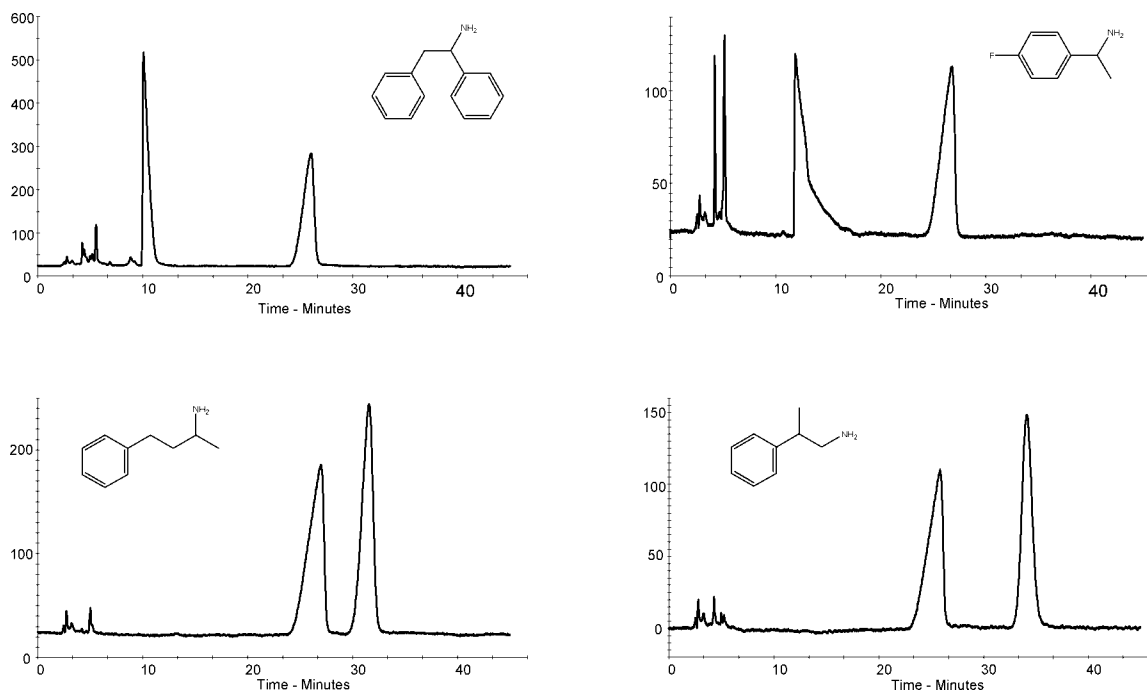


**Fig. 3.** Initial evaluation of separation of enantiomers of various amine racemates using microscale HPLC containing CSP 1. Conditions: Column, 150 mm × 0.3 mm CSP 1; Mobile phase, 15:85 10 mM H<sub>2</sub>SO<sub>4</sub> (aq) and 1 mM CH<sub>3</sub>COONH<sub>4</sub> (aq)/Acetonitrile; Flow, 2 μl/min; Temperature, ambient; Detection, UV at 215 nm.

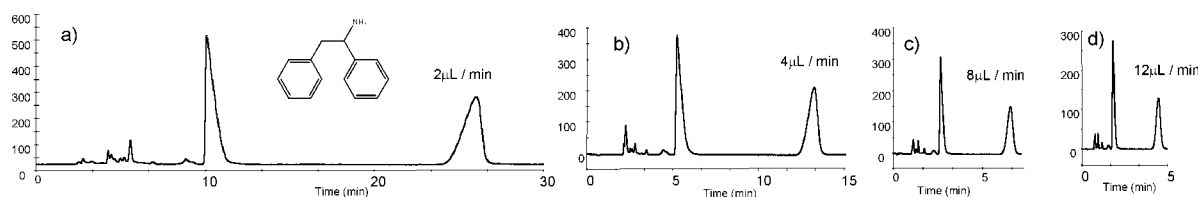


**Fig. 4.** Influence of flow rate on the separation of enantiomers on CSP 1 (15:85 10 mM  $\text{H}_2\text{SO}_4$  (aq) and 1 mM  $\text{CH}_3\text{COONH}_4$  (aq)/Acetonitrile).

been characterized by poor peak shapes, with chromatography often being carried out at slower flow rates or higher temperatures to counteract poor mass transfer characteristics. Interestingly, investigation of the influence of flow rate showed that the excellent resolution observed at 2  $\mu\text{L}/\text{min}$  (Fig. 4a) could be maintained even at an elevated flow rate of 12  $\mu\text{L}/\text{min}$  (Fig. 4d), which corresponds to 3 ml/min on a conventional 4.6 mm i.d. column. This sixfold improvement in analysis speed to afford baseline separation of underivatized amine enantiomers in fewer than 5 min will be a valuable tool for high-throughput analysis studies.

Similarly, the influence of modifier concentration was investigated to determine optimal conditions for fast baseline separation of enantiomers. Interestingly, both retention and enantioseparation were found to be only weakly dependant on water content of the eluent. Optimal fast chromatography could generally be developed for a variety of compounds using a simple eluent of 100% acetonitrile containing 10 mM sulfuric acid and 1 mM ammonium acetate (see Fig. 5). The fast chromatography and attractive peak-shapes obtained with this standard approach clearly illustrate the broad utility of CSP 1 for providing fast resolution of enantiomers of chiral primary amines. For many of these separations, further improvements in analysis

speed can be obtained either by increasing flow rate or by shortening the length of the column.

With the proven ability of CSP 1 to resolve the enantiomers of underivatized amines, we next turned to the analysis of underivatized amino acids, this compound class being the prototypical analytes studied by Cram and other groups involved in research in this area. As shown in Figure 6, the selectivity afforded by CSP 1 for the resolution of the enantiomers of these analytes is outstanding, with separation factors ranging from 3.7 (tryptophan) to 4.5 (phenylalanine). These results compare favorably with previous approaches for resolving the enantiomers of underivatized amino acids using crown ether stationary phases, ligand exchange CSPs, or CSPs derived from macrocyclic antibiotics.

While crown ether CSPs are well known to resolve the enantiomers of analytes containing primary amine functionality, we were curious to investigate the ability of CSP 1 to resolve the enantiomers of other types of compounds. Accordingly, several dozen racemates representing a variety of structural classes were evaluated. Interestingly, only those analytes containing underivatized primary amines were found to be well resolved, suggesting that the practical utility of CSP 1 may indeed be limited to amine-containing analytes.

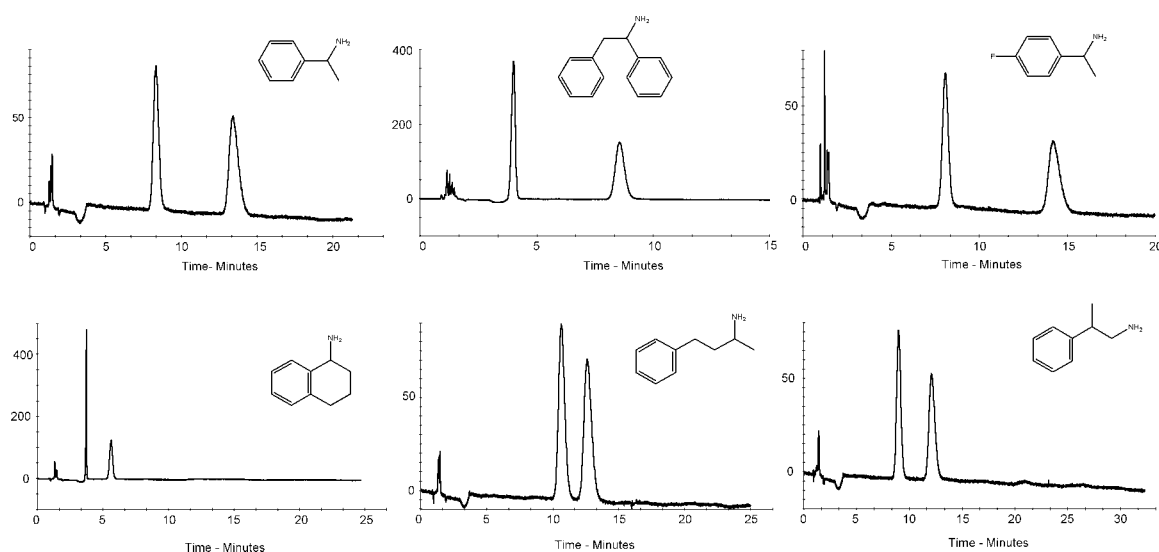


**Fig. 5.** Separation of the enantiomers of primary amine analytes on CSP 1. Conditions: Column, 150 mm  $\times$  0.3 mm CSP 1; Mobile phase, 100% Acetonitrile with 10 mM  $\text{H}_2\text{SO}_4$  and 1 mM  $\text{CH}_3\text{COONH}_4$ ; Flow, 8  $\mu\text{L}/\text{min}$ ; Temperature, ambient; Detection, UV at 215 nm.

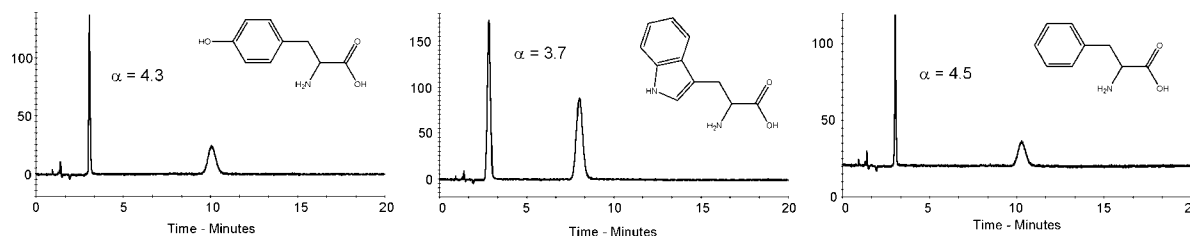


**Fig. 6.** Separation of amino acid enantiomers on CSP 1. Conditions: Column, 150 mm  $\times$  0.3 mm CSP 1; Mobile phase, 100% Acetonitrile with 10 mM  $\text{H}_2\text{SO}_4$  and 1 mM  $\text{CH}_3\text{COONH}_4$ ; Flow, 8  $\mu\text{L}/\text{min}$ ; Temperature, ambient; Detection, UV at 215 nm.

## CONCLUSION

In summary, the present evaluation demonstrates the utility of CSP 1 for providing rapid separation of the enantiomers of primary amines and amino acids. Furthermore, the study illustrates how by adopting the microcolumn HPLC format, a practically useful HPLC column can be created using only a small fraction of the material required for a conventional column, thereby potentially making a synthetically complex CSP commercially viable.

## LITERATURE CITED

- Welch CJ. The evolution of chiral stationary phase design in the Pirkle laboratories. *J Chromatogr* 1994;666:3–26.
- Okamoto Y, Yashima E, Yamamoto C. Optically active polymers with chiral recognition ability. *Top Stereochem* 2003;24:157–208.
- Xiao TL, Armstrong DW. Enantiomeric separations by HPLC using macrocyclic glycopeptide-based chiral stationary phases: an overview. *Methods Mol Biol* 2003;243(Chiral Separations):113–171.
- Ekborg-Ott K, Liu Y, Armstrong DW. Highly enantioselective HPLC separations using the covalently bonded macrocyclic antibiotic, ristocetin A, chiral stationary phase. *Chirality* 1998;10:434–483.
- www.sigmaaldrich.com.
- Pirkle WH, Welch CJ, Lamm B. Design, synthesis, and evaluation of an improved enantioselective naproxen selector. *J Org Chem* 1992;57:3854–3860.
- Pirkle WH, Welch CJ. An improved chiral stationary phase for the chromatographic separation of underivatized naproxen enantiomers. *J Liq Chromatogr* 1992;15:1947–1955.
- www.registech.com.
- Welch CJ, Protopopova MN, Bhat GA. Microscale synthesis and screening of combinatorial libraries of new chromatographic stationary phases. In: Blitz J, Little CB, editors. *Fundamental and applied aspects of chemically modified surfaces*. Cambridge: Royal Society of Chemistry; 1999. p 129–138.
- Li T. Peptide and peptidomimetic chiral selectors in liquid chromatography. *J Sep Sci* 2005;28:1927–1931.
- Lammerhofer M, Franco P, Lindner W. Quinine carbamate chiral stationary phases: systematic optimization of steric selector-select and binding increments and enantioselectivity by quantitative structure-enantioselectivity relationship studies. *J Sep Sci* 2006;29:1486–1496.
- Brahmachary E, Ling FH, Svec F, Frechet JM. Chiral recognition: design and preparation of chiral stationary phases using selectors derived from Ugi multicomponent condensation reactions and a combinatorial approach. *J Comb Chem* 2003;5:441–450.
- Hyun MH, Han SC, Lipshutz BH, Shin YJ, Welch CJ. Liquid chromatographic resolution of racemic amines, amino alcohols and related compounds on a chiral crown ether stationary phase. *J Chromatogr A* 2002;959:75–83.
- Novotny M. Recent advances in microcolumn liquid chromatography. *Anal Chem* 1988;60:500A–510A.
- Hernandez-Borges J, Aturki Z, Rocco A, Fanali S. Recent applications in nanoliquid chromatography. *J Sep Sci* 2007;30:1589–1610.
- Welch CJ, Sajonz P, Biba M, Gouker J, Fairchild J. Comparison of multiparallel microfluidic hplc instruments for high throughput analysis in support of pharmaceutical process research. *J Liq Chromatogr* 2006;29:2185–2220.
- Sajonz P, Schafer W, Gong X, Schultz S, Rosner T, Welch CJ. Multiparallel microfluidic hplc for high throughput normal phase chiral analysis. *J Chromatogr* 2007;1147:149–154.
- Sajonz P, Leonard WR, Biba M, Welch CJ. Multiparallel chiral method development screening using an 8-channel microfluidic HPLC system. *Chirality* 2006;18:803–813.
- Schafer WA, Hobbs S, Rehm J, Rakestraw DA, Orella C, McLaughlin M, Ge Z, Welch CJ. Mobile tool for HPLC reaction monitoring. *Org Process Res Dev* 2007;11:870–876.
- Welch CJ. Challenges and opportunities for the greening of separation science in the pharmaceutical industry. *Drug Discov World Fall* 2007;71–77.
- Sousa LR, Sogah GDY, Hoffman DH. Cram, Host-guest complexation. 12. Total optical resolution of amine and amino ester salts by chromatography. *J Am Chem Soc* 1978;100:4569–4576.
- Shinbo T, Yamaguchi T, Nishimura K, Sugiura M. Chromatographic separation of racemic amino acids by use of chiral crown ether-coated reversed-phase packings. *J Chromatogr* 1987;405:145–153.
- www.chiraltech.com.
- Lipshutz BH, Kayser F, Liu ZP. A modular approach to nonracemic cyclo-BINOLs. Preparation of symmetrically and unsymmetrically substituted ligands. *Tetrahedron Lett* 1998;39:7017–7020.

# Guest-Dependent Conformation of 18-Crown-6 Tetracarboxylic Acid: Relation to Chiral Separation of Racemic Amino Acids

HIROOMI NAGATA,<sup>1\*</sup> HIROYUKI NISHI,<sup>1</sup> MIYOKO KAMIGAUCHI,<sup>2</sup> AND TOSHIMASA ISHIDA<sup>3</sup>

<sup>1</sup>Mitsubishi Tanabe Pharma Corporation, Yodogawa-ku, Osaka 532-8505, Japan

<sup>2</sup>Kobe Pharmaceutical University, Higashinada-ku, Kobe 658-8558, Japan

<sup>3</sup>Osaka University of Pharmaceutical Sciences, Takatsuki, Osaka 569-11, Japan

**ABSTRACT** (+)-18-Crown-6 tetracarboxylic acid (18C6H<sub>4</sub>) has been used as a chiral selector for various amines and amino acids. To further clarify the structural scaffold of 18C6H<sub>4</sub> for chiral separation, single crystal X-ray analysis of its glycine<sup>+</sup> (1), H<sub>3</sub>O<sup>+</sup> (2), H<sub>5</sub>O<sub>2</sub><sup>+</sup> (3), NH<sub>4</sub><sup>+</sup> (4), and 2CH<sub>3</sub>NH<sub>3</sub><sup>+</sup> (5) complexes was performed and the guest-dependent conformation of 18C6H<sub>4</sub> was investigated. The crown ether ring of 18C6H<sub>4</sub> in **3**, **4**, and **5** took a symmetrical C<sub>2</sub> or C<sub>2</sub>-like conformation, whereas that in **1** and **2** took an asymmetric C<sub>1</sub> conformation, which is commonly observed in complexes with various optically active amino acids. The overall survey of the present and related complexes suggests that the molecular conformation of 18C6H<sub>4</sub> is freely changeable within an allowable range, depending on the molecular shape and interaction mode with the cationic guest. On the basis of the present results, we propose the allowable conformational variation of 18C6H<sub>4</sub> and a possible transition pathway from its primary conformation to the conformation suitable for chiral separation of racemic amines and amino acids. *Chirality* 20:820–827, 2008. © 2008 Wiley-Liss, Inc.

**KEY WORDS:** crown ether; chiral resolution; molecular conformation; amino acid; X-ray analysis; crystal structure

## INTRODUCTION

The optical purity of a drug is very important in terms of quality control, because one of the drug's enantiomers might show high toxicity in spite of another being effective as medicine. Recently, high performance liquid chromatography (HPLC) with chiral stationary phase (CSP) has extensively been used to directly separate enantiomers in optical purity test. Enantiomeric amines are usually separated by chiral crown ether columns,<sup>1–6</sup> while various racemic amino acids can effectively be separated using CSP chemically immobilized by (+)-18-crown-6 tetracarboxylic acid [(+)-18C6H<sub>4</sub>; Fig. 1] on silica gel.<sup>7–10</sup> In addition, (+)-18C6H<sub>4</sub> is also used as a chiral selector for amine compounds in capillary electrophoresis (CE)<sup>11–15</sup> or nuclear magnetic resonance (NMR).<sup>16–18</sup> To clarify the structural scaffold of (+)-18C6H<sub>4</sub> necessary for D/L-separation of racemic amino acids, we recently determined the crystal structures of (+)-18C6H<sub>4</sub> complexed with D- and L-isomers of tyrosine (Tyr), isoleucine (Ile), methionine (Met), phenylglycine (PheG), serine (Ser), and glutamic acid (Glu) by X-ray diffraction method,<sup>19,20</sup> and showed that all four carboxyl groups of (+)-18C6H<sub>4</sub> are deprotonatable and take the formula (+)-18C6H<sub>x</sub>,  $x = 0–4$ , charge =  $-4–0$ , depending on the interaction with the guest molecule. Consequently, we proposed that the structural scaffold of (+)-18C6H<sub>x</sub> necessary for chiral separation has mainly an asymmetrical bowl-like shape and is dependent on specific interactions between the amino and C $\alpha$ –H groups of the

optically active amino acid and the polar oxygen atoms of (+)-18C6H<sub>x</sub>. The crown ether ring of (+)-18C6H<sub>x</sub> complexed with an optically active amino acid commonly takes a convex/asymmetric conformation, whereas the conformation of (+)-18C6H<sub>4</sub> dihydrate<sup>21</sup> is planar/symmetric. This indicates that the transition of (+)-18C6H<sub>x</sub> from planar/symmetric to convex/asymmetric conformation is caused by clathration of the optical amino acid and is essential for chiral separation. Therefore, to further investigate the guest-dependent conformational change of (+)-18C6H<sub>x</sub> in more detail, low-molecular weight and optically inactive compounds were selected as guest molecule of (+)-18C6H<sub>x</sub>, hoping that such complex structure provides various intermediate structures that show transition from planar/symmetric to convex/asymmetric conformation. In this study, we report the crystal structures of (+)-18C6H<sub>x</sub> complexed with cationic glycine (**1**), H<sub>3</sub>O<sup>+</sup> (**2**), H<sub>5</sub>O<sub>2</sub><sup>+</sup> (**3**), NH<sub>4</sub><sup>+</sup> (**4**), and 2CH<sub>3</sub>NH<sub>3</sub><sup>+</sup> (**5**) and discuss the guest-dependent conformational change of (+)-18C6H<sub>x</sub>. The atomic numbering of (+)-18C6H<sub>4</sub> used in this work is shown in Figure 1.

\*Correspondence to: Hiroomi Nagata, Analytical Chemistry Research Department, CMC Research Laboratory, Mitsubishi Tanabe Pharma Corporation, Ltd., 3-16-89 Kashima, Yodogawa-ku, Osaka 532-8505, Japan.  
E-mail: nagata.hiroomi@md.mt-pharma.co.jp

Received for publication 27 September 2007; Accepted 10 January 2008  
DOI: 10.1002/chir.20550

Published online 27 February 2008 in Wiley InterScience (www.interscience.wiley.com).

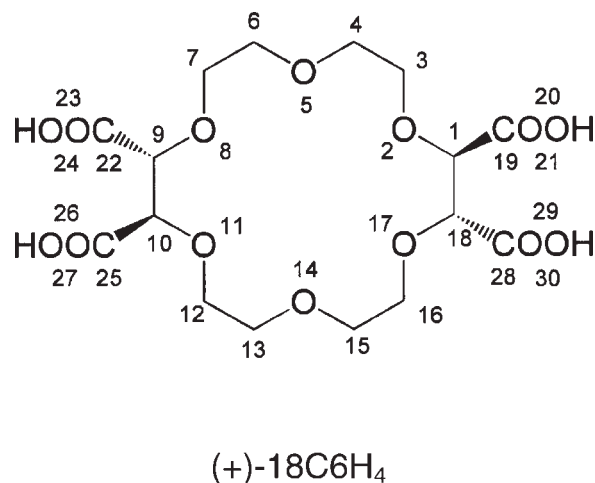


**Fig. 1.** Chemical structure and atomic numbering of (+)-18C6H<sub>4</sub> used in this work.

## EXPERIMENTAL

### X-Ray Analysis

All complex crystals, in the form of colorless prisms, were prepared from aqueous hydrochloric or perchloric acid solution containing an equimolar amount of (+)-18C6H<sub>4</sub> and Gly (**1**) or (+)-18C6H<sub>4</sub> alone (**2** and **3**), or containing the proper amount of ammonia (**4**) or methyl ammonia (**5**), by slow evaporation at 293 K. X-ray data were collected with a Rigaku RINT RAPID/R diffractometer using graphite-monochromated CuK $\alpha$  radiation ( $\lambda$  = 1.5418 Å) at 100 K. Details for cell parameter determination and data collection are summarized in Table 1. Intensity data within  $2\theta \leq 136.4^\circ$  were measured using an imaging plate area detector.

Each crystal structure was solved by the direct method using SIR-92.<sup>22</sup> Positional parameters of non-H atoms were refined by full-matrix least squares with anisotropic temperature parameters using SHELXL-97.<sup>23</sup> The positions of all H-atoms were determined by difference Fourier map. They were treated as riding with fixed isotropic displacement parameters and were not included as variables in the refinement. In complex **2**, two crystallographically independent perchlorate ions were located on the  $C_2$  symmetry axis with occupancy of 1/2. Very complicated disorder was observed in the perchlorate ion of Cl(400) with O(401)-O(404) and the oxygen atom O(27) of the carboxyl group of (+)-18C6H<sub>4</sub>. The occupancies of Cl(400) and O(27) were determined from refinement results and refined with isotropic temperature parameter. The bond-lengths and -angles of these atoms were not as accurate as usual because of incomplete disorder model and fragile crystal. However, this was not considered a problem in the investigation of interaction mode of host and guest molecules. In complex **3**, the perchlorate ion located at a  $C_2$  symmetric position was disordered with occupancy of 1/2. The positions of the three hydrogen atoms of the oxonium ion were determined by difference Fourier map. One of these hydrogen atoms was located at a  $C_2$  position as 1/2-occupancy atom. In complex **5**, the occupancy of crystal water O(700) was determined from its peak intensity as 1/2. Crystallographic data for the structures reported in this paper have been deposited with the Cambridge Crystallographic Data Centre [(**1**) CCDC 653874, (**2**) CCDC 653875, (**3**) CCDC 653876, (**4**) CCDC 653877, and (**5**) CCDC 653878].

### Molecular Orbital Calculation

Total energies of (+)-18C6H<sub>4</sub> in vacuo were calculated by the molecular orbital PM3 method<sup>24</sup> in MOPAC sys-

**TABLE 1.** Details of crystal data, intensity collection, and structure refinement

	1	2	3	4	5
Formula	C <sub>16</sub> H <sub>24</sub> O <sub>14</sub> C <sub>2</sub> H <sub>6</sub> NO <sub>2</sub> <sup>+</sup> H <sub>2</sub> OCl <sup>-</sup>	C <sub>16</sub> H <sub>24</sub> O <sub>14</sub> H <sub>3</sub> O <sup>+</sup> H <sub>2</sub> OClO <sub>4</sub> <sup>-</sup>	1/2C <sub>16</sub> H <sub>24</sub> O <sub>14</sub> 1/2H <sub>5</sub> O <sub>2</sub> <sup>+</sup> 1/2ClO <sub>4</sub> <sup>-</sup>	C <sub>16</sub> H <sub>23</sub> O <sub>14</sub> <sup>-</sup> NH <sub>4</sub> <sup>+</sup> 2H <sub>2</sub> O	C <sub>16</sub> H <sub>20</sub> O <sub>14</sub> <sup>4-</sup> 4CH <sub>3</sub> NH <sub>3</sub> <sup>+</sup> 5/2H <sub>2</sub> O
Molecular weight	569.90	576.85	288.42	493.42	609.62
Crystal system	Monoclinic	Monoclinic	Monoclinic	Monoclinic	Monoclinic
Space group	<i>P</i> 2 <sub>1</sub>	<i>C</i> 2	<i>C</i> 2	<i>P</i> 2 <sub>1</sub>	<i>P</i> 2 <sub>1</sub>
Unit cell dimensions					
<i>a</i> (Å)	9.874(1)	19.551(2)	14.399(1)	11.609(1)	8.3161(9)
<i>b</i> (Å)	10.778(1)	10.275(1)	7.6453(7)	7.6277(8)	11.206(1)
<i>c</i> (Å)	12.508(1)	15.982(2)	10.9339(9)	12.845(1)	16.030(1)
$\alpha$ (deg)	90	90	90	90	90
$\beta$ (deg)	110.978(6)	126.416(5)	109.127(5)	98.314(6)	95.039(6)
$\gamma$ (deg)	90	90	90	90	90
Volume (Å <sup>3</sup> )	1242.9(3)	2583.7(5)	1137.2(2)	1125.5(2)	1488.1(2)
<i>Z</i>	2	4	4	2	2
<i>F</i> (000)	600.0	1208.0	604.0	524.0	658.0
<i>D</i> <sub>x</sub> (g cm <sup>-3</sup> )	1.523	1.483	1.684	1.456	1.360
$\mu$ (CuK $\alpha$ ) (cm <sup>-1</sup> )	21.32	21.38	24.28	11.59	10.17
No. of reflections with $I > 2\sigma(I)$	3979	4080	1897	3737	4786
<i>R</i> ( $I > 2\sigma(I)$ )	0.034	0.082	0.030	0.042	0.040
<i>R</i> <sub>w</sub> ( $I > 2\sigma(I)$ )	0.091	0.231	0.079	0.113	0.113



tem. Atomic coordinates determined by X-ray analysis were used for molecular orbital calculations. The guest molecules, crystal waters, and counter ions were not included in the calculations. To compare energy stability of the respective different conformers under the same molecular situation, the neutral state of (+)-18C6H<sub>4</sub> was used for the calculation. Thus, H-atoms were added to the deprotonated carboxyl groups of (+)-18C6H<sub>3</sub><sup>−</sup> and (+)-18C6H<sub>0</sub><sup>4−</sup>. The conformers used for the calculations are as follows: complexes **1–5**, (+)-18C6H<sub>4</sub> dihydrate,<sup>21</sup> (+)-18C6H<sub>4</sub> hydrochloride,<sup>25</sup> (+)-18C6H<sub>x</sub> complexes with D-/L-Tyr, Ile, Met, PheG, Ser, and Glu.<sup>19,20</sup>

## RESULTS AND DISCUSSION

The chemical formulas of (+)-18C6H<sub>x</sub> complexes prepared in this study are given in Table 1. Although (+)-18C6H<sub>x</sub> in **1**, **2**, and **3** took a neutral form of (+)-18C6H<sub>4</sub>, (+)-18C6H<sub>x</sub> in **4** was in a monoanionic form with one of the four carboxyl groups being deprotonated ((+)-18C6H<sub>3</sub><sup>−</sup>). On the other hand, the four carboxyl groups in **5** were all deprotonated and existed in the tetra anionic form of (+)-18C6H<sub>0</sub><sup>4−</sup>. The host molecule in **1–4** accepted a monocationic guest molecule, on the other hand, the host in **5** anchored two monocationic guests.

### Conformation of Crown Ether Ring

The molecular conformations of (+)-18C6H<sub>x</sub> in complexes **1–5** are shown in Figure 2. In **1** and **2**, the crown ether ring of (+)-18C6H<sub>x</sub> takes a convex/asymmetric C<sub>1</sub> conformation [Fig. 2, (1) and (2)]. This conformation has also been observed in complexes of (+)-18C6H<sub>x</sub> with various optically active amino acids<sup>19,20</sup> and *R*-1-(1-naphthyl)-ethylamine.<sup>26</sup> Previously, we reported that the C<sub>1</sub> conformation of (+)-18C6H<sub>x</sub> could be further classified into three types, i.e. “conformers I, II, and III” (corresponding to Figs. 5d–5f), respectively), according to the difference of torsion angles around C10–O11–C12–C13–O14–C15–C16–O17 bond sequence of the crown ether ring (see Fig. 1).<sup>19</sup> (+)-18C6H<sub>x</sub> in **1** and **2** belongs to conformer III and I, respectively. On the other hand, the conformations of (+)-18C6H<sub>x</sub> in **3**, **4**, and **5** [Fig. 2, (3)–(5)] are considerably different from those in **1** and **2**. The crown ether ring takes a convex C<sub>2</sub> symmetric conformation in **3** where the C<sub>2</sub> crystallographic symmetry axis is located at the center of the crown ether ring. The crown ether rings in **4** and **5** are both planar and have all four carboxyl groups almost vertical to them. Thus, their macrocycle’s conformations could be pseudo-C<sub>2</sub> symmetric and pseudo-C<sub>2s</sub> symmetric, respectively. C<sub>2s</sub> symmetry is defined as the conformation in which a mirror C<sub>s</sub> symmetry crosses the C<sub>2</sub> symmetry at nearly right angle, as shown in Figure 2 (5). Similar conformation has been observed in (+)-18C6H<sub>4</sub> dihydrate<sup>21</sup> and (+)-18C6H<sub>2</sub><sup>2−</sup>-ethylenediamine complex.<sup>27</sup>

### Host–Guest Interaction

**Complex 1.** The Gly in **1** had a monocationic form with a protonated amino and a neutral carboxyl group in HCl salts. Gly torsion angle  $\psi$  [N–C $\alpha$ –C–O =  $-4.9^\circ$ ]<sup>3</sup> is similar to that in its  $\gamma$ -form crystal,<sup>28</sup> and its amino group

is almost located at the center of the circular crown ether ring (radius = about 3.0 Å) consisting of six oxygen atoms [O(2), O(5), O(8), O(11), O(14), and O(17)] and forms N–H $\cdots$ O hydrogen bonds and N $\cdots$ O electrostatic short contacts with the carboxyl oxygen atoms of (+)-18C6H<sub>4</sub> (Table 2). The short contacts<sup>29</sup> were observed for the C $\alpha$ –H $\cdots$ O, as shown in Figure 2 (1) and Figure 4 [C $\alpha$  $\cdots$ O(5) = 3.332(2) Å, C–H $\cdots$ O = 2.66 Å,  $\angle$ C–H $\cdots$ O = 122.5°; C $\alpha$  $\cdots$ O(11) = 3.208(3) Å, C–H $\cdots$ O = 2.67 Å,  $\angle$ C–H $\cdots$ O = 117.5°; C $\alpha$  $\cdots$ O(26) = 3.294(2) Å, C–H $\cdots$ O = 2.36 Å,  $\angle$ C–H $\cdots$ O = 174.9°]. These short contacts are commonly observed in complexes of (+)-18C6H<sub>4</sub> with various optical amino acids, such as Tyr, Ile, Met, PheG, Ser, and Glu,<sup>19,20</sup> and are considered to be a major force for chiral separation of racemic amino acids.

**Complex 2.** The oxonium ion formed by the salt bridge with perchloric acid is located at almost the same position as the amino group of Gly in **1** [Fig. 2, (2)]. The interactions of O–H $\cdots$ O/O $\cdots$ O atomic pairs in **2** are similar to those of N–H $\cdots$ O/N $\cdots$ O in **1** (Table 2).

**Complex 3.** According to the symmetry requirement of crystal packing, two C<sub>2</sub>-related water molecules took monocationic form by salt formation with one perchloric acid, thus forming a C<sub>2</sub>-symmetric H<sub>5</sub>O<sub>2</sub><sup>+</sup>, called “zundel ion” (details of this structure are discussed later). As shown in Figure 2 (3), H<sub>5</sub>O<sub>2</sub><sup>+</sup> ion simultaneously formed four hydrogen bonds with the C<sub>2</sub>-symmetric O(8) and O(8') atoms of the crown ether ring (O(100) $\cdots$ O(8) = 2.867(2), O–H $\cdots$ O = 1.88 Å,  $\angle$ O–H $\cdots$ O = 159.9°), and the carboxyl O(24) and O(24') atoms translated by one unit-cell along *b*-axis (O(100) $\cdots$ O(24) = 2.635(2), O–H $\cdots$ O = 1.82 Å,  $\angle$ O–H $\cdots$ O = 167.9°).

**Complex 4.** As shown in Figure 2 (4), the ammonium ion is located at the center of the one-side face of the crown ether ring and the opposite side is occupied with a water molecule. The ammonium ion forms N–H $\cdots$ O hydrogen bonds and N $\cdots$ O electrostatic short contacts with the oxygen atoms of the crown ether ring and the carboxyl groups (Table 2), and the water molecule forms hydrogen bonds with the oxygen atoms of two facing carboxyl groups, thus making the crown ether ring planar and the four carboxyl groups vertical to the ring.

**Complex 5.** As shown in Figure 2 (5), the (+)-18C6H<sub>0</sub><sup>4−</sup> molecule anchors two guest methylammonium ions located in each center of both faces of the planar crown ether ring and forms N–H $\cdots$ O hydrogen bonds and N $\cdots$ O electrostatic short contacts with the oxygen atoms of the crown ether ring and the carboxyl groups (Table 2).

### Structure of H<sub>5</sub>O<sub>2</sub><sup>+</sup> Ion

H<sub>5</sub>O<sub>2</sub><sup>+</sup> ion, called as “zundel ion,” consists of a dimeric structure of two water molecules and is described as [H<sub>2</sub>O $\cdots$ H<sup>+</sup> $\cdots$ H<sub>2</sub>O]. Therefore, it is believed that H<sub>5</sub>O<sub>2</sub><sup>+</sup> takes an intermediate structure between H<sub>2</sub>O and H<sub>3</sub>O<sup>+</sup> (oxonium ion) and plays an important role as a proton transporter in biological processes, such as enzymatic



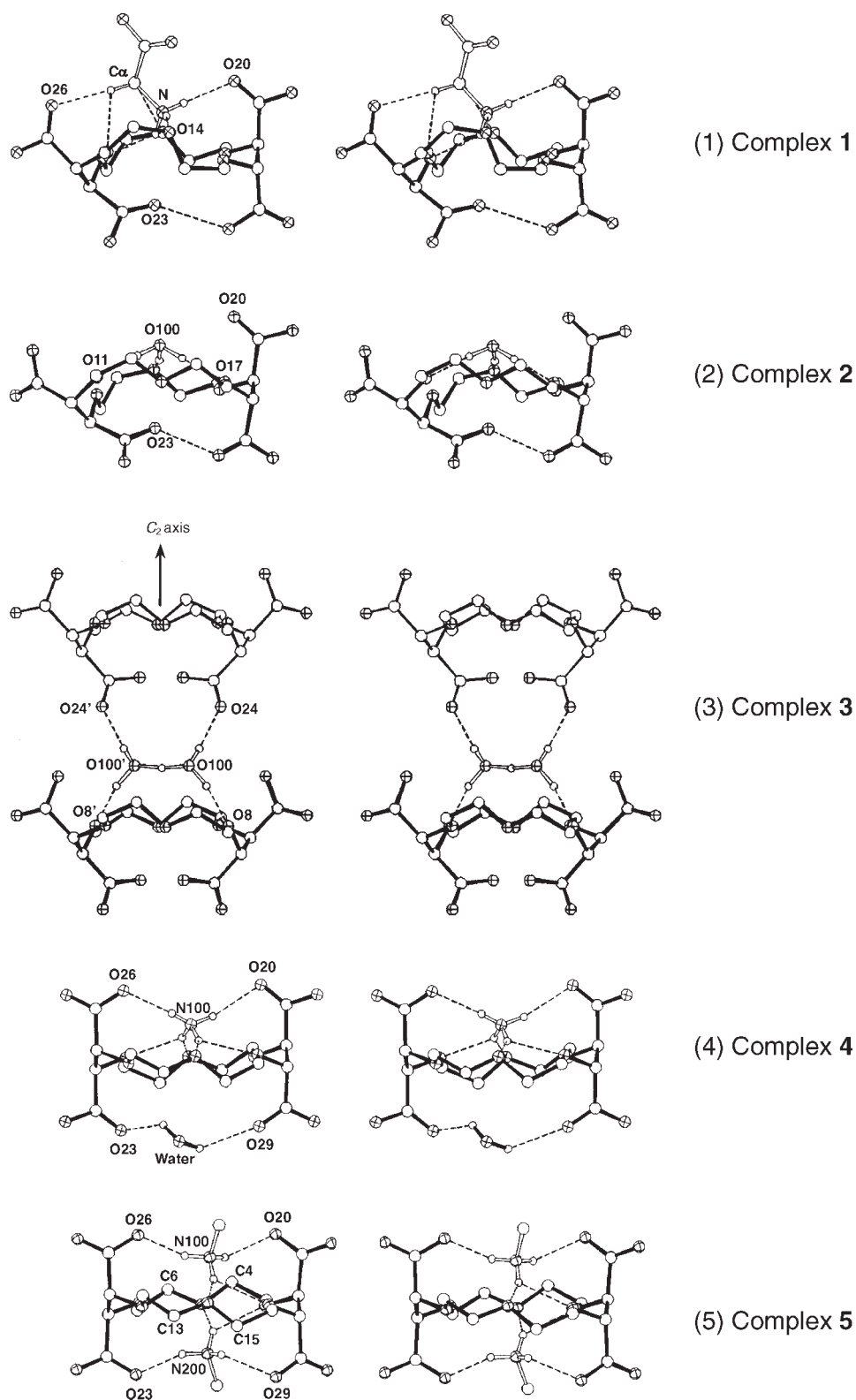


**Fig. 2.** Stereoscopic molecular conformations and interactions between host and guest molecules in complexes 1–5. (+)-18C6H<sub>4</sub> and each guest molecule are depicted with filled and open bonds, respectively. The molecule depicted with thin lines in complex 3 (upper side) represents (+)-18C6H<sub>4</sub> translated by one-unit cell along the *b*-axis. The dotted lines represent hydrogen bonds. The patterned circles represent O or N atom. The plain big and small circles represent C and H atoms, respectively.

**TABLE 2.** Possible hydrogen bonds and short contacts (Å) between N atom of Gly (1)/oxonium ion (2)/ammonium ion (4)/N atom of methyl ammonium (5) and O atoms of (+)-18C6H<sub>x</sub>

	1	2	4	5
X...O(2)	3.024(2)	3.009(5)	3.013(3)	
X-H...O				
∠X-H...O				
X...O(5)	3.021(2)	2.881(5)	3.146(3) <sup>a</sup>	3.064(2) <sup>b,i</sup>
X-H...O		1.83	2.40	2.28
∠X-H...O		160.6	146.0	138.8
X...O(8)	3.019(2)	3.062(7)	2.955(3) <sup>a</sup>	2.920(2) <sup>b,i</sup>
X-H...O	2.30		2.27	2.20
∠X-H...O	136.8		136.6	132.1
X...O(11)	2.867(2)	3.082(6)	3.074(3)	2.876(2) <sup>c,ii</sup>
X-H...O		2.03		2.24
∠X-H...O		176.5		124.0
X...O(14)	2.986(3)	(3.467(4))	3.111(3) <sup>d</sup>	2.906(2) <sup>c,ii</sup>
X-H...O	2.02		2.30	2.09
∠X-H...O	170.1		146.4	142.8
X...O(17)	3.060(2)	3.031(4)	2.956(2) <sup>d</sup>	
X-H...O		2.01	2.30	
∠X-H...O		174.1	127.7	
X...O(20)	2.892(2)	2.987(8)	3.070(3)	2.739(3) <sup>i</sup>
X-H...O	2.01		2.17	1.89
∠X-H...O	169.8		162.7	148.3
X...O(23)	3.331(2)	2.998(5)		2.929(2) <sup>ii</sup>
X-H...O				2.15
∠X-H...O				138.0
X...O(26)			2.911(3)	2.962(2) <sup>i</sup>
X-H...O			2.05	2.22
∠X-H...O			174.1	133.9
X...O(29)				2.743(2) <sup>ii</sup>
X-H...O				1.89
∠X-H...O				149.2

<sup>a-d</sup>Pair of branched hydrogen bonds.

<sup>i,ii</sup>Two methylammonium ions (i, ii) anchored independently by the crown ether ring.

reactions.<sup>30–33</sup> The structure of H<sub>5</sub>O<sub>2</sub><sup>+</sup> has extensively been studied by various physicochemical approaches, and the O...O distance of H<sub>5</sub>O<sub>2</sub><sup>+</sup> has been reported to be in the range of 2.4–2.5 Å. Using highly accurate X-ray analysis, we report in this study that H<sub>5</sub>O<sub>2</sub><sup>+</sup> ion, as shown in Figure 3, consists of C<sub>2</sub> symmetry-related two H<sub>2</sub>O molecules with the central hydrogen atom, having an occupancy of 1/2, located on the C<sub>2</sub> symmetry axis. The O...O distance in H<sub>5</sub>O<sub>2</sub><sup>+</sup> was 2.425(2) Å and the angle of O...H...O was slightly nonlinear (172.0°). This structure agrees well with that of H<sub>5</sub>O<sub>2</sub><sup>+</sup> in its gas phase (O...O = 2.431 Å; ∠O...H...O = 172°).<sup>34</sup>

#### Structural Scaffold of (+)-18C6H<sub>x</sub> in Chiral Interaction with Guest Molecule

Previously, we proposed a possible structural scaffold of (+)-18C6H<sub>x</sub> necessary for chiral separation of racemic amino acids<sup>19</sup> i.e., (i) the convex/asymmetrical C<sub>1</sub> conformation of (+)-18C6H<sub>x</sub>, which forms a bowl-like shape having

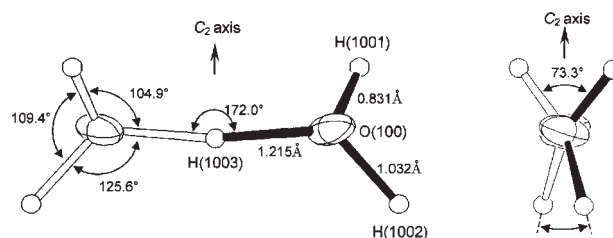


**Fig. 3.** Molecular structure, together with the bond lengths and angles, of H<sub>5</sub>O<sub>2</sub><sup>+</sup>, viewed from *a*- (left) and *c*-axis (right) directions in complex **3**. The atomic position of H(1003) is located at C<sub>2</sub> position with occupancy of 1/2. The closed and open lines are related to each other by crystallographic C<sub>2</sub> symmetry.

ing two hollows (one big and one small) on the rim (see Fig. 4), is necessary to form different binding modes between L- and D-enantiomers and (ii) N—H...O and Cα—H...O interactions between the amino acid and the oxygen atoms of (+)-18C6H<sub>x</sub> afford a driving force for chiral separation.

The structure of Gly can be considered as a common structure of L- and D-amino acids, because it provides the minimum structural element of amino acid, though it is achiral. Thus, the interaction mode between (+)-18C6H<sub>4</sub> and Gly in **1** completely satisfies the theory (i) and (ii).

#### Guest-Dependent Conformational Change of (+)-18C6H<sub>x</sub>

The conformational types of (+)-18C6H<sub>x</sub> could be divided into four; the first is planar/C<sub>2s</sub>-type observed in **5**,

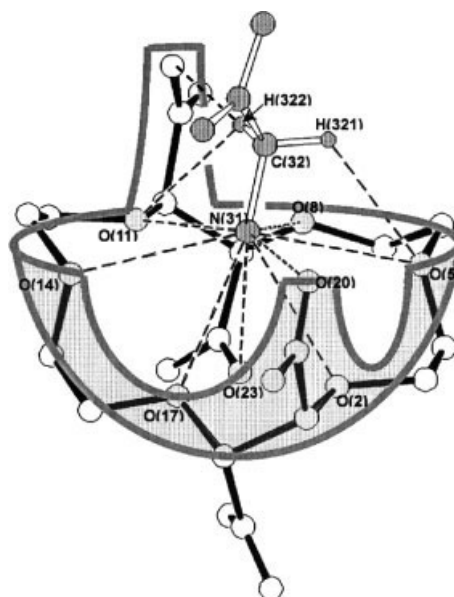


**Fig. 4.** Schematic interaction between Gly and (+)-18C6H<sub>4</sub> in complex **1**. The broken lines represent hydrogen bonds or electrostatic interactions. The conformation of (+)-18C6H<sub>4</sub> could be depicted as a bowl with two concave and one convex rim.

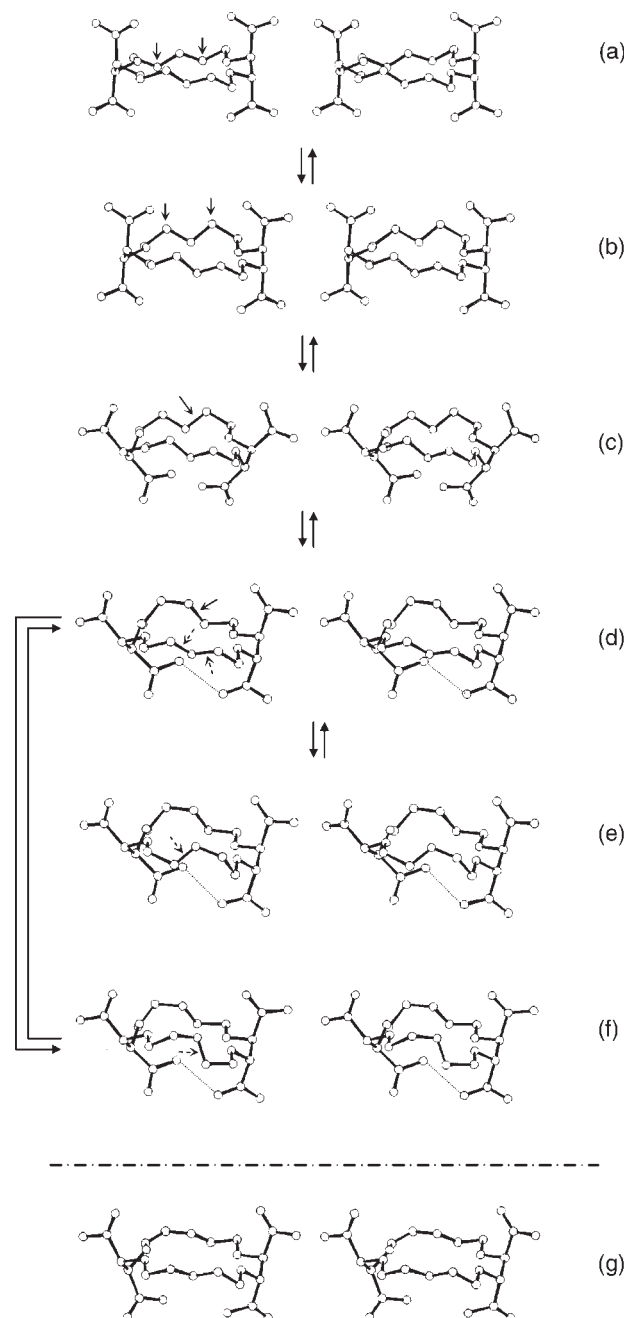


**Fig. 5.** Possible flow (in stereo) of transition of (+)-18C6H<sub>4</sub> from its planar/*C*<sub>2</sub>-type to convex/*C*<sub>1</sub>-type conformation. (a) Planar/*C*<sub>2s</sub>-type observed in (+)-18C6H<sub>4</sub> dihydrate<sup>21</sup> and complex 5. (b) Planar/*C*<sub>2</sub>-type observed in complex 4. (c) Convex/*C*<sub>2</sub>-type observed in complex 3. (d) Convex/*C*<sub>1</sub>-type (conformer I) observed in complex 2 and complexes with D-Tyr, D-Ile, L-Met, L-PheG, D-PheG, L-Ser and D-Ser.<sup>19,20</sup> (e) Convex/*C*<sub>1</sub>-type (conformer II) observed in complexes with L-Ile, D-Met and D-PheG.<sup>19</sup> (f) Convex/*C*<sub>1</sub>-type (conformer III) observed in complex 1 and complexes with L-Tyr, L-Glu and D-Glu.<sup>19,20</sup> (g) Convex/*C*<sub>1</sub>-type (pseudo-conformer I) observed in its hydrochloride.<sup>25</sup>

the second is planar/*C*<sub>2</sub>-type observed in 4, the third is convex/*C*<sub>2</sub>-type observed in 3, and the last is convex/*C*<sub>1</sub>-type observed in 1 and 2. Thus, it is obvious that the conformation of (+)-18C6H<sub>4</sub> is changeable, within an allowed range, depending on the molecular shape, optical isomer,

and number of cationic guests anchored to the crown ether ring.

As stated above, (+)-18C6H<sub>4</sub> must take an asymmetrical *C*<sub>1</sub>-type conformation (conformer I–III), not a symmetrical *C*<sub>2s</sub>- or *C*<sub>2</sub>-type conformation to achieve effective optical recognition according to theories (i) and (ii). Therefore, the present X-ray study provides a possible conformational flow of (+)-18C6H<sub>4</sub> from its free form to the chiral-discriminative form shown in Figure 5. This flow can be described as follows:

**Step 1.** The planar/*C*<sub>2s</sub>-type conformation of (+)-18C6H<sub>4</sub> dihydrate<sup>21</sup> could be the form on the HPLC column before amino acid solution is added. This conformation is changed to planar/*C*<sub>2</sub>-type conformation (Fig. 5b) by moving the C4 and C6 atomic positions as shown by the arrows in Figure 5b.

**Step 2.** The planar/*C*<sub>2</sub>-type conformation is then changed to convex/*C*<sub>2</sub>-type conformation (Fig. 5c) by distortion of the crown ether ring, promoted by interaction with a monocationic guest molecule.

**Step 3.** The convex/*C*<sub>2</sub>-type conformation is further changed to convex/*C*<sub>1</sub>-type conformation [conformer I (Fig. 5d) via a pseudo-conformer I (Fig. 5g)] by successive rotation around the C4–O5 bond as shown by the arrows in Figures 5c and 5d.

**Step 4.** Conformer I is then converted into an equilibrium state with conformers II and III by successive rotation around the C13–O14 or O14–O15 bond as shown by the arrows in Figures 5d–5f.

It is noteworthy in this conformational flow that successive rotation around the C4–O5 bond in the macrocycle (Figs. 5c and 5d) plays a critical role in formation of the asymmetric structure necessary for enantiomeric recognition and that conformer III (Fig. 5f) may be more suitable for optical recognition than conformers I and II, because it reflects most features of the asymmetric bowl-like shape (see Fig. 4).

On the other hand, to investigate the stability of the conformers corresponding to steps 1–4, total energy of each conformer was calculated by the PM3 method (Table 3). The maximum energy difference among same conformers is 1.75 eV for conformer III, which corresponds to about 40 kcal mol<sup>−1</sup>. Because the energy difference among same conformers is almost due to the slightly different bonding parameters (bond lengths and angles) used for the PM3 calculations, it would be reasonable to consider that the maximum permissible range of the energy difference is about 1.75 eV. Thus, the results indicate that each conformer, except pseudo-conformer I (Fig. 5g) observed in (+)-18C6H<sub>4</sub> hydrochloride,<sup>25</sup> is energetically equivalent, and the transition between the respective conformational steps is permissible without any energy barrier. However, the total energy of pseudo-conformer I was higher than those of other conformers by 2.56–4.31 eV, and thus this conformer could be set as an intermediate form between the convex/*C*<sub>2</sub>-type conformer (Fig. 5c) and convex/*C*<sub>1</sub>-type one (Fig. 5d). This indicates that there is an energy barrier for the conformational transition from the convex/

**TABLE 3. Total energy of various conformers of (+)-18C6H<sub>4</sub>**

Conformation	Total energy (electron volt)
Planar/ <i>C</i> <sub>2s</sub> -type	−6375.10 to −6375.71 <sup>a</sup>
Planar/ <i>C</i> <sub>2</sub> -type	−6374.73 <sup>b</sup>
Convex/ <i>C</i> <sub>2</sub> -type	−6375.93 <sup>c</sup>
Convex/ <i>C</i> <sub>1</sub> -type	
Conformer I	−6374.75 to −6375.67 <sup>d</sup>
Conformer II	−6374.55 to −6375.30 <sup>e</sup>
Conformer III	−6374.22 to −6375.97 <sup>f</sup>
Pseudo-conformer I	−6371.66 <sup>g</sup>

X-ray analyses of the present complexes were performed at 100 K, and others were done at room temperature,<sup>19,21,25</sup> 253 K<sup>19</sup> or 173 K<sup>20</sup>. The respective total energies of planar/*C*<sub>2s</sub>-type, planar/*C*<sub>2</sub>-type, convex/*C*<sub>2</sub>-type, and convex/*C*<sub>1</sub>-type (conformers I and II) are all within the range of those of convex/*C*<sub>1</sub>-type conformer III: −6374.22 to −6375.97 eV (energy range = 1.75 eV).

<sup>a</sup>Dihydrate<sup>21</sup> and complex 5.

<sup>b</sup>Complex 4.

<sup>c</sup>Complex 3.

<sup>d</sup>Complex 2 and complexes with D-Tyr, D-Ile, L-Met, L-PheG, D-PheG (Mol. A), L-Ser, and D-Ser.<sup>19,20</sup>

<sup>e</sup>Complexes with L-Ile, D-Met, and D-PheG (Mol. B).<sup>19</sup>

<sup>f</sup>Complex 1 and complexes with L-Tyr, L-Glu, and D-Glu.<sup>19,20</sup>

<sup>g</sup>Hydrochloride.<sup>25</sup>

*C*<sub>2</sub>-type to the convex/*C*<sub>1</sub>-type, which corresponds to a rate-limiting step in the guest-dependent conformational change of (+)-18C6H<sub>4</sub>.

Chiral separation of racemic amides or amino acids by HPLC and CE using (+)-18C6H<sub>4</sub> as chiral selector has usually been achieved in an acidic solution.<sup>7–15</sup> The present results show that collaborative interaction between the deprotonated carboxyl group (−COO<sup>−</sup>) of (+)-18C6H<sub>4</sub> and the protonated amino group (−NH<sub>3</sub><sup>+</sup>) of the guest molecule plays a major role in chiral separation. Interestingly, the crystal structure of complex 2 indicates that the H<sub>3</sub>O<sup>+</sup>-anchored (+)-18C6H<sub>4</sub>, which can exist abundantly in acidic aqueous solution, shifts from its original planar/*C*<sub>2s</sub> conformation to an asymmetric *C*<sub>1</sub> form. This means that a pH-dependent promotive effect toward the conformational change of (+)-18C6H<sub>4</sub> is necessary for chiral recognition.

## LITERATURE CITED

- Sousa LR, Sogah GDY, Hofmann DH, Cram DJ. Host-guest complexation. 12. Total optical resolution of amine and amino ester by chromatography. *J Am Chem Soc* 1978;100:4569–4576.
- Sogah GDY, Cram DJ. Host-guest complexation. 14. Host covalently bound to polystyrene resin for chromatographic resolution of enantiomers of amino acid and ester salts. *J Am Chem Soc* 1979;101:3035–3042.
- Shinbo T, Yamaguchi T, Nishimura K, Sugiura M. Chromatographic separation of racemic amino acids by using chiral crown ether-coated reversed-phase packings. *J Chromatogr* 1987;405:145–153.
- Shinbo T, Yamaguchi T, Yanagishita H, Kitamono D, Sakaki K, Sugiura M. Improved crown ether-based chiral stationary phase. *J Chromatogr* 1992;625:101–108.
- Machida Y, Nishi H, Nakamura K, Nakai H, Sato T. Enantiomer separation of amino compounds by a novel chiral stationary phase derived from crown ether. *J Chromatogr A* 1998;805:85–92.
- Machida Y, Nishi H, Nakamura K. Enantiomer separation of hydrophobic amino compounds by high-performance liquid chromatography using crown ether dynamically coated chiral stationary phase. *J Chromatogr A* 1999;830:311–320.
- Hirose K, Yongzhu J, Nakamura T, Nishioka R, Ueshige T, Tobe Y. Chiral stationary phase covalently bound with a chiral pseudo-18-crown-6 ether for enantiomer separation of amino compounds using a normal mobile phase. *Chirality* 2005;17:142–148.
- Machida Y, Nishi H, Nakamura K. Nuclear magnetic resonance studies for the chiral recognition of the novel chiral stationary phase derived from 18-crown-6 tetracarboxylic acid. *J Chromatogr A* 1998;810:33–41.
- Hyun MH, Jin JS, Lee W. Liquid chromatographic resolution of racemic amino acids and their derivatives on a new chiral stationary phase based on crown ether. *J Chromatogr A* 1998;822:155–161.
- Berkecz R, Sztojckov-Ivanov A, Ilisz I, Forro E, Fulop F, Hyun MH, Peter AJ. High-performance liquid chromatographic enantioseparation of -amino acid stereoisomers on a (+)-(18-crown-6)-2,3,11,12-tetracarboxylic acid-based chiral stationary phase. *J Chromatogr A* 2006;1125:138–143.
- Kuhn R, Wagner J, Walbroehl Y, Bereuter T. Potential and limitations of an optically active crown ether for chiral separation in capillary zone electrophoresis. *Electrophoresis* 1994;15:828–834.
- Kuhn R, Riester D, Fleckenstein B, Weismuller K. Evaluation of an optically active crown ether for the chiral separation of di- and tripeptides. *J Chromatogr A* 1995;716:371–379.
- Kuhn R. Enantiomeric separation by capillary electrophoresis using a crown ether as chiral selector. *Electrophoresis* 1999;20:2605–2613.
- Chen Z, Uchiyama K, Hobo T. 18-crown-6-Tetracarboxylic acid as a chiral additive for the simultaneous separation of o-, m-, and p-enantiomers of phenylalanine family by capillary electrophoresis. *Enantiomer* 2001;6:19–25.
- Chen Z, Uchiyama K, Hobo T. Interaction between 18-crown-6-tetracarboxylic acid and positional substituents of enantiomers and simultaneous separation of positional enantiomers of methyl-DL-tryptophans by capillary electrophoresis. *Electrophoresis* 2001;22:2136–2142.
- Wenzel TJ, Thurston JE. (+)-(18-Crown-6)-2,3,11,12-tetracarboxylic acid and its Ytterbium(III) complex as chiral NMR discriminating agents. *J Org Chem* 2000;65:1243–1248.
- Machida Y, Kagawa M, Nishi H. Nuclear magnetic resonance studies for the chiral recognition of (+)-(R)-18-crown-6-tetracarboxylic acid to amino compounds. *J Pharm Biomed Anal* 2003;30:1929–1942.
- Lovely AE, Wenzel TJ. Chiral NMR discrimination of piperidines and piperazines using (18-crown-6)-2,3,11,12-tetracarboxylic acid. *J Org Chem* 2006;71:9178–9182.
- Nagata H, Nishi H, Kamigauchi M, Ishida T. Structural scaffold of 18-crown-6 tetracarboxylic acid for optical resolution of chiral amino acid: X-ray crystal analyses and energy calculations of complexes of D- and L-isomers of tyrosine, isoleucine, methionine and phenylglycine. *Org Biomol Chem* 2004;2:3470–3475.
- Nagata H, Nishi H, Kamigauchi M, Ishida T. Structural scaffold of 18-Crown-6 tetracarboxylic acid for optical resolution of chiral amino acid: X-ray crystal analyses of complexes of D- and L-isomers of serine and glutamic acid. *Chem Pharm Bull* 2006;54:452–457.
- Dutton PJ, Fronczek FR, Fyles TM, Gandour RD. A host for the water dimer. *J Am Chem Soc* 1990;112:8984–8985.
- Altomare A, Cascarano G., Giacovazzo C, Guagliardi A, Burla M, Polidori G, Camali M. SIR-92, Program for the solution of crystal structures. *J Appl Cryst* 1994;27:435.
- Sheldrick GM. SHELXL97, Program for the refinement of crystal structures. Germany: University of Gottingen; 1997.
- Stewart JJP. Program for the molecular orbital calculation. *J Comput Chem* 1989;10:209.
- Behr JP, Dumas P, Moras D. The H<sub>3</sub>O<sup>+</sup> cation: molecular structure of an oxonium-macrocyclic polyether complex. *J Am Chem Soc* 1982;104:4540–4543.
- Machida Y, Nishi H, Nakamura K. Crystallographic studies for the chiral recognition of the novel chiral stationary phase derived from (+)-(R)-18-crown-6 tetracarboxylic acid. *Chirality* 1999;11:173–178.

27. Daly JJ, Schonholzer J. Molecular structure of the ethylenediammonium complex of a tetracarboxy-macrocyclic receptor molecule. *Helv Chim Acta* 1981;64:1444–1451.
28. Iitaka Y. The crystal structure of  $\gamma$ -glycine. *Acta Crystallogr* 1961;14:1–10.
29. Steiner T. Weak hydrogen bonding. Part 1: Neutron diffraction data of amino acid C $\alpha$ -H suggest lengthening of the covalent C-H bond in C-H $\cdots$ O interactions. *J Chem Soc Perkin Trans2* 1995;1315–1319.
30. Marx D, Tuckerman ME, Hutter J, Parrinello M. The nature of the hydrated excess proton in water. *Nature* 1999;397:601–604.
31. Ludwig R. New insight into the transport mechanism of hydrated hydroxide ions in water. *Angew Chem Int Ed* 2003;42:258–260.
32. Cheruzel LE, Pometun MS, Cecil MR, Mashuta MS, Wittebort RJ, Buchanan RM. Structures and solid-state dynamics of one-dimensional water chains stabilized by imidazole channels. *Angew Chem Int Ed* 2003;42:5452–5455.
33. Tuckerman ME, Marx D, Parrinello M. The nature and transport mechanism of hydrated hydroxide ions in aqueous solution. *Nature*, 2002;417:925–929.
34. Vener MV, Sauer J. Environmental effects on vibrational proton dynamics in H<sub>5</sub>O<sub>2</sub><sup>+</sup>: DFT study on crystalline H<sub>5</sub>O<sub>2</sub><sup>+</sup>ClO<sub>4</sub><sup>-</sup>. *Phys Chem Chem Phys* 2005;7:258–263.



# 3-Substituted BINOL Schiff Bases and Their Reductive Products for Catalytic Asymmetric Addition of Diethylzinc to Aldehydes

BING LIU,<sup>1,2</sup> ZHI-BING DONG,<sup>1</sup> CAO FANG,<sup>1</sup> HAI-BIN SONG,<sup>1</sup> AND JIN-SHAN LI<sup>1\*</sup>

<sup>1</sup>State Key Laboratory of Elemento-Organic Chemistry, Nankai University, Tianjin 300071, People's Republic of China

<sup>2</sup>Key Laboratory of Food Nutrition and Safety, Ministry of Education of China, Tianjin Key Laboratory of Food Nutrition and Safety, Tianjin University of Science and Technology, Tianjin 300457, People's Republic of China

**ABSTRACT** Three new chiral 3-substituted BINOL Schiff bases and their reductive 3-arylaminoethylBINOL products have been synthesized and used for the asymmetric addition reaction of diethylzinc to aldehydes in the presence of titanium tetraisopropoxide. The reaction provided optically active secondary alcohols in high yield (86–100%) and good enantioselectivity (up to 92% ee). *Chirality* 20:828–832, 2008. © 2008 Wiley-Liss, Inc.

**KEY WORDS:** BINOL; titanium; Schiff base; asymmetric addition; aldehyde

## INTRODUCTION

The catalytic enantioselective alkylation of aldehydes is a potentially useful method for preparing chiral secondary alcohols which are important synthetic intermediates for many natural products or precursors.<sup>1–3</sup> Most previous studies have focused on using  $\beta$ -aminoalcohols,<sup>4–9</sup> diols,<sup>10–12</sup> or diamines<sup>13,14</sup> as chiral ligands in the asymmetric addition of diethylzinc to aldehydes and these have given moderate to excellent results. 1,1'-Bi-2-naphthol (BINOL) and its derivatives are the most effective chiral ligands in asymmetric catalysis.<sup>15–18</sup> Since the chiral diol ligands BINOL,<sup>19–20</sup> H<sub>4</sub>-BINOL<sup>21</sup> and H<sub>8</sub>-BINOL<sup>22</sup> have been successfully applied for the asymmetric addition of dialkylzinc to aldehydes, most studies have focused on the 3,3'-disubstituted BINOL ligands. However, few 3-mono-substituted BINOLs have been reported.<sup>23–26</sup> Recently Harada and Kanda reported that 3-substituted BINOLs exhibited an enhanced catalytic activity compared to 3,3'-disubstituted BINOLs in the reaction.<sup>27</sup> Similar phenomena also appeared in our previous research.<sup>28,29</sup> On the basis of this research, a new kind of chiral ligands exhibiting an enhanced asymmetric catalytic activity could possibly be obtained by introducing amino and imino groups into the 3-position of BINOL through the methylene bridge.

In this work, we have synthesized three new 3-substituted BINOL Schiff bases [(*R*)-1, (*R*)-2, (*R*)-3] and their 3-arylaminoethylBINOL reductive products [(*R*)-4, (*R*)-5, (*R*)-6] and used them in asymmetric addition of diethylzinc to aldehydes in the presence of titanium tetraisopropoxide (Scheme 1).

## EXPERIMENTS

### General Methods

The <sup>1</sup>H and <sup>13</sup>C NMR spectra were recorded on a Bruker AC-300 instrument in CDCl<sub>3</sub> solution with TMS as internal standard. Optical rotations were measured on a Perkin-Elmer 241 polarimeter. Elemental analysis was performed with a Yanaco CHN Corder MT-3 elemental ana-

lyzer. High-resolution mass spectra (MALDI-HRMS) were measured on an Ionspec FT MS 7.0T spectrometer. All experiments which are sensitive to moisture or air were carried out under an argon atmosphere using standard Schlenk techniques. Diethylzinc (1.94 M in hexane) was purchased from Aldrich. All anhydrous solvents were purified and dried by standard techniques just before use. (*R*)-3-Formyl-1,1'-binaphthol was prepared according to the literature method.<sup>30</sup>

### The Preparation of New Chiral 3-Substituted BINOL Ligands (*R*)-3-(4-Tolylimino)methyl-1,1'-binaphthol (*R*)-1

To a solution of (*R*)-3-formyl-1,1'-binaphthol (1.40 g, 4.46 mmol) in 20 mL dry ethanol was added *p*-toluidine (0.49 g, 4.55 mmol). The reaction process was monitored by TLC. After refluxing for 7 h, the reaction mixture was concentrated to dryness. The residue was purified by column chromatography (hexane/ethyl acetate 5:1) to give (*R*)-1 (1.63 g, 91% yield) as a yellow solid. m.p. 116–118°C. [ $\alpha$ ]<sub>D</sub><sup>25</sup> = +174.5 (*c* = 0.4, CH<sub>2</sub>Cl<sub>2</sub>). <sup>1</sup>H NMR (300 MHz, CDCl<sub>3</sub>)  $\delta$ : 13.56 (br, 1H), 8.94 (s, 1H), 8.17 (s, 1H), 7.92–7.95 (m, 2H), 7.86–7.89 (d, *J* = 7.70, 1H), 7.27–7.41 (m, 8H), 7.15–7.20 (m, 3H), 5.11 (br, 1H), 2.39 (s, 3H). <sup>13</sup>C NMR (75 MHz, CDCl<sub>3</sub>)  $\delta$ : 162.34, 160.90, 155.57, 151.51, 137.69, 135.34, 130.13, 129.36, 129.30, 129.06, 128.26, 126.55, 124.83, 124.77, 124.12, 123.33, 121.54, 121.07, 117.71, 113.89, 21.08. Anal. Calc. for C<sub>28</sub>H<sub>21</sub>NO<sub>2</sub> (403.16): C, 83.35; H, 5.25; N, 3.47. Found: C, 83.18; H, 5.30; N, 3.54%.

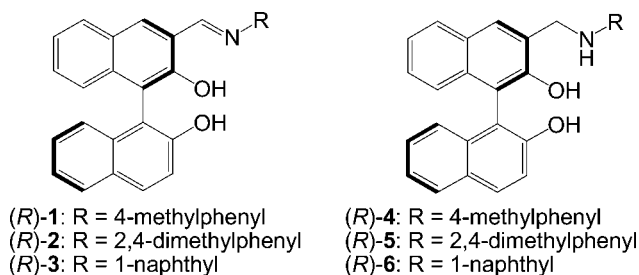
\*Correspondence to: Jin-Shan Li, State Key Laboratory of Elemento-Organic Chemistry, Nankai University, Tianjin 300071, People's Republic of China. E-mail: jinshanli@nankai.edu.cn

Contract grant sponsor: National Natural Science Foundation of China; Contract grant number: 20372037

Received for publication 6 September 2007; Accepted 7 February 2008

DOI: 10.1002/chir.20559

Published online 12 March 2008 in Wiley InterScience (www.interscience.wiley.com).



Scheme 1. 3-substituted BINOL Schiff bases and 3-arylaminomethyl-BINOLs.

**(*R*)-3-(2,4-Dimethylphenylimino)methyl-1,1'-binaphthol (*R*)-2**

(*R*)-3-(2,4-Dimethylphenylimino)methyl-1,1'-binaphthol (*R*)-2: yellow solid. 93% yield, m.p. 112–114°C.  $[\alpha]_D^{25} = +152.0$  ( $c = 0.4$ , CH<sub>2</sub>Cl<sub>2</sub>). <sup>1</sup>H NMR (300 MHz, CDCl<sub>3</sub>)  $\delta$ : 13.43 (br, 1H), 8.56 (s, 1H), 8.17 (s, 1H), 7.92–7.94 (m, 2H), 7.86–7.88 (d,  $J = 7.66$ , 1H), 7.27–7.41 (m, 4H), 7.07–7.24 (m, 6H), 5.16 (br, 1H), 2.35 (s, 3H), 2.31 (s, 3H). <sup>13</sup>C NMR (75 MHz, CDCl<sub>3</sub>)  $\delta$ : 160.98, 155.60, 151.55, 144.60, 137.40, 135.66, 133.63, 135.35, 132.85, 131.62, 130.10, 129.35, 129.24, 129.03, 128.26, 127.91, 127.57, 126.50, 124.91, 124.88, 124.10, 123.31, 121.71, 117.78, 117.30, 114.52, 113.85, 20.98, 18.22. Anal. Calcd. for C<sub>29</sub>H<sub>23</sub>NO<sub>2</sub> (417.17): C, 83.43; H, 5.55; N, 3.35. Found: C, 83.14; H, 5.69; N, 3.39%.

**(*R*)-3-(Naphthalen-1-ylimino)methyl-1,1'-binaphthol (*R*)-3**

(*R*)-3-(Naphthalen-1-ylimino)methyl-1,1'-binaphthol (*R*)-3: yellow solid. 97% yield, m.p. 118–120°C.  $[\alpha]_D^{25} = +207.0$  ( $c = 0.4$ , CH<sub>2</sub>Cl<sub>2</sub>). <sup>1</sup>H NMR (300 MHz, CDCl<sub>3</sub>)  $\delta$ : 13.34 (br, 1H), 9.01 (s, 1H), 8.20 (s, 1H), 8.23 (s, 1H), 7.94–7.98 (m, 2H), 7.85–7.90 (t,  $J = 7.83$ , 2H), 7.80–7.83 (m, 1H), 7.30–7.55 (m, 10H), 7.20–7.22 (m, 1H), 5.18 (br, 1H). <sup>13</sup>C NMR (75 MHz, CDCl<sub>3</sub>)  $\delta$ : 163.11, 162.34, 155.50, 151.57, 145.78, 135.90, 134.03, 133.62, 130.21, 129.55, 129.40, 129.19, 128.32, 128.00, 127.85, 127.57, 126.82, 126.65, 126.60, 125.82, 124.92, 124.85, 124.28, 123.38, 121.70, 120.77, 117.78, 114.38, 114.15, 113.91, 28.16. HRMS Calcd. for C<sub>31</sub>H<sub>21</sub>NO<sub>2</sub> ( $M^+$ ): 439.1657; Found: 440.1645 ( $M^+ + H$ ).

**(*R*)-3-(4-Toluidino)methyl-1,1'-binaphthol (*R*)-4**

(*R*)-3-(4-Tolylimino)methyl-1,1'-binaphthol (*R*)-1 (0.95 g, 2.36 mmol) was dissolved in 25 mL dry ethanol and 25 mL CH<sub>2</sub>Cl<sub>2</sub> and cooled to 0°C. NaBH<sub>4</sub> (0.36 g, 9.43 mmol) was added portionwise. The reaction mixture was stirred at room temperature for 30 min and then quenched with saturated aq. NH<sub>4</sub>Cl. The reaction mixture was concentrated to dryness. The residue was extracted with ethyl acetate, and the extract was washed with water and brine, and dried over Na<sub>2</sub>SO<sub>4</sub>. After removal of solvent the residue was purified by column chromatography (hexane/ethyl acetate 5:1) to give (*R*)-4 (0.87 g, 91% yield) as a white solid. m.p. 88–92°C.  $[\alpha]_D^{25} = +36.0$  ( $c = 0.4$ , CHCl<sub>3</sub>). <sup>1</sup>H NMR (300 MHz, CDCl<sub>3</sub>)  $\delta$ : 7.84–7.95 (m, 4H), 7.32–7.39 (m, 5H), 7.12–7.16 (t,  $J = 10.20$  Hz, 2H), 7.02 (d,  $J = 8.15$  Hz,

2H), 6.75 (d,  $J = 8.30$  Hz, 2H), 4.65 (s, 2H), 2.25 (s, 3H). <sup>13</sup>C NMR (75 MHz, CDCl<sub>3</sub>)  $\delta$ : 152.63, 152.14, 144.91, 133.52, 133.24, 132.62, 130.74, 129.85, 129.52, 129.40, 129.28, 129.15, 129.00, 128.33, 128.10, 127.10, 127.00, 126.76, 124.51, 124.35, 124.11, 123.67, 117.68, 115.27, 112.71, 112.37, 47.59, 20.45. HRMS Calcd for C<sub>28</sub>H<sub>23</sub>NO<sub>2</sub> ( $M^+$  405.1707); found: 405.1723.

**(*R*)-3-(2,4-Dimethylphenylamino)methyl-1,1'-binaphthol (*R*)-5**

(*R*)-3-(2,4-Dimethylphenylamino)methyl-1,1'-binaphthol (*R*)-5: yellow solid. 83% yield, m.p. 90–92°C.  $[\alpha]_D^{25} = +37.5$  ( $c = 0.4$ , CHCl<sub>3</sub>). <sup>1</sup>H NMR (300 MHz, CDCl<sub>3</sub>)  $\delta$ : 7.83–7.95 (m, 4H), 7.24–7.38 (m, 5H), 7.11–7.16 (t,  $J = 6.90$  Hz, 2H), 6.93 (d, 2H), 6.75 (d,  $J = 8.7$  Hz, 1H), 4.68 (s, 2H), 2.24 (s, 3H), 2.18 (s, 3H). <sup>13</sup>C NMR (75 MHz, CDCl<sub>3</sub>)  $\delta$ : 152.67, 152.15, 133.51, 133.20, 131.25, 130.75, 129.41, 129.28, 129.04, 128.67, 128.33, 128.11, 127.47, 127.10, 127.00, 126.85, 124.53, 124.34, 124.20, 124.11, 123.67, 122.32, 117.68, 112.79, 112.69, 112.34, 47.27, 20.38, 17.46. HRMS Calcd for C<sub>29</sub>H<sub>25</sub>NO<sub>2</sub> ( $M^+$  419.1885); found: 419.1880.

**(*R*)-3-(Naphthalen-1-ylamino)methyl-1,1'-binaphthol (*R*)-6**

(*R*)-3-(Naphthalen-1-ylamino)methyl-1,1'-binaphthol (*R*)-6: white solid. 87% yield. m.p. 210–211°C.  $[\alpha]_D^{25} = +55.6$  ( $c = 0.4$ , CHCl<sub>3</sub>). <sup>1</sup>H NMR (300 MHz, CDCl<sub>3</sub>)  $\delta$ : 8.00 (s, 1H), 7.96 (d,  $J = 8.91$  Hz, 1H), 7.80–7.90 (m, 4H), 7.44–7.48 (m, 2H), 7.28–7.41 (m, 6H), 7.15 (d,  $J = 8.30$  Hz, 2H), 6.83–6.88 (m, 1H), 6.65 (br, 1H), 4.84 (s, 2H). <sup>13</sup>C NMR (75 MHz, CDCl<sub>3</sub>)  $\delta$ : 152.42, 152.06, 142.72, 134.35, 133.46, 133.05, 131.09, 129.48, 129.17, 128.75, 128.39, 128.22, 127.24, 127.20, 126.73, 126.40, 125.88, 125.16, 124.39, 124.24, 123.85, 119.99, 119.14, 117.74, 112.07, 111.92, 106.82, 40.17. HRMS Calcd for C<sub>31</sub>H<sub>23</sub>NO<sub>2</sub> ( $M^+$  441.1723); found: 441.1723.

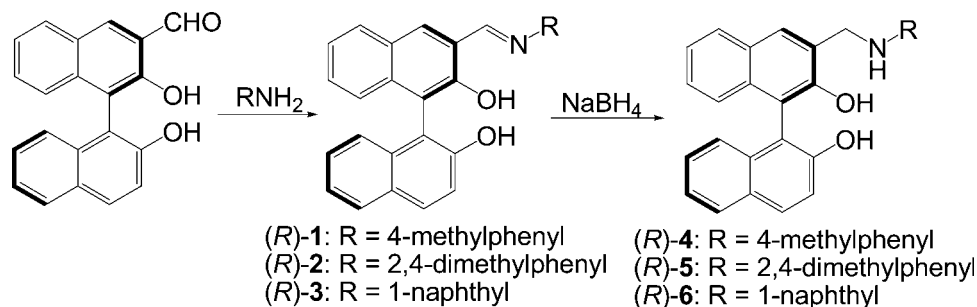
**A Typical Procedure for the Asymmetric Addition of Diethylzinc to Aldehydes**

Titanium tetrakisopropoxide (0.36 mL, 1.2 mmol) was added to a solution of (*R*)-6 (0.044 g, 0.10 mmol) in 3 mL dry CH<sub>2</sub>Cl<sub>2</sub> at room temperature and the reaction mixture was stirred for 30 min followed by addition of diethylzinc (1.94 M in hexane, 1.16 mL) with continuous stirring for 15 min. The solution was cooled to 0°C and benzaldehyde (0.106 g, 1 mmol) was added. After 5 h the reaction was quenched with 20 mL of saturated NH<sub>4</sub>Cl solution. The reaction mixture was filtered to remove the insoluble material and the filtrate was extracted with 3 × 20 mL CH<sub>2</sub>Cl<sub>2</sub>. The combined organic layers were dried over MgSO<sub>4</sub> and concentrated to the solvent free. The residue was purified by column chromatography on silica gel affording 1-phenyl-1-propanol as a pale yellow liquid. The enantiomeric excess of the products was determined by GC on a chiral  $\beta$ -DEX 120 capillary column.

**RESULTS AND DISCUSSION**

3-Substituted BINOL Schiff bases were synthesized by the reaction of (*R*)-3-formyl-1,1'-binaphthol with various ar-





**Scheme 2.** Synthesis of 3-substituted BINOL Schiff bases and 3-arylaminoethylBINOLs.

omatic amines in 90–97% yield.<sup>31</sup> By the reduction of BINOL Schiff bases using  $\text{NaBH}_4$ , 3-arylaminoethylBINOLs were synthesized in 83–91% yield (Scheme 2).

The colorless crystals of (S)-6 were obtained from methanol solution. The crystal structure of (S)-6 was determined by X-ray diffraction (see Fig. 1). Crystallographic data for ligand (S)-6:  $\text{C}_{32}\text{H}_{27}\text{NO}_3$ , formula weight 473.55, Monoclinic, *P*1,  $a = 12.328(3)$  Å,  $b = 7.8825(16)$  Å,  $c = 13.896(3)$  (14) Å,  $\alpha = 90^\circ$ ,  $\beta = 113.82(3)^\circ$ ,  $\gamma = 90^\circ$ ,  $V = 1235.3(4)$  Å<sup>3</sup>,  $Z = 2$ ,  $D_{\text{calcd}} = 1.273$  g/cm<sup>3</sup>,  $T = 293(2)$  K,  $\mu$  (Mo K $\alpha$ ) = 0.081 mm<sup>-1</sup>,  $R$ 1 ( $wR$ 2) = 0.0357 (0.0868), crystal dimensions 0.20 × 0.18 × 0.12 mm.<sup>†</sup> The dihedral angles of C(20)–C(19)–C(21)–N(1) and C(21)–N(1)–C(22)–C(31) are 117.2 and 161.4°, respectively. The dihedral angle between the two naphthalene systems is 77.5°.

We examined the reaction of benzaldehyde with diethylzinc catalyzed by the six chiral ligands in the presence of titanium tetraisopropoxide. The active catalyst was formed in situ by mixing the ligand with titanium tetraisopropoxide.<sup>32</sup> The influence of solvent and chiral ligand loading as well as the molar ratio of chiral ligand and titanium tetraisopropoxide on the addition reaction was systematically

investigated. The obtained results were summarized in Table 1.

When the amount of (R)-3 was reduced from 20 to 10 mol %, there was a decrease in enantioselectivity (entries 1, 2). However, the amount of the ligand from 10 to 5 mol % led to a slight increase while that from 5 to 3 mol % led to a large decrease in enantioselectivity (entries 3, 4, 6). As a result the best amount of the ligand was 5 mol %. The molar ratio of ligand to metal was examined from 1/12, 1/7, 1/3 to metal-free in the addition reaction and it was found that the best molar ratio of ligand to metal was set up to be 1 to 7 (entries 4, 5, 7). For the three Schiff base ligands, (R)-3 showed improved catalytic prop-

**TABLE 1.** Catalytic asymmetric addition of diethylzinc (1.94 M in hexane) to benzaldehyde

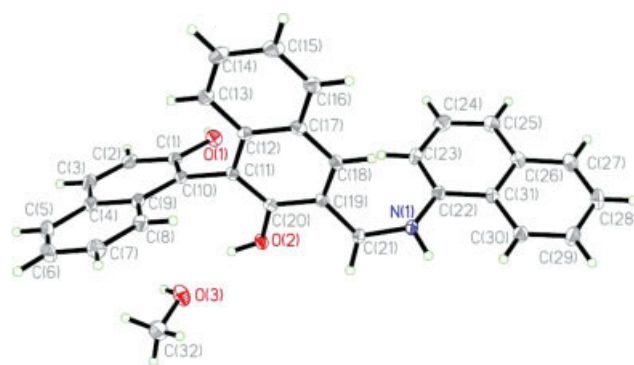
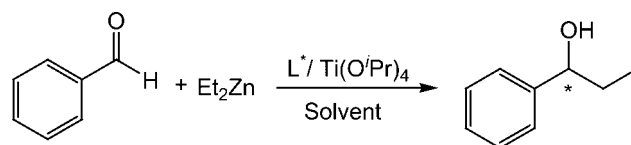


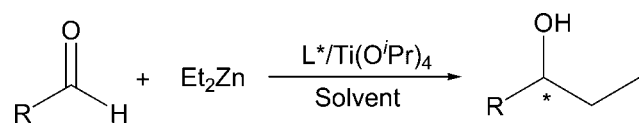
**Fig. 1.** The molecular structure of (S)-6 including a methanol molecule. [Color figure can be viewed in the online issue, which is available at [www.interscience.wiley.com](http://www.interscience.wiley.com).]

<sup>†</sup>CCDC 632117 contains the supplementary crystallographic data for this paper. These data can be obtained free of charge via [www.ccdc.cam.ac.uk/conts/retrieving.html](http://www.ccdc.cam.ac.uk/conts/retrieving.html) (or from the Cambridge Crystallographic Data Centre, 12 Union Road, Cambridge CB2 1EZ, UK; fax +44 1223 336033; or deposit@ccdc.com.ac.uk).

Entry	L*	L* (mol %)	L* / Ti(O <sup>i</sup> Pr) <sub>4</sub>	Solvent	Yield <sup>a</sup> (%)	ee <sup>b</sup> (%)
1	(R)-3	20	1/12	PhMe	86	77
2	(R)-3	10	1/12	PhMe	94	52
3	(R)-3	10	1/7	PhMe	94	56
4	(R)-3	5	1/7	PhMe	96	65
5	(R)-3	5	1/3	PhMe	89	58
6	(R)-3	3	1/7	PhMe	89	34
7	(R)-3	5	–	PhMe	94	12
8	(R)-1	5	1/7	PhMe	89	57
9	(R)-2	5	1/7	PhMe	92	53
10	(R)-6	20	1/12	PhMe	90	83
11	(R)-6	10	1/12	PhMe	94	81
12	(R)-6	10	1/7	PhMe	97	77
13	(R)-6	5	1/7	PhMe	93	64
14	(R)-6	10	1/12	CH <sub>2</sub> Cl <sub>2</sub>	93	87
15	(R)-6	10	1/7	CH <sub>2</sub> Cl <sub>2</sub>	96	84
16	(R)-4	10	1/12	CH <sub>2</sub> Cl <sub>2</sub>	87	85
17	(R)-5	10	1/12	CH <sub>2</sub> Cl <sub>2</sub>	82	85

<sup>a</sup>Isolated yield.

<sup>b</sup>Data were determined by GC analysis using a chiral column (Chiral beta-DEX 120 capillary column).

**TABLE 2.** Enantioselective addition of diethylzinc to aldehydes with  $L^*/Ti(O^iPr)_4$ 

Entry	Chiral ligand	R	Yield <sup>a</sup> (%)	ee <sup>b</sup> (%)	Config. <sup>c</sup>
1	( <i>R</i> )- <b>3</b> (5)	C <sub>6</sub> H <sub>5</sub>	96	65	<i>R</i>
2	( <i>R</i> )- <b>3</b> (5)	<i>p</i> -ClC <sub>6</sub> H <sub>4</sub>	86	44	<i>R</i>
3	( <i>R</i> )- <b>3</b> (5)	<i>p</i> -BrC <sub>6</sub> H <sub>4</sub>	93	61	<i>R</i>
4	( <i>R</i> )- <b>3</b> (5)	<i>p</i> -MeOC <sub>6</sub> H <sub>4</sub>	90	66	<i>R</i>
5	( <i>R</i> )- <b>3</b> (5)	1-Naphthyl	99	67	<i>R</i>
6	( <i>R</i> )- <b>3</b> (5)	PhCH=CH	86	63	<i>R</i>
7	( <i>R</i> )- <b>6</b> (10)	C <sub>6</sub> H <sub>5</sub>	93	87	<i>R</i>
8	( <i>R</i> )- <b>6</b> (10)	<i>p</i> -ClC <sub>6</sub> H <sub>4</sub>	96	88	<i>R</i>
9	( <i>R</i> )- <b>6</b> (10)	<i>p</i> -BrC <sub>6</sub> H <sub>4</sub>	99	89	<i>R</i>
10	( <i>R</i> )- <b>6</b> (10)	<i>p</i> -MeOC <sub>6</sub> H <sub>4</sub>	95	80	<i>R</i>
11	( <i>R</i> )- <b>6</b> (10)	<i>o</i> -MeOC <sub>6</sub> H <sub>4</sub>	95	82	<i>R</i>
12	( <i>R</i> )- <b>6</b> (10)	1-Naphthyl	100	92	<i>R</i>
13	( <i>R</i> )- <b>6</b> (10)	PhCH=CH	99	87	<i>R</i>

<sup>a</sup>Isolated yield.<sup>b</sup>Data were determined by GC analysis using a chiral column (Chiral beta-DEX 120 capillary column).<sup>c</sup>Determined by comparison of the sign of specific rotation value with Ref. 32.

erties in this reaction (entries 4, 65% ee) while (*R*)-**1** and (*R*)-**2** showed a slight decrease in enantioselectivity (entries 8, 9; 57 and 53% ee respectively).

With chiral ligand (*R*)-**6**, its amount from 20 to 10 mol% led to a slight decrease, but the amount from 10 to 5 mol% led to a large decrease in enantioselectivity (entries 10–13). By comparison of the parallel reactions carried out at different molar ratio of the ligand to metal (entries 11, 12), it was found that 1/12 was the optimal molar ratio for the reaction, which gave the highest enantioselectivity. Solvent evaluation revealed that dichloromethane was more favorable than toluene for this reaction in terms of enantioselectivity. For the three chiral 3-arylaminoethylBINOL ligands, (*R*)-**6** showed improved catalytic properties in this reaction (entry 14, 87% ee) while (*R*)-**4** and (*R*)-**5** showed a slight decrease in enantioselectivity (entries 16, 17; 85% ee).

With the ligands (*R*)-**3** and (*R*)-**6**, we also examined the asymmetric addition of diethylzinc to a variety of aldehydes under the optimized reaction conditions. The experimental results were summarized in Table 2.

In the addition reaction catalyzed by Schiff base ligand (*R*)-**3**, it was found that the electron-withdrawing substituent of the substrate benzaldehyde (e.g., chloro or bromo) decreased enantioselectivity (entries 2, 3) while electron-donating groups such as methoxy increased enantioselectivity (entry 4). However, the situation for 3-arylaminoethylBINOL ligand (*R*)-**6** was just opposite. The electron-withdrawing substituent was found to increase the enantioselectivity (entries 8, 9) while electron-donating group to decrease the enantioselectivity (entries 10, 11). The sterically hindered 1-naphthaldehyde gave the

best result (entry 12, 92% ee). In addition,  $\alpha,\beta$ -unsaturated cinnamaldehyde also gave 87% ee (entry 13).

In summary, we have prepared chiral BINOL Schiff bases (*R*)-**1**, (*R*)-**2**, (*R*)-**3** and their reductive products (*R*)-**4**, (*R*)-**5**, (*R*)-**6**. It was found that the six chiral BINOL ligands catalyze the asymmetric addition of diethylzinc to aldehydes giving secondary alcohols in high yield and good enantioselectivity. The (*R*)-**6**-Ti complex was found to be an effective catalyst in the asymmetric addition of diethylzinc to aldehydes.

## LITERATURE CITED

- Noyori R. Asymmetric catalysis in organic synthesis. New York: Wiley; 1994. Chapter 5.
- Noyori R, Kitamura M. Enantioselective addition of organometallic reagents to carbonyl compound: chirality transfer/multiplication and amplification. *Angew Chem Int Ed Engl* 1991;30:49–69.
- Soai K, Niwa S. Enantioselective addition of organozinc reagents to aldehydes. *Chem Rev* 1992;92:833–856.
- Paleo MR, Cabeza I, Sardina FJ. Enantioselective addition of diethylzinc to aldehydes catalyzed by *N*-(9-Phenylfluoren-9-yl)  $\beta$ -amino alcohols. *J Org Chem* 2000;65:2108–2113.
- Hanyu N, Mino T, Sakamoto M, Fujita T. Facile synthesis of amino bicyclo[2.2.1]heptyl alcohol and its application for enantioselective additions of diethylzinc to aldehydes. *Tetrahedron Lett* 2000;41:4587–4590.
- Hanyu N, Aoki T, Mino T, Sakamoto M, Fujita T. Enantioselective addition of diethylzinc to aldehydes catalyzed by optically active 1,4-aminoalcohols. *Tetrahedron: Asymmetry* 2000;11:2971–2979.
- Superchi S, Mecca T, Giorgio E, Rosini C. 1,1'-Binaphthylazepine-based ligands for asymmetric catalysis. II. New aminoalcohols as chiral ligands in the enantioselective addition of ZnEt<sub>2</sub> to aromatic aldehydes. *Tetrahedron: Asymmetry* 2001;12:1235–1239.
- Priego J, Mancheno OG, Cabrera S, Carretero JC. 2-Aminosubstituted 1-sulfinylferrocenes as chiral ligands in the addition of diethylzinc to aromatic aldehydes. *J Org Chem* 2002;67:1346–1353.
- Fontes M, Verdager X, Sola L, Pericas M, Riera A. 2-Piperidino-1,1,2-triphenylethanol: a highly effective catalyst for the enantioselective arylation of aldehydes. *J Org Chem* 2004;69:2532–2543.
- Heckel A, Seebach D. Immobilization of TADDOL with a high degree of loading on porous silica gel and first applications in enantioselective catalysis. *Angew Chem Int Ed* 2000;39:163–165.
- Fu B, Du DM, Wang JB. Synthesis of novel C<sub>2</sub>-symmetric chiral bis(oxazoline) ligands and their application in the enantioselective addition of diethylzinc to aldehydes. *Tetrahedron: Asymmetry* 2004;15:119–126.
- Schinnerl M, Seitz M, Kaiser A, Reiser O. Applications of bis(oxazoline) ligands in catalysis: asymmetric 1,2- and 1,4-addition of ZnR<sub>2</sub> to carbonyl compounds. *Org Lett* 2001;3:4259–4262.
- Niwa S, Soai K. Asymmetric synthesis using chiral piperazines. III. Enantioselective addition of dialkylzincs to aryl aldehydes catalysed by chiral piperazines. *J Chem Soc Perkin Trans 1* 1991;28:2717–2720.
- Conti S, Falorni M, Giacomelli G, Soccolini F. Chiral ligands containing heteroatoms. 10. 1-(2-pyridyl)alkylamines as chiral catalysts in the addition of diethylzinc to aldehydes: temperature dependence on the enantioselectivity. *Tetrahedron* 1992;48:8993–9000.
- Pu L. 1,1'-Binaphthyl dimers, oligomers, and polymers: molecular recognition, asymmetric catalysis, and new materials. *Chem Rev* 1998;98:2405–2494.
- Chen Y, Yekta S, Yudin AK. Modified BINOL ligands in asymmetric catalysis. *Chem Rev* 2003;103:3155–3212.
- Kořcovskú P, Vyskočil S, Smřčina M. Non-symmetrically substituted 1,1'-Binaphthyls in enantioselective catalysis. *Chem Rev* 2003;103:3213–3245.
- Brunel JM. BINOL: a versatile chiral reagent. *Chem Rev* 2005;105:857–897.

19. Mori M, Nakai T. Asymmetric catalytic alkylation of aldehydes with diethylzinc using a chiral binaphthol-titanium complex. *Tetrahedron Lett* 1997;38:6233–6236.
20. Zhang FY, Yip CW, Cao R, Chan ASC. Enantioselective addition of diethylzinc to aromatic aldehydes catalyzed by Ti(BINOL) complex. *Tetrahedron: Asymmetry* 1997;8:585–589.
21. Shen X, Guo H, Ding KL. The synthesis of a novel non-C<sub>2</sub> symmetric H<sub>4</sub>-BINOL ligand and its application to titanium-catalyzed enantioselective addition of diethylzinc to aldehydes. *Tetrahedron: Asymmetry* 2000;11:4321–4327.
22. Zhang FY, Chan ASC. Enantioselective addition of diethylzinc to aromatic aldehydes catalyzed by titanium-5,5',6,6',7,7',8,8'-octahydro-1,1'-bi-2-naphthol complex. *Tetrahedron: Asymmetry* 1997;8:3651–3655.
23. Matsui K, Takizawa S, Sasai H. Bifunctional organocatalysts for enantioselective aza-Morita-Baylis-Hillman reaction. *J Am Chem Soc* 2005;127:3680–3681.
24. Matsui K, Tanaka K, Horii A, Takizawa S, Sasai H. Conformational lock in a Brønsted acid-Lewis base organocatalyst for the aza-Morita-Baylis-Hillman reaction. *Tetrahedron: Asymmetry* 2006;17:578–583.
25. Yoshida T, Morimoto H, Kumagai N, Matsunaga S, Shibasaki M. Non-C<sub>2</sub>-symmetric, chirally economical, and readily tunable linked-binols: design and application in a direct catalytic asymmetric Mannich-Type reaction. *Angew Chem Int Ed* 2005;44:3470–3474.
26. Ihori Y, Yamashita Y, Ishitani H, Kobayashi S. Chiral zirconium catalysts using multidentate BINOL derivatives for catalytic enantioselective Mannich-Type reactions; ligand optimization and approaches to elucidation of the catalyst structure. *J Am Chem Soc* 2005;127:15528–15535.
27. Harada T, Kanda K. Enantioselective alkylation of aldehydes catalyzed by a highly active titanium complex of 3-substituted unsymmetric BINOL. *Org Lett* 2006;8:3817–3819.
28. Guo QS, Liu B, Lu YN, Jiang FY, Song HB, Li JS. Synthesis of 3 or 3,3'-substituted BINOL ligands and their application in the asymmetric addition of diethylzinc to aromatic aldehydes. *Tetrahedron: Asymmetry* 2005;16:3667–3671.
29. Guo QS, Lu YN, Liu B, Xiao J, Li JS. A facile synthesis of 3 or 3,3'-substituted binaphthols and their applications in the asymmetric addition of diethylzinc to aldehydes. *J Organomet Chem* 2006;691:1282–1287.
30. Lin J, Rajaram AR, Pu L. Enantioselective fluorescent recognition of chiral acids by 3- and 3,3'-aminomethyl substituted BINOLs. *Tetrahedron* 2004;60:11277–11281.
31. Dave R, Sasaki NA. Synthesis of chiral C/N-functionalized morpholine alcohols: study of their catalytic ability as ligand in asymmetric diethylzinc addition to aldehyde. *Tetrahedron: Asymmetry* 2006;17:388–401.
32. Dai WM, Zhu HJ, Hao XJ. Chiral ligands derived from abrine. VI. Importance of a bulky *N*-alkyl group in indole-containing chiral  $\beta$ -tertiary amino alcohols for controlling enantioselectivity in addition of diethylzinc toward aldehydes. *Tetrahedron: Asymmetry* 2000;11:2315–2337.

# $\alpha$ -Aminophosphonates as Novel Organocatalysts for Asymmetric Michael Addition of Carbonyl Compounds to Nitroolefins

QIN TAO, GUO TANG,\* KAN LIN, AND YU-FEN ZHAO

*Department of Chemistry and Key Laboratory for Chemical Biology of Fujian Province,  
College of Chemistry and Chemical Engineering, Xiamen University, Xiamen 361005, People's Republic of China*

**ABSTRACT** A cyclic  $\alpha$ -aminophosphonate was found to be a novel organocatalyst for Michael type addition reactions of carbonyl compounds to nitroolefins to afford the corresponding adducts in high enantio- and diastereoselectivities. *Chirality* 20:833–838, 2008. © 2008 Wiley-Liss, Inc.

**KEY WORDS:** asymmetric Michael addition;  $\alpha$ -aminophosphonate; cyclohexanone; aldehydes; nitroolefins

## INTRODUCTION

Asymmetric Michael addition to nitroalkenes has been developed as a powerful tool in organic synthesis, because of carbon-carbon bond-formation. Optically active nitroalkane Michael adducts are versatile building blocks for agricultural and pharmaceutical compounds.<sup>1,2</sup> Organocatalytic asymmetric Michael addition of ketones to nitroolefins, pioneered by List et al.<sup>3</sup> and Barbas and coworkers,<sup>4</sup> has attracted great attention. Pyrrolidine-pyridine,<sup>5</sup> pyrrolidine-thiourea, derivatives,<sup>6</sup> and fluoroupyrrolidine sulfonamide<sup>7</sup> and chiral diamine,<sup>8</sup> have also served as powerful asymmetric catalysts for such Michael additions. Herein, we wish to add a new example to these entries by revealing for the first time that readily available cyclic  $\alpha$ -aminophosphonates<sup>9–11</sup> can also serve as efficient catalysts for Michael addition.

There are many methods available to synthesize aminophosphonates.<sup>12–14</sup> These compounds are well studied as diverse and useful biological active reagents, but applications as organocatalysts for asymmetric Michael addition reactions have not been reported hitherto. Although they have been synthesized, there is only one report of cyclic  $\alpha$ -aminophosphonates as catalysts for an aldol reaction.<sup>15</sup> Given the importance of organocatalytic reactions, we believe the strategy described in this article may be useful for other processes.

Since cyclic  $\alpha$ -aminophosphonic acids are analogues of proline, the cyclic  $\alpha$ -aminophosphonates could be too. These, in turn, are highly enantioselective catalysts for direct asymmetric aldol reactions,<sup>16</sup> asymmetric Michael additions,<sup>17</sup> and Mannich reactions.<sup>18</sup> We envisaged that cyclic  $\alpha$ -aminophosphonates might be better than proline as catalysts for these reactions. First we investigated Michael addition reactions. The catalyst **II** was synthesized in three steps from (S)-phenylglycinol according to published procedures<sup>9</sup> and catalyst **I** by a modification thereof (Scheme 1).

## EXPERIMENTAL SECTION

### General

Silica gel (300–400 mesh) from Yantai Silica Gel Factory was used for chromatography. Optical rotation was measured on a Perkin-Elmer 341 automatic polarimeter. IR spectra were recorded on a Nicolet Avatar 360-IR. <sup>1</sup>H NMR and <sup>13</sup>C NMR spectra were recorded on a Bruker 400M instrument, and tetramethylsilane was used as internal standard. Data for <sup>1</sup>H NMR are reported as follows: chemical shift (ppm), and multiplicity (s singlet, d doublet, m multiplet). Enantiomeric excesses were determined by HPLC analysis using an Elite EC 2000 system with Chiralcel OD or Chiralpak AS-H columns.

### Material

Commercial reagents were used as received, unless otherwise stated. The *trans*-substituted nitroolefins were prepared by known procedures.<sup>19,20</sup>

**Preparation of catalysts I and II.** Catalyst **II** is known. Data are in agreement with previously reported results.<sup>9</sup> Catalyst **I** was prepared by a modification of **II**.

(3*S*,5*R*,7*aR*)-5-(Benzotriazol-1-yl)-3-phenyl[2,1-*b*]oxazolo-pyrrolidine (**1**): Prepared from (S)-2-amino-2-phenylethanol according to the literature procedures.<sup>9</sup>

Diisopropyl (3*S*,5*R*,7*aR*)-3-phenylhexahydropyrrolo[2,1-*b*]-[1,3]oxazol-5-yl phosphonate (**2**): To a solution of **1** (3.1 g,

This article contains supplementary material available via the Internet at <http://www.interscience.wiley.com/jpages/0899-0042/suppmat>.

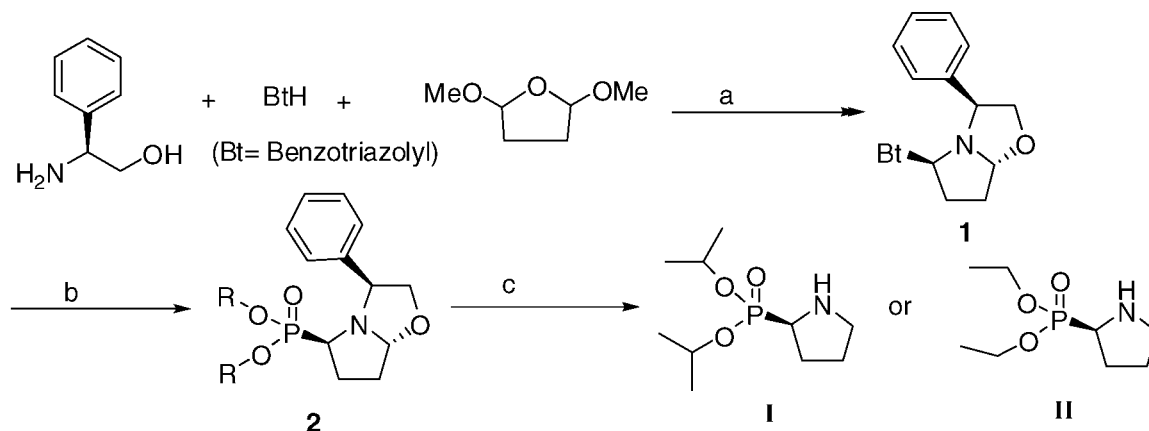
Contract grant sponsor: Chinese Ministry of Education Key Project; Contract grant numbers: 104201

\*Correspondence to: Guo Tang, Department of Chemistry and Key Laboratory for Chemical Biology of Fujian Province, College of Chemistry and Chemical Engineering, Xiamen University, Xiamen 361005, People's Republic of China. E-mail: t12g21@xmu.edu.cn

Received for publication 17 November 2007; Accepted 7 February 2008

DOI: 10.1002/chir.20552

Published online 1 April 2008 in Wiley InterScience ([www.interscience.wiley.com](http://www.interscience.wiley.com)).



Conditions: a.  $\text{CH}_2\text{Cl}_2$ , 24h.

b.  $\text{P}(\text{OR})_3$  (2 eq.),  $\text{ZnBr}_2$  (0.3 eq.),  $\text{CH}_2\text{Cl}_2$ ,  $0^\circ\text{C}$ , 20h. R = ethyl or isopropyl **2a**: R = isopropyl, **2b**: R = ethyl

c.  $\text{H}_2$ ,  $\text{Pd}(\text{OH})_2/\text{C}$ ,  $\text{HCl-EtOH}$ , 24h.

**Scheme 1.** Synthesis of catalysts **I** and **II**.

10 mmol) in dry  $\text{CH}_2\text{Cl}_2$  (200 ml) were added sequentially triisopropylphosphite (4.5 ml, 20 mmol) and  $\text{ZnBr}_2$  (1 mmol). The reaction mixture was stirred at  $0^\circ\text{C}$  for 20 h. The reaction was then quenched with 2 M NaOH, and the product was extracted with  $\text{CH}_2\text{Cl}_2$ . The combined organic extracts were washed with brine, dried with  $\text{Na}_2\text{SO}_4$ , and evaporated in vacuo. Column chromatography on silica gel, with hexane/EtOAc 2/1 as eluent, yielded 2.68 g (75%) of **2a** as a colorless oil.  $^1\text{H}$  NMR (400 MHz,  $\text{CDCl}_3$ ):  $\delta$  1.11 (d,  $J$  = 6.2 Hz, 3H), 1.18 (d,  $J$  = 6.2 Hz, 3H), 1.20 (d,  $J$  = 6.2 Hz, 3H), 1.25 (d,  $J$  = 6.2 Hz, 3H), 1.95–2.13 (m, 2H), 2.21–2.26 (m, 2H), 3.17–3.22 (dt,  $J$  = 2.7 Hz and 7.4 Hz, 1H), 3.64–3.67 (dd,  $J$  = 5.9 Hz and 8.4 Hz, 1H), 4.30–4.33 (dd,  $J$  = 7.1 Hz and 8.3 Hz, 1H), 4.43 (t,  $J$  = 6.5 Hz, 1H), 4.56–4.66 (m, 2H), 5.00–5.02 (m, 1H), 7.20–7.42 (m, 5H) ppm.  $^{13}\text{C}$  NMR ( $\text{CDCl}_3$ , 100 MHz):  $\delta$  23.7 ( $J$  = 5.2 Hz), 24.0 ( $J$  = 3.4 Hz and 8.0 Hz), 25.5, 30.3 ( $J$  = 7.4 Hz), 61.2, 63.7, 69.2 ( $J$  = 4.6 Hz), 70.2 ( $J$  = 7.6 Hz), 70.7 ( $J$  = 6.9 Hz), 72.2, 77.2 ( $J$  = 32.1 Hz), 99.0 ( $J$  = 16.2 Hz), 126.6, 126.8, 128.1, 142.3 ppm. IR (film): 3453, 2972, 2936, 2874, 1389, 1236, 1104, 992  $\text{cm}^{-1}$ . HRMS calcd for  $\text{C}_{18}\text{H}_{28}\text{NO}_4\text{P}$  = 354.1834 (M + H); found: 354.1932.  $[\alpha]_D^{20}$  = +58.44 ( $c$  = 0.9, EtOH).

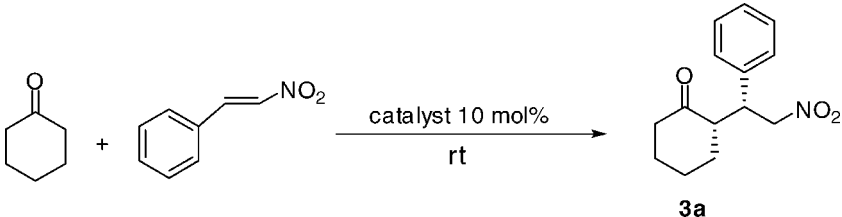
**Diisopropyl (2R)-tetrahydro-1H-pyrrol-2-ylphosphonate I:** A solution of starting material (1 mmol) in ethanol (60 ml) with 10%  $\text{Pd}(\text{OH})_2/\text{C}$  (50 mg) was charged with hydrogen at a pressure of 40 psi at rt for 24 h. After filtration of the catalyst, the filtrate was treated with HCl in EtOAc (2 M) and stirred at rt for 30 min. The solvent was concentrated in vacuo, and then neutralized with NaOH (1 M), and the aqueous suspension was extracted with  $\text{CH}_2\text{Cl}_2$ . The combined organic extracts were washed with brine, dried with  $\text{Na}_2\text{SO}_4$ , and evaporated in vacuo, and the residue purified by column chromatography using  $\text{CH}_2\text{Cl}_2/\text{MeOH}$  45/1 as eluent to give **I** in 85% yield as a yellow oil.  $^1\text{H}$  NMR ( $\text{CDCl}_3$ , 400 MHz):  $\delta$  1.33 (d,  $J$  = 6.2 Hz, 12H), 1.75–2.04 (m, 4H), 2.66 (br s, 1H), 2.90–2.96 (m, 1H), 3.05–3.10 (m, 1H), 3.26–3.31 (m, 1H), 4.71–4.80 (m, 2H)

ppm.  $^{13}\text{C}$  NMR ( $\text{CDCl}_3$ , 100 MHz):  $\delta$  23.9 ( $J$  = 4.2 Hz), 25.7 ( $J$  = 8.2 Hz), 26.7, 47.4 ( $J$  = 11.0 Hz), 53.5, 55.2, 70.3 ( $J$  = 8.2 Hz), 70.5 ( $J$  = 7.0 Hz) ppm. IR (film): 3438, 2977, 2873, 1385, 1230, 1107, 984  $\text{cm}^{-1}$ . HRMS calcd for  $\text{C}_{10}\text{H}_{22}\text{NO}_3\text{P}$  = 236.1416 (M + H); found: 236.1419.  $[\alpha]_D^{20}$  = –6.19 ( $c$  = 1.1, EtOH).

#### General procedure for the Michael addition reaction

Cyclohexanone (196 mg, 2 mmol) and catalyst **I** (7.62 mg, 0.02 mmol) in 0.2 mL of  $\text{CHCl}_3$  were stirred at rt for 20 min. Then *trans*- $\beta$ -nitrostyrene (29.8 mg, 0.2 mmol) was added and the resulting mixture was stirred at rt for 30 h. The reaction mixture was evaporated under vacuum, and then purified by column chromatography on silica gel, eluted by hexane/EtOAc = 10:1 then 5:1 to give the desired products **3a** (46.3 mg, 94%). The desired products as (S)-2-((R)-2-nitro-1-phenylethyl)cyclohexanone (**3a**),<sup>6,7</sup> (S)-2-((R)-1-(4-chlorophenyl)-2-nitroethyl)cyclohexanone (**3b**),<sup>7</sup> (S)-2-((R)-1-(2-chlorophenyl)-2-nitroethyl)cyclohexanone (**3c**),<sup>8</sup> (S)-2-((R)-1-(2,4-dichlorophenyl)-2-nitroethyl)cyclohexanone (**3d**),<sup>6</sup> (S)-2-((R)-1-(4-bromophenyl)-2-nitroethyl)cyclohexanone (**3e**),<sup>8</sup> (S)-2-((R)-1-(4-fluorophenyl)-2-nitroethyl)cyclohexanone (**3f**),<sup>8</sup> (S)-2-((R)-1-(2-methoxyphenyl)-2-nitroethyl)cyclohexanone (**3g**),<sup>7,8</sup> (S)-2-((S)-1-(furan-2-yl)-2-nitroethyl)cyclohexanone (**3h**),<sup>6</sup> (S)-2,2-dimethyl-4-nitro-3-phenylbutanal (**4a**)<sup>6,7</sup> (R)-2-ethyl-(S)-3-phenyl-4-nitrobutanal (**4b**)<sup>21</sup> are known.

**(R)-2-((S)-1-(4-bromophenyl)-2-nitroethyl)butanal 4c.** Yellow oil, dr = 3:1 (*syn:anti*), *ee* 96%.  $^1\text{H}$  NMR ( $\text{CDCl}_3$ , 400 MHz):  $\delta$  0.84 (t,  $J$  = 7.5 Hz, 3H), 1.48–1.54 (m, 2H), 2.64–2.70 (m, 1H), 3.77 (dt,  $J$  = 4.8, 9.9 Hz, 3H), 4.57–4.74 (m, 2H), 7.08–7.08 (m, 2H), 7.47–7.49 (m, 2H), 9.71 (d,  $J$  = 2.3 Hz, 1H) ppm. HRMS calcd for  $\text{C}_{12}\text{H}_{14}\text{BrNO}_3$  = 322.0055 (M + Na); found: 322.0062.  $[\alpha]_D^{20}$  = +10.20 ( $c$  = 1.2,  $\text{CHCl}_3$ ). The *ee* of the product was determined by HPLC analysis (Chiralcel OD, *i*-PrOH/

**TABLE 1.** Effects of solvents and different catalysts on asymmetric Michael addition reaction of cyclohexanone and *trans*- $\beta$ -nitrostyrene<sup>a</sup>


Entry	Catalyst	Solvent	Time (h)	Yield <sup>b</sup> (%)	Dr <sup>c</sup> ( <i>syn:anti</i> )	Ee <sup>c</sup> ( <i>syn</i> ) (%)
1	I	CHCl <sub>3</sub>	30	94	50:1	79
2	II	CHCl <sub>3</sub>	38	90	16:1	73
3	I	CH <sub>2</sub> Cl <sub>2</sub>	48	88	16:1	58
4	I	benzene	50	90	17:1	64
5	I	toluene	46	82	17:1	60
6	I	DMSO	40	—	—	—
7	I	H <sub>2</sub> O	40	—	—	—

<sup>a</sup>Cyclohexanone (2 mmol) and catalyst (0.02 mmol) in 0.2 ml solvent was stirred, then *trans*- $\beta$ -nitrostyrene (0.2 mmol) was added. The product was purified by column chromatography on silica gel, and the absolute configuration was determined by the comparison of the specific rotation of the product with literature data.

<sup>b</sup>Isolated yield after column chromatography.

<sup>c</sup>Determined by <sup>1</sup>H NMR.<sup>d</sup>Determined by chiral HPLC analysis (Chiralpak AS-H, *i*-PrOH/hexane = 10/90).<sup>6</sup>

hexane = 20/80, flow rate = 1.0 ml/min,  $\lambda_{\max}$  = 254 nm):  $t_{\min}$  = 15.37 min,  $t_{\max}$  = 14.05 min.

**(*R*)-2-((*S*)-2-nitro-1-phenylethyl)octanal 4d.** Pale yellow oil, dr = 13:1 (*syn:anti*), ee 82%. <sup>1</sup>H NMR (CDCl<sub>3</sub>, 400 MHz):  $\delta$  0.82 (t,  $J$  = 7.0 Hz, 3H), 1.11–1.40 (m, 10H), 2.66–2.73 (m, 1H), 3.77 (dt,  $J$  = 5.2, 9.7 Hz, 1H), 4.61–4.73 (m, 2H), 7.16–7.18 (m, 2H), 7.29–7.37 (m, 3H), 9.69 (d,  $J$  = 2.8 Hz, 1H) ppm. <sup>13</sup>C NMR (CDCl<sub>3</sub>, 100 MHz):  $\delta$  13.9, 22.4, 26.3, 27.3, 29.0, 29.1, 31.3, 31.7, 43.1, 53.9, 78.4, 128.0, 128.1, 129.1, 136.8, 203.2 ppm. HRMS calcd for C<sub>16</sub>H<sub>23</sub>NO<sub>3</sub> = 300.1576 (M + Na); found: 300.1580.  $[\alpha]_D^{20}$  = +29.23 ( $c$  = 1.3, CHCl<sub>3</sub>). The ee of the product was determined by HPLC analysis (Chiralcel OD, *i*-PrOH/hexane = 20/80, flow rate = 1.0 ml/min,  $\lambda_{\max}$  = 254 nm):  $t_{\min}$  = 10.08 min,  $t_{\max}$  = 11.44 min.

**(*R*)-2-((*S*)-1-(4-fluorophenyl)-2-nitroethyl)octanal 4e.** Pale yellow oil, dr = >99:1 (*syn:anti*), ee 87%. <sup>1</sup>H NMR (CDCl<sub>3</sub>, 400 MHz):  $\delta$  0.83 (t,  $J$  = 7.1 Hz, 3H), 1.12–1.39 (m, 10H), 2.65–2.70 (m, 1H), 3.77 (dt,  $J$  = 4.9, 9.9 Hz, 1H), 4.57–4.72 (m, 2H), 7.02–7.07 (m, 2H), 7.14–7.26 (m, 2H), 9.70 (d,  $J$  = 2.6 Hz, 1H) ppm. <sup>13</sup>C NMR (CDCl<sub>3</sub>, 100 MHz):  $\delta$  13.9, 22.4, 26.2, 27.3, 29.0, 31.3, 42.4, 53.8, 78.4, 116.0, 116.2, 129.6, 129.7, 132.5, 132.6, 202.9 ppm. HRMS calcd for C<sub>16</sub>H<sub>22</sub>FNO<sub>3</sub> = 318.1482 (M + Na); found: 318.1489.  $[\alpha]_D^{20}$  = +21.70 ( $c$  = 1.1, CHCl<sub>3</sub>). The ee of the product was determined by HPLC analysis (Chiralcel OD, *i*-PrOH/hexane = 20/80, flow rate = 1.0 ml/min,  $\lambda_{\max}$  = 254 nm):  $t_{\min}$  = 9.90 min,  $t_{\max}$  = 8.72 min.

**(*R*)-2-((*S*)-1-(4-methoxyphenyl)-2-nitroethyl)octanal 4f.** Yellow oil, dr = 17:1 (*syn:anti*), ee 80%. <sup>1</sup>H NMR (CDCl<sub>3</sub>, 400 MHz):  $\delta$  0.82 (t,  $J$  = 7.0 Hz, 3H), 1.12–1.36 (m, 10H), 2.61–2.68 (m, 1H), 3.72 (dt,  $J$  = 5.1, 9.6 Hz, 1H), 3.79 (s, 3H), 4.56–4.70 (m, 2H), 6.86–6.88 (m, 2H), 7.07–

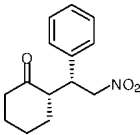
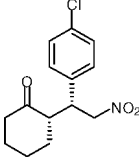
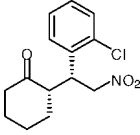
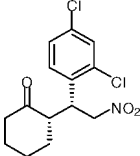
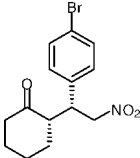
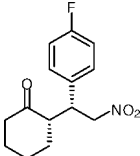
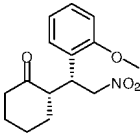
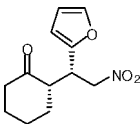
7.10 (m, 2H), 9.69 (d,  $J$  = 2.8 Hz, 1H) ppm. <sup>13</sup>C NMR (CDCl<sub>3</sub>, 100 MHz):  $\delta$  13.9, 22.4, 26.3, 27.3, 29.0, 31.3, 42.4, 54.0, 55.2, 78.7, 114.4, 128.5, 129.0, 159.2, 203.4 ppm. HRMS calcd for C<sub>17</sub>H<sub>25</sub>NO<sub>4</sub> = 330.1682 (M + Na); found: 330.1690.  $[\alpha]_D^{20}$  = +19.31 ( $c$  = 1.3, CHCl<sub>3</sub>). The ee of the product was determined by HPLC analysis (Chiralcel OD, *i*-PrOH/hexane = 10/90, flow rate = 1.0 ml/min,  $\lambda_{\max}$  = 254 nm):  $t_{\min}$  = 15.51 min,  $t_{\max}$  = 17.05 min.

## RESULTS AND DISCUSSION

Initially, using **I** and **II** (10 mol%) as catalysts for cyclohexanone and *trans*- $\beta$ -nitrostyrene, as shown in this article (Table 1), catalyst **I** has better effects both in diastereo- and enantioselectivity, so **I** was adopted by us. Various solvents were examined at room temperature, in strong polar solvents such as DMSO (entry 6) and water (entry 7), traces of the desired products were detected after 40 h, but in less polar solvents such as chloroform, the reactions gave high yields, good stereoselectivity, and needed less time. However, in less polar solvents such as benzene, toluene and dichloromethane, the stereoselectivities declined.

To test the catalytic activity of this cyclic  $\alpha$ -amino-phosphonate, Michael addition reactions were carried out between cyclohexanone and a wide range of nitroolefins as substrates (Table 2). The reaction conditions shown for the reactions in Table 1 were used, with **I** as catalyst and CHCl<sub>3</sub> as solvent. As shown here, these reactions proceeded efficiently (85–97% yields), with high enantio- and diastereo-selectivities (up to 79% and >99:1, respectively). *trans*- $\beta$ -Nitroolefins having functionalities such as a halogen atom (entries 2–6), or methoxy group (entry 7) on the benzene ring and heterocyclic groups (entry 8), could be used in this catalytic process.

**TABLE 2. Cyclic  $\alpha$ -aminophosphonate-catalyzed I Michael addition reaction of cyclohexanone to nitroolefins**

Entry	Product	Time (h)	Yield <sup>a</sup> (%)	Dr <sup>b</sup> ( <i>syn:anti</i> )	Ee <sup>c</sup> ( <i>syn</i> ) (%)
1	 <p><b>3a</b></p>	30	94	50:1	79
2	 <p><b>3b</b></p>	24	97	33:1	72
3	 <p><b>3c</b></p>	32	86	>99:1	66
4	 <p><b>3d</b></p>	26	95	>99:1	72
5	 <p><b>3e</b></p>	30	88	17:1	71
6	 <p><b>3f</b></p>	28	91	25:1	64
7	 <p><b>3g</b></p>	30	90	>99:1	61
8	 <p><b>3h</b></p>	28	85	10:1	44

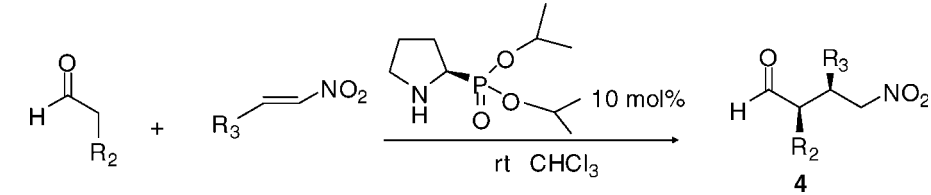
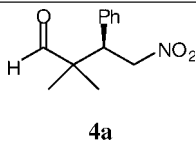
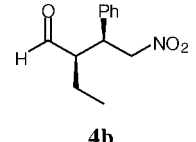
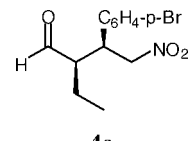
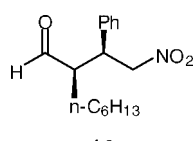
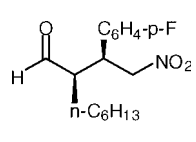
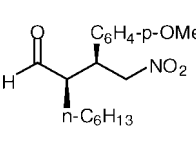
<sup>a</sup>Isolated yield after column chromatography.

<sup>b</sup>Determined by <sup>1</sup>H NMR.

<sup>c</sup>Determined by chiral HPLC analysis (Chiralpak AS-H, *i*-PrOH/hexane = 10/90).<sup>6,8</sup>



**TABLE 3.** Effects of donor structure cyclic  $\alpha$ -aminophosphonate-catalyzed Michael addition reaction of aldehydes and nitroolefins

					
Entry	Product	Time (h)	Yield <sup>a</sup> (%)	Dr <sup>b</sup> ( <i>syn:anti</i> )	Ee <sup>c</sup> ( <i>syn</i> ) (%)
1	 4a	30	78	–	91 <sup>d</sup>
2	 4b	24	80	6:1	87
3	 4c	26	78	3:1	96
4	 4d	26	81	13:1	82
5	 4e	28	78	>99:1	87
6	 4f	28	75	17:1	80

<sup>a</sup>Isolated yield after column chromatography.<sup>b</sup>Determined by <sup>1</sup>H NMR.<sup>c</sup>Determined by chiral HPLC analysis (Chiralpak OD, *i*-PrOH/hexane = 15/85 or 20/80, flow rate = 1 ml/min,  $\lambda_{\text{max}}$  = 254 nm).<sup>d</sup>Determined by chiral HPLC analysis (Chiralpak AS *i*-PrOH/hexane = 10/90).<sup>6</sup>

In addition to cyclohexanone, aldehydes could also be used successfully as substrates in the above reaction (Table 3),<sup>21–24</sup> to afford the corresponding adducts in high yields with high stereoselectivities. Interestingly, we noticed that the diastereoselectivity improved as the alkyl chain becomes longer (entries 2 and 4). Good selectivities were obtained with both halogen (entries 3 and 5) and methoxy (entry 6) on the benzene ring.

To account for the present enantio- and diastereo-selective Michael addition reactions, there are two cases to con-

sider. With cyclohexanone, the *si* face of the enamine is shielded, therefore the reaction takes place on the *re* face, to give 2*S* stereochemistry in the product. According to Seebach's model,<sup>25–31</sup> the nitroolefin approaches the enamine in a synclinal fashion, due to the favorable electrostatic interactions between the partially positive nitrogen atom of the enamine in the transition state and the partially positive nitro group. Thus the (*R*)-1-configuration is obtained and the product therefore has *syn* stereochemistry. With aldehydes the less hindered face of the enam-

ine is the *si* face, which is approached by the nitroolefin to give the observed stereochemistry, the result is similar to reports by Barbas and coworkers<sup>4</sup> and Hayashi et al.<sup>32</sup>

We have reported for the first time that versatile cyclic  $\alpha$ -aminophosphonates could be used as catalysts in the asymmetric Michael addition of cyclohexanone to nitroolefins to give high yield of the corresponding adducts with good diastereoselectivity, and aldehydes give excellent enantioselectivity. Ongoing studies using other amino-phosphinates as organocatalysts and applications to Mannich reactions are now in progress.

## LITERATURE CITED

- Kranse N, Hoffmann-Röder A. Recent advances in catalytic enantioselective Michael additions. *Synthesis* 2001;2:171–196.
- Sulzer-Mossé S, Alexakis A. Chiral amines as organocatalysts for asymmetric conjugate addition to nitroolefins and vinyl sulfones *via* enamine activation. *Chem Commun* 2007;3123–3135.
- List B, Pojarliev P, Martin HJ. Efficient proline-catalyzed Michael additions of unmodified ketones to nitro olefins. *Org Lett* 2001;3:2423–2425.
- Betancort JM, Barbas CF III. Catalytic direct asymmetric Michael reactions: taming naked aldehyde donors. *Org Lett* 2001;3:3737–3740.
- Ishii T, Fujioka S, Sekiguchi Y, Kotsuki H. A new class of chiral pyrrolidine-pyridine conjugate base catalysts for use in asymmetric Michael addition reactions. *J Am Chem Soc* 2004;126:9558–9559.
- Cao CL, Ye MC, Sun XL, Tang Y. Pyrrolidine-thiourea as a bifunctional organocatalyst: highly enantioselective Michael addition of cyclohexanone to nitroolefins. *Org Lett* 2006;8:2901–2904.
- Zu L, Wang J, Li H, Wang W. A recyclable fluororous (S)-pyrrolidine sulfonamide promoted direct, highly enantioselective Michael addition of ketones and aldehydes to nitroolefins in water. *Org Lett* 2006;8:3077–3079.
- Vishnumaya, Singh VK. Highly enantioselective water-compatible organocatalyst for Michael reaction of ketones to nitroolefins. *Org Lett* 2007;9:1117–1119.
- Katritzky AR, Cui XL, Yang BZ, Steel PJ. Asymmetric syntheses of 2-substituted and 2,5-disubstituted pyrrolidines from (3*S*,5*R*,7*aR*)-5-(benzotriazol-1-yl)-3-phenyl-2,1-*b*-oxazopyrrolidine. *J Org Chem* 1999;64:1979–1985.
- Kaname M, Mashige H, and Yoshifuji Shigeyuki. Chemical conversion of cyclic  $\alpha$ -amino acids to cyclic  $\alpha$ -aminophosphonic acids. *Chem Pharm Bull* 2001;49:531–536.
- Kaname M, Arakawa Y, Yoshifuji S. Synthesis of novel (*R*)- and (*S*)-piperidine-3-phosphonic acids and transformation into (*R*)- and (*S*)-pyrrolidine-2-phosphonic acids. *Tetrahedron Lett* 2001;42:2713–2716.
- Kukhar VP, Hudson HR. *Aminophosphonic and aminophosphinic acids*. Chichester: Wiley; 2000. 660 p.
- Kolodiaznyi OI. Asymmetric synthesis of organophosphorus compounds. *Tetrahedron Asymmetry* 1998;9:1279–1332.
- Kukhar VP, Soloshonok VA, Solodenko VA. Asymmetric synthesis of phosphorus analogs of amino acids. *Phosphorus Sulfur Silicon* 1994;92:239–264.
- Dinér P, Amedjkouh M. Aminophosphonates as organocatalysts in the direct asymmetric aldol reaction: towards *syn* selectivity in the presence of Lewis bases. *Org Biomol Chem* 2006;4:2091–2906.
- Sakthivel K, Notz W, Bui T, Barbas CF III. Amino acid catalyzed direct asymmetric aldol reactions: a bioorganic approach to catalytic asymmetric carbon-carbon bond-forming reactions. *J Am Chem Soc* 2001;123:5260–5267.
- Hanessian S, Pham V. Catalytic asymmetric conjugate addition of nitroalkanes to cycloalkenones. *Org Lett* 2000;2:2975–2978.
- Cordova A, Notz W, Zhong G, Betancort JM, Barbas CF III. A highly enantioselective amino acid-catalyzed route to functionalized  $\alpha$ -amino acids. *J Am Chem Soc* 2002;124:1842–1843.
- Jang YJ, Shih YK, Liu JY, Kuo WY, Yao CF. Improved one-pot synthesis of styryl tetrahydrofurans and cyclohexanes by radical addition to  $\beta$ -nitrostyrenes in the presence of benzoyl peroxide. *Chem—Eur J* 2003;9:2123–2128.
- Kumaran G, Kulkarni GH. Effect of the  $\alpha$ -alkyl substituent of conjugated nitroolefins on the formation of cyclic nitronic esters vs. nitrocyclopropanes in their reaction with sulfur ylides. *Synthesis* 1995;1545–1548.
- Li Y, Liu XY, Zhao G. Effective and recyclable dendritic catalysts for the direct asymmetric Michael addition of aldehydes to nitrostyrenes. *Tetrahedron Asymmetry* 2006;17:2034–2039.
- Zu LS, Li H, Wang J, Yu XH, Wang W. Highly enantioselective aldehyde-nitroolefin Michael addition reactions catalyzed by recyclable fluororous (S) diphenylpyrrolinol silyl ether. *Tetrahedron Lett* 2006;47:5131–5134.
- Albertshofer K, Thayumanavan R, Utsumi N, Tanaka F, Barbas CF III. Amine-catalyzed Michael reactions of an aminoaldehyde derivative to nitroolefins. *Tetrahedron Lett* 2007;48:693–696.
- Barros MT, Phillips AMF. Chiral piperazines as efficient catalysts for the asymmetric Michael addition of aldehydes to nitroalkenes. *Eur J Org Chem* 2007;178–185.
- Seebach D, Golinski J. Synthesis of open-chain 2,3-disubstituted 4-nitroketones by diastereoselective Michael-addition of (*e*)-enamines to (*e*)-nitroolefins. A topological rule for C, C-bond forming processes between prochiral centres. *Helv Chim Acta* 1981;64:1413–1423.
- Blarer SJ, Schweizer WB, Seebach D. Asymmetrische Michael-Additionen. Praktisch vollständigdiastereo- und enantioselective Alkylierungen des Enamins aus Cyclohexanon und Prolinylmethyläther durch  $\omega$ -Nitrostyrole zu u-2-(1'-Aryl-2'-nitroäthyl)cyclohexanon. *Helv Chim Acta* 1982;65:1637–1654.
- Blarer SJ, Seebach D. Asymmetrische Michael-Additionen. Stereoselektive Alkylierungen des (*R*)- und (*S*)-Enamins aus Cyclohexanon und 2-(Methoxymethyl)pyrrolidin durch  $\alpha$ -(Methoxycarbonyl)zimtsäure-methylester. *Chem Ber* 1983;116:2250–2260.
- Blarer SJ, Seebach D. Asymmetrische Michael-Additionen. Regio-, diastereo- und enantioselective Alkylierungen der Enamine aus  $\beta$ -Tetralonen und (*S*)-2-(Methoxymethyl) pyrrolidin (“Prolinolmethylether”) durch  $\omega$ -Nitrostyrole. *Chem Ber* 1983;116:3086–3096.
- Seebach D, Beck AK, Golinski J, Hay JN, Laube T. Über den sterischen Verlauf der Umsetzung von Enaminen aus offenkettigen Aldehyden und Ketonen mit Nitroolefinen zu 2,3-disubstituierten 4-Nitroketonen. *Helv Chim Acta* 1985;68:162–172.
- Seebach D, Brook MA. Reversed stereochemical course of the Michael addition of cyclohexanone to  $\beta$ -nitrostyrenes by using 1-(trimethylsiloxy)cyclohexene/dichloro(diisopropoxy)titanium. *Helv Chim Acta* 1985;68:319–324.
- Seebach D, Missbach M, Calderari G, Eberle M. [3 + 3]-Carbocyclizations of nitroallylic esters and enamines with stereoselective formation of up to six new stereogenic centers. *J Am Chem Soc* 1990;112:7625–7638.
- Hayashi Y, Gotoh H, Hayashi T, Shoji M. Diphenylprolinol silyl ethers as efficient organocatalysts for the asymmetric Michael reaction of aldehydes and nitroalkenes. *Angew Chem Int Ed* 2005;44:4212–4215.

# Synthesis and Application of Chiral $\beta$ -Amino Disulfides as Ligands for the Enantioselective Addition of Diethylzinc to Aldehydes

ANTONIO L. BRAGA,<sup>1\*</sup> FÁBIO Z. GALETTO,<sup>1</sup> OSCAR E. D. RODRIGUES,<sup>2</sup> CLAUDIO C. SILVEIRA,<sup>1</sup> AND MARCIO W. PAIXÃO<sup>3</sup>

<sup>1</sup>*Departamento de Química, Universidade Federal de Santa Maria, Santa Maria, RS, Brazil*

<sup>2</sup>*Centro Universitário Franciscano, Santa Maria, RS, Brazil*

<sup>3</sup>*Instituto de Química, Universidade de São Paulo, São Paulo, SP, Brazil*

**ABSTRACT** A new class of chiral  $\beta$ -amino disulfides was synthesized from readily available and inexpensive starting materials by a straightforward method and their abilities as ligands were examined in the enantioselective addition of diethylzinc to aldehydes. Enantiomeric excesses of up to 99% have been obtained using 0.5 mol % of the chiral catalysts. *Chirality* 20:839–845, 2008. © 2008 Wiley-Liss, Inc.

**KEY WORDS:** asymmetric catalysis; chiral ligands; thiols; sulfur; zinc

## INTRODUCTION

Addition of organometallic reagents to carbonyl compounds is one of the most common and fundamental reactions for the formation of carbon–carbon bonds, and the asymmetric version of this reaction is particularly useful for generating optically active secondary alcohols.<sup>1–3</sup> The importance of this structural feature arises mainly from the fact that it is part of many natural products or precursors as an important synthetic intermediate for various other functionalities, e.g., amine, halide, ester, and ether. Concerning this subject, several highly stereoselective additions to prochiral aldehydes have been reported,<sup>4–8</sup> and among the various organometallic compounds,<sup>9,10</sup> di-organozincs serve as excellent alkyl nucleophiles.<sup>11–17</sup> The development and functional understanding of chiral ligands for catalytic asymmetric synthesis is of increasing importance in modern synthetic chemistry; and in particular, the addition of diethylzinc to aldehydes has become a classical test to design new ligands for asymmetric catalysis.<sup>1</sup> Chiral  $\beta$ -amino alcohols are often used as ligands in this reaction<sup>18–24</sup> because of its easy access normally direct from the respective amino acids. Rationalizations about the stereoselectivity in asymmetric addition of dialkylzinc reagents to aldehydes using these ligands as model were performed by various research groups, giving an important tool to understand mechanistically the way and to improve the development of new classes of chiral catalysts.<sup>25</sup>

In the last few years, a significant improvement in enantioselectivity has been observed by the use of amino sulfur or selenium moieties as catalysts for the enantioselective addition of diethylzinc to aldehydes.<sup>26–32</sup> Sulfur containing ligands<sup>33</sup> like  $\beta$ -amino thiols and  $\beta$ -amino disulfides derivatives from ephedrine,<sup>34–36</sup> norephedrine,<sup>37–39</sup> (S)-proline,<sup>40–42</sup> (S)-phenylglycine,<sup>43</sup> (S)-valine,<sup>44,45</sup> (R)-cysteine,<sup>5,46–50</sup> (R)-cystine,<sup>51</sup> and others<sup>52–58</sup> have gained more and more interest as catalysts in this stereoselective reac-

tion. In a similar way, chiral amino diselenides have been efficiently used as catalysts for this addition,<sup>28–32</sup> but due to the most difficult accessibility of these compounds, only a few number of reports can be found in literature.

As part of our broader program to explore the preparation and use of chiral organochalcogen compounds in asymmetric catalysis,<sup>59–64</sup> especially ligands binding via sulfur or selenium, we describe in this article the development of a new class of [S, N]-ligands in a straightforward synthetic route, using inexpensive and easily available starting materials and their application as chiral ligands in the enantioselective addition of diethylzinc to aldehydes.

## EXPERIMENTAL SECTION

### General Procedures

Melting Points are uncorrected. Optical rotations were measured on a Perkin-Elmer 341 Polarimeter. <sup>1</sup>H and <sup>13</sup>C NMR spectra were recorded at 400 and 100 MHz, respectively, with tetramethylsilane as internal standard. High-resolution mass spectra were recorded on a Bruker BioApex 70 eV spectrometer. Gas chromatography (GC) was performed using a Varian 3800 gas chromatograph with Hydrodex  $\beta$ -3P column. HPLC analyses were carried out on a Shimadzu SCL-10 Avp chromatograph using a Diacel Chiralcel OD column; solvent, 99:1 hexane/isopropanol; flow rate 0.5 mL/min; 254 nm detection. Column chromatography was performed using Merck Silica Gel (230–400 mesh) following the methods described by Still et al.<sup>65</sup> Thin layer chromatography (TLC) was performed using

Contract grant sponsors: CAPES, CNPq and FAPERGS.

\*Correspondence to: Antonio L. Braga, Departamento de Química, Universidade Federal de Santa Maria, 97105-900 Santa Maria, RS, Brazil.

E-mail: albraga@quimica.ufsm.br

Received for publication 2 November 2007; Accepted 1 February 2008

DOI: 10.1002/chir.20554

Published online 1 April 2008 in Wiley InterScience (www.interscience.wiley.com).

Merck Silica Gel GF<sub>254</sub>, 0.25 mm thickness. For visualization, TLC plates were either placed under ultraviolet light, or stained with iodine vapor, or acidic vanillin. Most reactions were monitored by TLC for disappearance of starting material. The following solvents were dried and purified by distillation from the reagents indicated: tetrahydrofuran from sodium with a benzophenone ketyl indicator; dichloromethane from calcium hydride; acetonitrile from phosphorus pentoxide. All other solvents were ACS or HPLC grade unless otherwise noted. Air- and moisture-sensitive reactions were conducted in flame-dried or oven dried glassware equipped with tightly fitted rubber septa and under a positive atmosphere of dry argon. Reagents and solvents were handled using standard syringe techniques. Temperatures above room temperature were maintained by use of a mineral oil bath with an electrically heated coil connected to a Variac controller.

**General procedure for the synthesis of amino disulfides 4.** In a 50-mL round-bottomed flask with a reflux condenser, under an argon atmosphere, lithium disulfide was generated by reaction of elemental sulfur (0.0384 g, 1.2 mmol) with lithium triethylborohydride (1 M in THF, 1.2 mL, 1.2 mmol) in dry THF (5 mL). The suspension was heated at reflux and stirred for at least 20 min, and a THF (10 mL) solution of aziridine **2** (1.0 mmol) was added drop wise within 20 min. The resulting solution was stirred for 12 h at room temperature. The mixture was quenched with a saturated NH<sub>4</sub>Cl solution (20 mL), extracted with CH<sub>2</sub>Cl<sub>2</sub> and the combined organic fractions were collected, dried over MgSO<sub>4</sub> and filtered; the solvent was then removed in vacuo yielding crude products **4a–d**, which were purified by flash chromatography (Hexane:ethyl acetate 90:10).

**$\beta$ -Amino disulfide 4a.** Yield: 0.447 g (84%). White solid. m.p. 144–146°C.  $[\alpha]_D^{20} = -11$  ( $c = 1.0$ , CH<sub>2</sub>Cl<sub>2</sub>). <sup>1</sup>H NMR (400 MHz, CDCl<sub>3</sub>):  $\delta = 7.30$ – $7.18$  (m, 10 H), 4.94–4.92 (m, 2 H), 4.12–4.09 (m, 2 H), 2.91–2.81 (m, 8 H), 1.42 (s, 18 H) ppm. <sup>13</sup>C NMR (100 MHz, CDCl<sub>3</sub>):  $\delta = 155.2$ , 137.5, 129.3, 128.4, 126.5, 79.4, 51.1, 43.4, 38.8, 28.3 ppm. HRMS (ESI): calcd for C<sub>28</sub>H<sub>40</sub>N<sub>2</sub>NaO<sub>4</sub>S<sub>2</sub> [M + Na]<sup>+</sup> 555.232722; found 555.232721. The enantiomeric purity was determined by HPLC analysis (column, Chiralcel-OD; eluent, hexane/2-propanol 98:02; flow rate, 1 mL/min; *R* isomer,  $t_R = 16.3$  min, *S* isomer,  $t_R = 17.2$  min) and found to be >99.9%.

**$\beta$ -Amino disulfide 4b.** Yield: 0.345 g (79%). White solid. m.p. 104–105°C.  $[\alpha]_D^{20} = +69$  ( $c = 1.0$ , CH<sub>2</sub>Cl<sub>2</sub>). <sup>1</sup>H NMR (400 MHz, CDCl<sub>3</sub>):  $\delta = 4.78$ – $4.76$  (m, 2 H), 3.69–3.67 (m, 2 H), 2.90–2.89 (m, 4 H), 1.94–1.90 (m, 2 H), 1.44 (s, 18 H), 0.96 (d,  $J = 8.2$  Hz, 6 H), 0.92 (d,  $J = 8.2$  Hz, 6 H) ppm. <sup>13</sup>C NMR (100 MHz, CDCl<sub>3</sub>):  $\delta = 155.8$ , 79.2, 55.4, 42.8, 32.5, 30.8, 19.5, 17.7 ppm. HRMS (ESI): calcd for C<sub>20</sub>H<sub>40</sub>N<sub>2</sub>NaO<sub>4</sub>S<sub>2</sub> [M + Na]<sup>+</sup> 459.232722; found 459.232721.

**$\beta$ -Amino disulfide 4c.** Yield: 0.362 g (78%). White solid. m.p. 67–69°C.  $[\alpha]_D^{20} = -37$  ( $c = 1.0$ , CH<sub>2</sub>Cl<sub>2</sub>). <sup>1</sup>H NMR (400 MHz, CDCl<sub>3</sub>):  $\delta = 4.95$ – $4.91$  (m, 2 H), 3.91–3.87 (m, 2 H), 2.82–2.81 (m, 2 H), 2.79–2.78 (m, 2 H),

1.70–1.67 (m, 2 H), 1.44 (s, 22 H), 0.94 (d,  $J = 9.4$  Hz, 12 H) ppm. <sup>13</sup>C NMR (100 MHz, CDCl<sub>3</sub>):  $\delta = 155.4$ , 79.1, 48.3, 45.2, 42.9, 28.4, 25.0, 23.1, 22.0 ppm. HRMS (ESI): calcd for C<sub>22</sub>H<sub>44</sub>N<sub>2</sub>NaO<sub>4</sub>S<sub>2</sub> [M + Na]<sup>+</sup> 487.264022; found 487.265880.

**$\beta$ -Amino disulfide 4d.** Yield: 0.371 g (80%). White solid. m.p. 70–72°C.  $[\alpha]_D^{20} = +10$  ( $c = 1.0$ , CH<sub>2</sub>Cl<sub>2</sub>). <sup>1</sup>H NMR (400 MHz, CDCl<sub>3</sub>):  $\delta = 4.79$ – $4.76$  (m, 2 H), 3.75–3.72 (m, 2 H), 2.99–2.89 (m, 4 H), 1.66–1.64 (m, 2 H), 1.45 (s, 18 H), 1.12–1.10 (m, 4 H), 0.93–0.89 (m, 12 H) ppm. <sup>13</sup>C NMR (100 MHz, CDCl<sub>3</sub>):  $\delta = 155.6$ , 79.1, 54.3, 42.3, 37.2, 28.4, 24.9, 15.4, 11.5 ppm. HRMS (ESI): calcd for C<sub>22</sub>H<sub>44</sub>N<sub>2</sub>NaO<sub>4</sub>S<sub>2</sub> [M + Na]<sup>+</sup> 487.264022; found 487.265879.

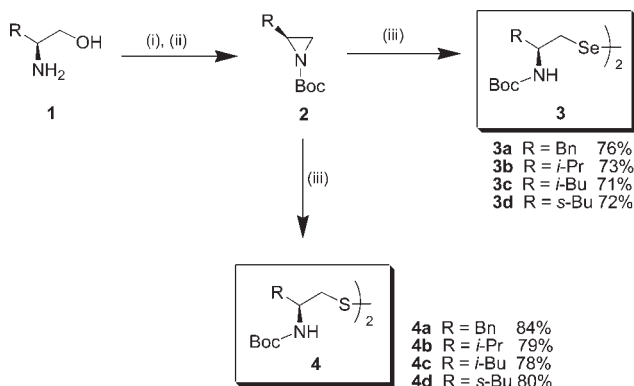
**Procedure for the synthesis of thioether 6.** In a 25-mL round-bottomed flask, under argon atmosphere, the thiolate anion was generated by the reaction of diethyl disulfide (0.0734 g, 0.6 mmol) with NaBH<sub>4</sub> (0.057 g, 1.5 mmol) in a mixture of THF (1.5 mL) and EtOH (0.5 mL). The suspension was allowed to stir for at least 20 min, and a THF (10 mL) solution of aziridine **2a** (0.233 g, 1.0 mmol) was added drop wise within 20 min. The resulting solution was stirred for 12 h at room temperature. The mixture was quenched with a saturated NH<sub>4</sub>Cl solution (20 mL), extracted with CH<sub>2</sub>Cl<sub>2</sub> and the combined organic fractions were collected, dried over MgSO<sub>4</sub> and filtered; the solvent was then removed in vacuo yielding crude thioether **6**, which was purified by flash chromatography (Hexane:ethyl acetate, 90:10). Yield: 0.220 g (75%) Spectral data consistent with those reported in the literature.<sup>66</sup>

**General procedure for the enantioselective addition of diethylzinc to aldehydes.** In a 25-mL round-bottomed flask, a solution of toluene (7 mL), aldehyde (1.0 mmol), and the ligand **4a–d** (0.5 mol%, 12.5  $\mu$ mol) was stirred for 30 min at room temperature. Diethylzinc (1 M in hexane, 2.5 mL, 2.5 mmol) was slowly injected and stirring was continued for 24 h at room temperature. Cooling (0°C) of the reaction mixture was followed by the slow addition of HCl (aq, 1 M, 5 mL). The organic layer was separated and washed again with HCl (aq, 1 M, 3 mL). Drying with MgSO<sub>4</sub>, filtration, and evaporation of the solvent in vacuo yielded the crude secondary alcohols. Purification was performed by bulb-to-bulb distillation under reduced pressure (ca. 0.1 mbar).

**(*R*)-1-phenylpropan-1-ol.** Yield: 0.122 g (90%). <sup>1</sup>H NMR (400 MHz, CDCl<sub>3</sub>):  $\delta = 7.32$ – $7.13$  (m, 5 H), 4.54 (t,  $J = 6.6$  Hz, 1 H), 1.87–1.67 (m, 2 H), 0.85 (t,  $J = 7.4$  Hz, 3 H) ppm. <sup>13</sup>C NMR (100 MHz, CDCl<sub>3</sub>):  $\delta = 144.5$ , 128.3, 127.3, 125.9, 75.9, 31.8, 10.0 ppm.

**(*R*)-1-(2-methoxyphenyl)propan-1-ol.** Yield: 0.133 g (80%). <sup>1</sup>H NMR (400 MHz, CDCl<sub>3</sub>):  $\delta = 7.30$ – $7.13$  (m, 2 H), 6.69–6.67 (m, 2 H), 4.77 (t,  $J = 6.4$  Hz, 1 H), 3.75 (s, 3 H), 2.94 (m, 1 H), 1.75 (q,  $J = 7$  Hz, 2 H), 0.91 (t,  $J = 7.4$  Hz, 3 H) ppm. <sup>13</sup>C NMR (100 MHz, CDCl<sub>3</sub>):  $\delta = 156.2$ , 132.3, 127.8, 126.7, 120.4, 110.2, 71.5, 30.0, 10.2 ppm.

**(*R*)-1-(4-methoxyphenyl)propan-1-ol.** Yield: 0.125 g (75%). <sup>1</sup>H NMR (400 MHz, CDCl<sub>3</sub>):  $\delta = 7.29$ – $7.01$  (m, 4



**Scheme 1.** Synthesis of  $\beta$ -amino diselenides **3** and  $\beta$ -amino disulfides **4** reagents and conditions: (I)  $\text{Boc}_2\text{O}$ ,  $\text{CH}_3\text{CN}$ , r.t., 3 h; (II) KOH, TSCl, THF, reflux, 4 h; (III)  $\text{Li}_2\text{Se}_2$  or  $\text{Li}_2\text{S}_2$ , THF, r.t., 12 h.

H), 4.35 (t,  $J = 6.1$  Hz, 1 H), 3.55 (s, 3 H), 1.85–1.63 (m, 2 H), 0.91 (t,  $J = 7.0$  Hz, 3 H) ppm.  $^{13}\text{C}$  NMR (100 MHz,  $\text{CDCl}_3$ ):  $\delta = 158.4, 137.9, 128.9, 113.4, 75.3, 55.1, 31.9, 10.0$  ppm.

**(*R*)-1-(pyridin-2-yl)propan-1-ol.** Yield: 0.107 g (78%).  $^1\text{H}$  NMR (400 MHz,  $\text{CDCl}_3$ ):  $\delta = 8.47$  (m, 1 H), 7.57–7.01 (m, 3 H), 4.65 (t,  $J = 5.7$  Hz, 1 H), 1.93–1.75 (m, 2 H), 1.12–0.87 (m, 3 H) ppm.  $^{13}\text{C}$  NMR (100 MHz,  $\text{CDCl}_3$ ):  $\delta = 162.1, 150.1, 137.0, 122.6, 122.1, 79.1, 31.6, 10.0$  ppm.

**(*R*)-dodecan-3-ol.** Yield: 0.100 g (54%).  $^1\text{H}$  NMR (400 MHz,  $\text{CDCl}_3$ ):  $\delta = 3.35$ – $3.29$  (m, 1 H), 1.48–1.19 (m, 19 H), 0.91–0.86 (m, 6 H) ppm.  $^{13}\text{C}$  NMR (100 MHz,  $\text{CDCl}_3$ ):  $\delta = 70.5, 36.8, 31.9, 31.5, 30.1, 29.6, 29.5, 29.4, 25.2, 22.7, 14.2, 10.2$  ppm.

**(*R*)-octan-3-ol.** Yield: 0.066 g (51%).  $^1\text{H}$  NMR (400 MHz,  $\text{CDCl}_3$ ):  $\delta = 3.65$ – $3.51$  (m, 1 H), 1.59–1.23 (m, 10 H), 1.09–0.86 (m, 6 H) ppm.  $^{13}\text{C}$  NMR (100 MHz,  $\text{CDCl}_3$ ):  $\delta = 73.2, 36.8, 31.9, 30.0, 25.3, 22.6, 13.9, 9.8$  ppm.

#### Conditions for the Analysis of Chiral Secondary Alcohols

**Chiral capillary GC.** Hydrodex  $\beta$ -3P column 25 m  $\times$  0.25 mm. Carrier gas,  $\text{H}_2$  (5 mL/min); detector, FID, 280°C; injector, 220°C.

**Chiral HPLC.** Chiralcel OD column; solvent, 99:1 hexane/isopropanol; flow rate 0.5 mL/min; 254 nm UV detector.

The racemic alcohols products were obtained by addition of  $\text{EtMgBr}$  to aldehydes. The conditions of analysis and retention times of the *R* and *S* isomers have been reported elsewhere.<sup>67,68</sup>

## RESULTS AND DISCUSSION

We have previously reported that the use of only 0.5 mol % of the chiral amino diselenides **3a–d** as ligands in the enantioselective addition of diethylzinc to aldehydes, afforded the respective secondary alcohols in up to 99% *ee*.<sup>69</sup> To the best of our knowledge, these ligands were the first class of chiral amino diselenides with the selenium

atom attached to an alkyl group. From now, we set out to extend this study through the synthesis of other similar ligands, possessing potentially stereogenic chalcogenide donors. Scheme 1 depicts the synthesis of these two classes of ligands:  $\beta$ -amino diselenides **3a–d**, previously reported, and the new  $\beta$ -amino disulfides **4**. These compounds would allow us to study electronically and structurally the effects of these different catalysts and hopefully provide insight into further ligand design.

The chiral amino chalcogenides **3a–d** and **4a–d** were easily prepared from the corresponding commercially available  $\alpha$ -amino alcohols **1**, which were further quantitatively converted into the *N*-Boc-protected derivatives by reaction with di-*tert*-butyl dicarbonate in acetonitrile. Chiral aziridines **2** were obtained in good yields by treatment of *N*-Boc amino alcohols with *p*-toluenesulfonyl chloride and potassium hydroxide in boiling THF. Finally, the sulfur or selenium atom was efficiently introduced by regioselective ring opening employing  $\text{Li}_2\text{Y}_2$ <sup>70</sup> ( $\text{Y} = \text{S}, \text{Se}$ ) as nucleophile. The attack was selective in the less hindered carbon<sup>71,72</sup> of aziridines ring **2a–d**, furnishing the aliphatic chiral amino diselenides **3a–d** and disulfides **4a–d** without any loss of enantiomeric purity, as determined by HPLC analysis using Daicel Chiralcel OD column. The regiochemistry was determined by analysis of NMR data, confirming the regioselective aziridine ring opening without detection of a second regioisomer.

With this sterically and electronically varied set of enantiopure dichalcogenides, we have examined their efficiency as chiral ligands in the enantioselective addition of diethylzinc to aldehydes. Aiming to determine the optimum conditions, we performed studies about effects that can influence this catalysis, such as load of catalyst and temperature.

**TABLE 1.** Enantioselective addition of diethylzinc to benzaldehyde varying the loading of ligand **4a**

Entry	Loading of <b>4a</b> (mol %)	Yield <sup>a</sup> (%)	<i>ee</i> <sup>b</sup> (%)
1	10	92	95 (R)
2	5	92	95 (R)
3	2.5	91	95 (R)
4	1	91	95 (R)
5	0.5	90	95 (R)
6	0.25	43	62 (R)
7 <sup>c</sup>	0.5	94	83 (R)
8 <sup>d</sup>	0.5	48	90 (R)

<sup>a</sup>Determined by GC analysis.

<sup>b</sup>Determined by chiral GC analysis with use of a Hydrodex  $\beta$ -3P column; the absolute configuration was determined by comparing the sign of the optical rotation.

<sup>c</sup>Reaction was carried out at 50°C for 20 h.

<sup>d</sup>Reaction was carried out at 0°C for 48 h.



In a preliminary stage, ligand **4a** was tested in the addition of diethylzinc to benzaldehyde to determine the optimal loading of catalyst. Yields and enantioselectivities for 1-phenyl-1-propanol have been collected in Table 1.

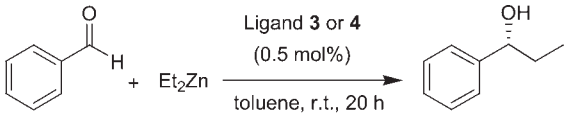
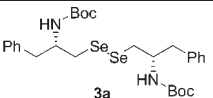
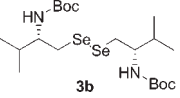
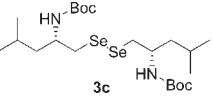
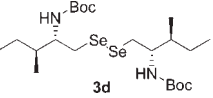
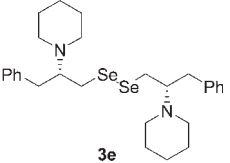
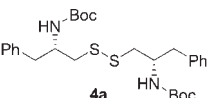
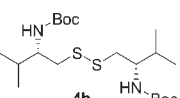
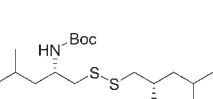
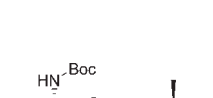
Concentrations varying from 0.25 to 10 mol % were tested and it could be observed that the *ee* of the alkylated product remained very high in the most of the cases (Table 1, entries 1–6). Even when 0.5 mol % of ligand **4a** was used, enantiomeric excess of 1-phenyl-1-propanol was 95% and the conversion was still high (Table 1, entry 5). However, at lower catalyst concentration, yield and enantiomeric excess of this secondary alcohol markedly decreased (Table 1, entry 6). This result can be rationalized due to the high affinity of sulfur with zinc, forming a highly effective catalytic cycle. At this point, it has to be mentioned that the described ligand systems display a high reactivity compared to most of the other ligand systems described in the literature.<sup>73,74</sup>

In addition, we investigated the temperature effect on the enantiomeric excess of the product in the same (1,2)-addition reaction. We also observed that this process is sensible to this effect, in terms of yield and selectivity. When the reaction was carried out at room temperature, the conversion was of 90%, and the *ee* of 95% (Table 1, entry 5). By increasing the temperature, a negative effect in terms of *ee* was observed while the yields remained practically constant (Table 1, entry 7). Probably, the increment of temperature supply to this reaction and additional energy necessary to form a nonfavorable transition state, decreasing the *ee* in this case. By lowering the temperature to 0°C, we observed a drastic decrease in the yield (Table 1, entry 8), probably due to a decreasing in the efficiency of complexation; while the *ee* remained practically the same obtained at room temperature.

With these results in hand, the efficiency of the other disulfides prepared was also examined. The reactions were performed under standard conditions: 0.5 mol % of ligand **4**, benzaldehyde (1 mmol), diethylzinc (2.5 mmol) in toluene, at room temperature. Aiming to perform a comparative study between ligands **3** and **4** to verify the influence of chalcogen atom as effective ligand, the enantioselectivities observed with diselenides **3**<sup>69</sup> to the respective secondary alcohols are also given in the following Tables.

As shown in Table 2, all the ligands has presented high levels of enantiocontrol, affording (*R*)-1-phenyl-1-propanol in enantiomeric excesses ranging from 91 to 95%. The steric hindrance from the different alkyl groups in the side chains of aminoalcohols plays an important role in the selectivity, and the ligands **3a** and **4a** (Table 2, Entries 1 and 6) shown better levels of enantioselection in comparison with the other less bulky *R*-substituents. Concerning the influence of the chalcogen atom, selenium and sulfur showed practically the same efficiency. This result can be rationalized by the high tendency of both atoms coordinate to a metal center (zinc) forming an efficient catalytic complex. The steric effect on the amine moiety was also studied using the modified catalyst **3e**.<sup>69</sup> Although this ligand had shown good performance, the results obtained with **3a** are still higher in terms of conversion and enantio-

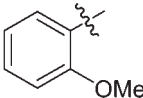
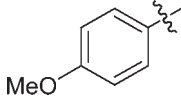
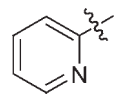
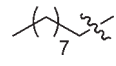
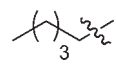
**TABLE 2.** Screening of ligands **3a–e** and **4a–d** in the catalytic enantioselective addition of diethylzinc to benzaldehyde

			
Entry	Ligand	Yield <sup>a</sup> (%)	<i>ee</i> <sup>b</sup> (%)
1		91	95 (R)
2		71	91 (R)
3		80	92 (R)
4		72	91 (R)
5		82	90 (R)
6		90	95 (R)
7		70	92 (R)
8		79	94 (R)
9		70	92 (R)

<sup>a</sup>Determined by GC analysis.

<sup>b</sup>Determined by chiral GC analysis using a Hydrodex β-3P column; and the absolute configuration was determined comparing the sign of optical rotation.

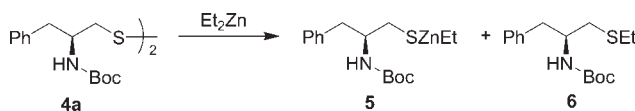
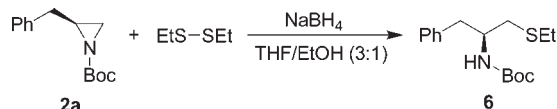
**TABLE 3.** Enantioselective addition of diethylzinc to aldehydes using **3a** or **4a**

$\text{R}^1\text{CHO} + \text{Et}_2\text{Zn} \xrightarrow[\text{toluene, r.t., 20 h}]{\text{Ligand } \mathbf{3a} \text{ or } \mathbf{4a} \text{ (0.5 mol\%)}} \text{R}^1\text{CH(OH)Et}$				
Entry	Ligand	R <sup>1</sup>	Yield <sup>a</sup> (%)	ee (%)
1 <sup>a</sup>	<b>3a</b>		93	95 (R)
2 <sup>b</sup>	<b>4a</b>		80	95 (R)
3 <sup>b</sup>	<b>3a</b>		93	>99 (R)
4 <sup>b</sup>	<b>4a</b>		75	>99 (R)
5 <sup>c</sup>	<b>3a</b>		85	91 (R)
6 <sup>c</sup>	<b>4a</b>		78	98 (R)
7 <sup>c</sup>	<b>3a</b>		56	45 (R)
8 <sup>c</sup>	<b>4a</b>		54	>99 (R)
9 <sup>c</sup>	<b>3a</b>		63	>99 (R)
10 <sup>c</sup>	<b>4a</b>		51	70 (R)

<sup>a</sup>Conversion was determined by GC analysis.<sup>b</sup>Determined by chiral GC analysis using a Hydrodex  $\beta$ -3P column; the absolute configuration was determined by comparing the sign of optical rotation.<sup>c</sup>Determined by chiral HPLC analysis using a Daicel Chiralcel OD column.

meric excess, as well as the simplicity of the catalyst (Table 2, compare entries 1 vs. 5).

To extend the scope of the optimal ligand **4a** as chiral catalysts in this reaction, several aromatic and aliphatic aldehydes were screened. As shown in the Table 3, for aromatic aldehydes, high yields and levels of enantioselection of the respective (*R*)-secondary alcohols were observed by the use of both catalysts (entries 1–6) and in the best cases, *ees* up to 99% were achieved (see entries 3 and 4). When the less reactive aliphatic aldehydes were employed, the results had shown an unexpected way. By using the diselenide **3a**, the selectivity was excellent for hexanal (minor chain), and very poor to decanal (Table 3,

**Scheme 2.** Formation of the catalytically active species.**Scheme 3.** Synthesis of thioether **6**.

entries 7 and 9). Surprisingly, by using the disulfide **4a** the selectivity observed had an opposite way: (*R*)-dodecan-3-ol was obtained in up to 99% *ee* while (*R*)-octan-3-ol was achieved in only a moderated enantiomeric excess (Table 3, entries 8 vs. 10). Apparently, the size of the chalcogen atom in the structure of the ligand plays an important influence in terms of selectivity.

The stereochemistry of the products is in accordance with the mechanistic rationalization described in Noyori's work.<sup>1,75,76</sup>

To elucidate the mechanistic aspects, we assumed that the disulfide linkage is cleaved by nucleophilic attack of diethylzinc, resulting in the thiolate **5** and the thioether **6** (Scheme 2), according to the results reported by Kellogg<sup>35</sup> and Wirth.<sup>30</sup>

Aiming to identify the catalytically active species, we prepared the compound **6** via **2a** ring-opening reaction by attack of EtSSEt/NaBH<sub>4</sub><sup>77</sup> as shown in Scheme 3.

We believe that the active catalyst of the reaction is the species **5**, since in an additional experiment, the thioether **6** did not catalyze the alkylation reaction of benzaldehyde.

## CONCLUSIONS

In summary, a new series of chiral  $\beta$ -amino disulfides was synthesized in a straightforward synthetic route from readily available and inexpensive starting materials. These compounds have been evaluated in the enantioselective addition of diethylzinc to aldehydes, furnishing the corresponding optically active secondary alcohols in high yields and enantiomeric excesses by using a very small amount of catalyst. Most importantly, by the use of these compounds it was possible to perform a comparative study with the analog diselenides **3** reported by our group. As a result of this study, a larger class of complementary dichalcogenide ligands **3** and **4** for the addition of diethylzinc to aldehydes, especially to aliphatic aldehydes, is now available. Studies dealing with the mechanism of the reaction and application of this catalyst system in other asymmetric catalytic reactions<sup>78</sup> and as building blocks for peptides synthesis<sup>79</sup> are currently in progress in our laboratory.

## ACKNOWLEDGMENT

F.Z.G thanks CAPES for a Ph.D fellowship.

## LITERATURE CITED

- Noyori R, Kitamura M. Enantioselective addition of organometallic reagents to carbonyl compounds-chirality transfer, multiplication and amplification. *Angew Chem Int Ed Engl* 1991;30:49–69.
- Noyori R. *Asymmetric catalysis in organic chemistry*. New York: Wiley; 1994.
- Soai K, Niwa S. Enantioselective addition of organozinc reagents to aldehydes. *Chem Rev* 1992;92:833–856.



4. Pu L, Yu HB. Catalytic asymmetric organozinc additions to carbonyl compounds. *Chem Rev* 2001;101:757–824; and references therein.
5. Braga AL, Milani P, Paixão MW, Zeni G, Rodrigues OED, Alves EF. Aziridine sulfides and disulfides as catalysts for the enantioselective addition of diethylzinc to aldehydes. *Chem Commun* 2004;2488–2489.
6. Braga AL, Rubim RM, Schrekker HS, Wessjohann LA, Bolster MWG, Zeni G, Sehnem JA. The facile synthesis of chiral oxazoline catalysts for the diethylzinc addition to aldehydes. *Tetrahedron: Asymmetry* 2003;14:3291–3295.
7. Braga AL, Lüdtke DS, Schneider PH, Vargas F, Schneider A, Wessjohann LA, Paixão MW. Catalytic enantioselective aryl transfer: asymmetric addition of boronic acids to aldehydes using pyrrolidinylmethanols as ligands. *Tetrahedron Lett* 2005;46:7827–7830.
8. Braga AL, Lüdtke DS, Vargas F, Paixão MW. Catalytic enantioselective arylation of aldehydes: boronic acids as a suitable source of transferable aryl groups. *Chem Commun* 2005;2512–2514.
9. Ye M, Logaraj S, Jackman LM, Hillegass K, Hirsh KA, Bollinger AM, Grosz AL, Mani V. Enantioselective addition of alkyl lithium reagent to aldehydes induced by chiral lithium alkoxides. *Tetrahedron* 1994;50:6109–6116.
10. Schon M, Naef R. New 1-amino-1,2-diphenylethanols as ligands for the enantioselective addition of alkyl lithiums to benzaldehyde. *Tetrahedron: Asymmetry* 1999;10:169–176.
11. Frantz DE, Fässler R, Carreira EM. Facile enantioselective synthesis of propargylic alcohols by direct addition of terminal alkynes to aldehydes. *J Am Chem Soc* 2000;122:1806–1807.
12. Lipshutz BH, Shin YL. Polystyrene-bound cyclo-BINOLs. New heterogeneous ligands for asymmetric catalysis. *Tetrahedron Lett* 2000;41:9515–9521.
13. Zhu HJ, Jiang JX, Saebo S, Pittman CU Jr. Chiral ligands derived from Abrine 8. An experimental and theoretical study of free ligand conformational preferences and the addition of diethylzinc to benzaldehyde. *J Org Chem* 2005;70:261–267.
14. Martínez AG, Vilar ET, Fraile AG, Cerero SdlM, Moroto BL. Understanding the catalytic role of flexible chiral  $\alpha$ -amino alcohols: the 1-(2-aminoethyl)norbornan-2-ol model. *Tetrahedron* 2005;61:3055–3064.
15. Fennie MW, DiMauro EF, O'Brien EM, Annamalai V, Kozlowski MC. Mechanism and scope of salen bifunctional catalysts in asymmetric aldehyde and  $\alpha$ -ketoester alkylation. *Tetrahedron* 2005;61:6249–6265.
16. Cobb AJA, Marson CM. Asymmetric synthesis using catalysts containing multiple stereogenic centers and a trans-1,2-diaminocyclohexane core; reversal of predominant enantioselectivity upon N-alkylation. *Tetrahedron* 2005;61:1269–1279.
17. Dahman S, Bräse S. Planar and central chiral [2.2] paracyclophane-based *N,O*-ligands as highly active catalysts in the diethylzinc addition to aldehydes. *Chem Commun* 2002;26–27.
18. Paleo MR, Cabeza I, Sardina FJ. Enantioselective addition of diethylzinc to aldehydes catalyzed by *N*-(9-phenylfluoren-9-yl)  $\beta$ -amino alcohols. *J Org Chem* 2000;65:2108–2113.
19. Nugent WA. MIB: an advantageous alternative to DAIB for the addition of organozinc reagents to aldehydes. *Chem Commun* 1999;1369–1370.
20. Mino T, Oishi K, Yamashita M. Enantioselective addition of diethylzinc to aryl aldehydes catalyzed by ADPD imine catalysts. *Synlett* 1998;965–966.
21. Xu Q, Wu X, Pan X, Chan ASC, Yang TK. Synthesis of new pyridyl alcohols and their use as catalysts in the asymmetric addition of diethylzinc to aldehydes. *Chirality* 2002;14:28–31.
22. Cicchi S, Crea S, Goti A, Brandi A. Synthesis of new enantiopure  $\gamma$ -aminoalcohols: their use as catalysts in the alkylation of benzaldehyde by diethylzinc. *Tetrahedron: Asymmetry* 1997;8:293–301.
23. Wilken J, Groger H, Kossenjans M, Martens J. Synthesis and application of new (threo)- and (erythro)-amino alcohols based on octahydrocyclopenta[b]pyrrole system in the catalytic enantioselective addition of diethylzinc to benzaldehyde. *Tetrahedron: Asymmetry* 1997;8:2761–2771.
24. Xu Q, Wang G, Pan X, Chan ASC. The syntheses of new optically active 2-methylquinoline derivatives and their application in the enantioselective addition of diethylzinc to aldehydes. *Tetrahedron: Asymmetry* 2001;12:381–385.
25. Bolm C, Müller J. Spectroscopic studies on the  $\beta$ -hydroxysulfoximine-catalyzed enantioselective alkylation of aldehydes. *Tetrahedron* 1994;50:4355–4362.
26. Anderson JC, Cubbon R, Harding M, James DS. Concepts for ligand design in asymmetric catalysis: a study of chiral amino thiol ligands. *Tetrahedron: Asymmetry* 1998;9:3461–3490; and references therein.
27. Kang J, Kim JB, Kim JW, Lee D. The effects of sulfur substitution in chiral amino thiols on the enantioselective addition of organozinc reagents to aldehydes: a novel method for estimation of free energies of dimerization in monomer-dimer equilibria. *J Chem Soc Perkin Trans 2* 1997;189–194.
28. Wirth T. Enantioselective alkylation of aldehydes catalyzed by new chiral diselenides. *Tetrahedron Lett* 1995;36:7849–7852.
29. Wirth T, Santi C. Synthesis of non-racemic nitrogen-containing diselenides as efficient precursor catalysts in the diethylzinc addition to benzaldehyde. *Tetrahedron: Asymmetry* 1999;10:1019–1023.
30. Wirth T, Kulicke KJ, Fragale G. Chiral diselenides from benzylamines: catalysts in the diethylzinc addition to aldehydes. *Helv Chim Acta* 1996;79:1957–1966.
31. Braga AL, Lüdtke DS, Vargas F, Braga RC. Catalytic applications of chiral organoselenium compounds in asymmetric synthesis. *Synlett* 2006;1453–1466.
32. Braga AL, Lüdtke DS, Vargas F. Enantioselective synthesis mediated by catalytic chiral organoselenium compounds. *Curr Org Chem* 2006;10:1921–1938.
33. Mellah M, Voituriez A, Schulz E. Chiral sulfur ligands for asymmetric catalysis. *Chem Rev* 2007;107:5133–5209.
34. Hof RP, Poelert MA, Peper NCMW, Kellogg RM. Sulfur derivatives of ephedra alkaloids—new and highly efficient chiral catalysts. *Tetrahedron: Asymmetry* 1994;5:31–34.
35. Fitzpatrick K, Hulst R, Kellogg RM. Thiol and disulfide derivatives of ephedra alkaloids. II. A mechanistic study of their effect on the addition of diethylzinc to benzaldehyde. *Tetrahedron: Asymmetry* 1995;6:1861–1864.
36. Hulst R, Heres H, Fitzpatrick K, Peper NCMW, Kellogg RM. Catalytic enantioselective alkylation of benzaldehyde with diethylzinc using chiral nonracemic (thio)-phosphoramidates. *Tetrahedron: Asymmetry* 1996;7:2755–2760.
37. Jin MJ, Ahn SJ, Lee KS. New chiral catalysts for the highly enantioselective addition of diethylzinc to aldehydes. *Tetrahedron Lett* 1996;37:8767–8770.
38. Soai K, Ohno Y, Inoue Y, Tsuruoka T, Hirose Y. Catalytic enantioselective alkylation of aldehydes using chiral hydrogen phosphoramidates and hydrogen phosphinamides and their thio analogs. *Recl Trav Chim Pays-Bas* 1995;114:145–152.
39. Jimeno C, Moyano A, Pericas MA, Riera A. A purely synthetic, diversity amenable version of norephedrine thiols for the highly enantioselective diethylzinc addition to aldehydes. *Synlett* 2001;1155–1157.
40. Gibson CL. Enantioselective addition of diethylzinc to aldehydes catalysed by a  $\beta$ -amino disulfide derived from L-proline. *Chem Commun* 1996;645–646.
41. Gibson CL. An L-proline-based  $\beta$ -amino tertiary thiol: synthesis and use as a catalyst in the enantioselective addition of diethylzinc to aldehydes. *Tetrahedron: Asymmetry* 1999;10:1551–1561.
42. Eriksen HS, Oyaga SC, Sherrington DC, Gibson CL. Polymer-supported  $\beta$ -amino thioesters as catalysts for the enantioselective addition of diethylzinc to aldehydes. *Synlett* 2005;1235–1238.
43. Fulton DA, Gibson CL. Synthesis of a scalemic  $\beta$ -amino disulfide from (S)-phenylglycine and (R)-styrene oxide and use as a catalyst in enantioselective additions of diethylzinc to aldehydes. *Tetrahedron Lett* 1997;38:2019–2022.
44. Tseng SL, Yang TK. The application of chiral amino thiols as catalysts in the enantioselective addition of diethylzinc to aldehydes. *Tetrahedron: Asymmetry* 2004;15:3375–3380.

45. Anderson JC, Harding M. The importance of nitrogen substituents in chiral amino thiol ligands for the asymmetric addition of diethylzinc to aromatic aldehydes. *Chem Commun* 1996;393–394.
46. Braga AL, Alves EF, Silveira CC, Zeni G, Appelt HR, Wessjohann LA. A new cysteine-derived ligand as catalyst for the addition of diethylzinc to aldehydes: the importance of a 'free' sulfide site for enantioselectivity. *Synthesis* 2005;588–594.
47. Braga AL, Lüdtke DS, Wessjohann LA, Paixão MW, Schneider PH. A chiral disulfide derived from (*R*)-cysteine in the enantioselective addition of diethylzinc to aldehydes: loading effect and asymmetric amplification. *J Mol Catal A* 2005;229:47–50.
48. Braga AL, Appelt HR, Schneider PH, Rodrigues OED, Silveira CC, Wessjohann LA. New C-2-symmetric chiral disulfide ligands derived from (*R*)-cysteine. *Tetrahedron* 2001;57:3291–3295.
49. Braga AL, Appelt HR, Schneider PH, Silveira CC, Wessjohann LA. A new functionalized, chiral disulfide derived from L-cysteine: (*R,R*)-bis[(3-benzoyloxazolan-4-yl)-methane] disulfide as a catalyst in the diethylzinc addition to aldehydes. *Tetrahedron: Asymmetry* 1999;10:1733–1738.
50. Meng QL, Li YL, He Y, Guan YD. Novel thiazolidine derivatives as chiral catalysts in the enantioselective addition of diethylzinc to aldehydes. *Tetrahedron: Asymmetry* 2000;11:4255–4261.
51. Braga AL, Vargas F, Silveira CC, Andrade LH. Synthesis of new chiral imidazolidine disulfides derived from L-cystine and their application in the enantioselective addition of diethylzinc to aldehydes. *Tetrahedron Lett* 2002;43:2335–2337.
52. Kellogg RM, Hof RP. (Nonracemic) thiols and Zn-II. Structural and catalytic aspects of some natural and non-natural zinc thiolates. *J Chem Soc Perkin Trans 1* 1996;1651–1657.
53. Mão JC, Wan BS, Wang RL, Wu F, Lu SW. Concise synthesis of novel practical sulfamide-amine alcohols for the enantioselective addition of diethylzinc to aldehydes. *J Org Chem* 2004;69:9123–9127.
54. Braga AL, Milani P, Vargas F, Paixão MW, Sehnem JA. Modular chiral thiazolidine catalysts in asymmetric aryl transfer reactions. *Tetrahedron: Asymmetry* 2006;17:2793–2797.
55. Wang SX, Chen FE. Novel polymer-supported chiral catalysts for the asymmetric addition of diethylzinc to aldehydes. *Chem Pharm Bull* 2007;55:1011–1013.
56. Yang WG, Wu S, Shi M. Progress of organozinc reagents in asymmetric addition reactions catalyzed by sulfur-containing chiral ligands. *Chin J Org Chem* 2007;27:197–208.
57. Hui XP, Chen CA, Wu KH, Gau HM. Polystyrene-supported *N*-sulfonylated amino alcohols and their applications to titanium(IV) complexes catalyzed enantioselective diethylzinc additions to aldehydes. *Chirality* 2007;19:10–15.
58. Hatano M, Miyamoto T, Ishihara K. Recent progress in selective additions of organometal reagents to carbonyl compounds. *Curr Org Chem* 2007;11:127–157.
59. Braga AL, Vargas F, Sehnem JA, Braga RC. Efficient synthesis of chiral  $\beta$ -seleno amides via ring-opening reaction of 2-oxazolines and their application in the palladium-catalyzed asymmetric allylic alkylation. *J Org Chem* 2005;70:9021–9024.
60. Vargas F, Sehnem JA, Galetto FZ, Braga AL. Modular chiral  $\beta$ -selenium-, sulfur-, and tellurium amides: synthesis and application in the palladium-catalyzed asymmetric allylic alkylation. *Tetrahedron* 2008;64:392–398.
61. Braga AL, Paixão MW, Milani P, Silveira CC, Rodrigues OED, Alves EF. New aziridine sulfide ligands for palladium-catalyzed asymmetric allylic alkylation. *Synlett* 2004;1297–1299.
62. Silveira CC, Vieira AS, Braga AL, Russowsky D. Stereoselective manich-type reaction of chlorotitanium  $\alpha$ -phenylseleno esters enolates with aromatic aldimines. *Tetrahedron* 2005;61:9312–9318.
63. Braga AL, Appelt HR, Silveira CC, Wessjohann LA, Schneider PH. Facile and practical enantioselective synthesis of propargylic alcohols by direct addition of alkynes to aldehydes catalyzed by chiral disulfide-oxazolidine ligands. *Tetrahedron* 2002;58:10413–10416.
64. Braga AL, Silva SJN, Lüdtke DS, Drekenner RL, Silveira CC, Rocha JBT, Wessjohann LA. Chiral diselenide ligands for the asymmetric copper-catalyzed conjugate addition of Grignard reagents to enones. *Tetrahedron Lett* 2002;43:7329–7331.
65. Still WC, Kahn M, Mitra A. Rapid chromatographic technique for preparative separations with moderate resolution. *J Org Chem* 1978;43:2923–2925.
66. Granander J, Sott R, Hilmersson G. Chiral lithium amido sulfide ligands for asymmetric addition reactions of alkyllithium reagents to aldehydes. *Tetrahedron: Asymmetry* 2003;14:439–447.
67. Huang WS, Hu QS, Pu L. A highly general catalyst for the enantioselective reaction of aldehydes with diethylzinc. *J Org Chem* 1998;63:1364–1365 (see also supporting information).
68. Huang WS, Pu L. The first highly enantioselective catalytic diphenylzinc additions to aldehydes: synthesis of chiral diarylcarbinols by asymmetric catalysis. *J Org Chem* 1999;64:4222–4223.
69. Braga AL, Paixão MW, Lüdtke DS, Silveira CC, Rodrigues OED. Synthesis of new chiral aliphatic amino diselenides and their application as catalysts for the enantioselective addition of diethylzinc to aldehydes. *Org Lett* 2003;5:2635–2638 (see also supporting information).
70. Gladysz JA, Hornby JL, Garbe JE. Convenient one-flask synthesis of dialkyl selenides and diselenides via lithium triethylborohydride reduction of sex. *J Org Chem* 1978;43:1204–1208.
71. Tanner D. Chiral aziridines—their synthesis and use in stereoselective transformations. *Angew Chem Int Ed Engl* 1994;33:599–619.
72. McCoull W, Davis FA. Recent synthetic applications of chiral aziridines. *Synthesis* 2000;1347–1365.
73. Wipf P, Pierce JG, Wang XD. Investigation of ligand loading and asymmetric amplification in CHAOx-catalyzed asymmetric diethylzinc additions. *Tetrahedron: Asymmetry* 2003;14:3605–3611.
74. Lauterwasser F, Vanderheiden S, Brase S. Planar- and central-chiral *N,O*-[2.2]paracyclophane ligands: non-linear-like effects and activity. *Adv Syn Cat* 2006;348:443–448.
75. Kitamura M, Okada S, Suga S, Noyori RJ. Enantioselective addition of dialkylzinc to aldehydes promoted by chiral amino alcohols. Mechanism and nonlinear effect. *J Am Chem Soc* 1989;111:4028–4036.
76. Yamakawa M, Noyori RJ. An ab initio molecular orbital study on the amino alcohol-promoted reaction of dialkylzinc and aldehydes. *J Am Chem Soc* 1995;117:6327–6335.
77. Osborn HMI, Sweeney JB, Howson Bill. Ring-opening of *N*-tosyl aziridines by sulphur-stabilized nucleophiles. *Synlett* 1993;675–676.
78. Paixão MW, de Godoi M, Rhoden CRB, Westermann B, Wessjohann LA, Lüdtke DS, Braga AL. The application of chiral, non-racemic *N*-alkylephedrine and *N,N*-dialkylnorephedrine as ligands for the enantioselective aryl transfer reaction to aldehydes. *J Mol Catal A* 2007;261:120–124.
79. Braga AL, Lüdtke DS, Paixão MW, Alberto EE, Stefani HA, Juliano L. Straightforward synthesis of non-natural selenium containing amino acid derivatives and peptides. *Eur J Org Chem* 2005;4260–4264.

# Synthesis of Dendritic Stationary Phases with Surface-Bonded L-Phenylalanine Derivate as Chiral Selector and Their Evaluation in HPLC Resolution of Racemic Compounds

CHUAN-QI YIN,<sup>1,2</sup> BAO-JIANG HE,<sup>2</sup> SHAO-HUA HUANG,<sup>2</sup> JUN-YI ZHANG,<sup>2</sup> ZHENG-WU BAI,<sup>2</sup> AND ZAO-YING LI<sup>1\*</sup>

<sup>1</sup>College of Chemistry and Molecular Sciences, Wuhan University, Wuhan, Hubei Province, China

<sup>2</sup>College of Chemical Engineering and Pharmacy, Wuhan Institute of Chemical Technology, Wuhan, Hubei Province, China

**ABSTRACT** Four dendrimers were synthesized on aminopropyl-modified silica gel using methyl acrylate and ethylene diamine as building blocks by divergent method. Four generations of chiral stationary phases (CSPs) were prepared by coupling of L-2-(*p*-toluenesulfonamido)-3-phenylpropionyl chloride to corresponding dendrimers. The derivatives prepared on silica gel were characterized by FT-IR, <sup>1</sup>H NMR, and elemental analysis. The selector loadings of these four generations of CSPs generally showed a decrease tendency with the increase of generation numbers of dendrimers. The enantio-separation properties of these CSPs were preliminarily investigated by high-performance liquid chromatography. The CSP derived from the three-generation dendrimer exhibited the best enantioseparation capability. Effects of the mobile phase composition and molecular structures of racemic mixtures on enantioseparation were further studied. *Chirality* 20:846–855, 2008. © 2008 Wiley-Liss, Inc.

**KEY WORDS:** dendrimer; chiral stationary phase; enantioseparation; high-performance liquid chromatography

## INTRODUCTION

Chiral separation of racemic mixtures remains an area of interest, due to its importance in the development and manufacture of single enantiomer drugs.<sup>1,2</sup> High-performance liquid chromatograph (HPLC) based on the application of chiral CSPs is an effective way to separate a racemic mixture into its enantiomers.<sup>3–5</sup> Up to date, many works focus on the preparation of various CSPs to meet the requirements of determination and bulk preparation of chiral compounds.<sup>6–9</sup>

Dendrimers are monodisperse polymers that represent a class of highly ordered oligomeric or polymeric structures with a specific number of functional groups in precisely defined locations.<sup>10–13</sup> Although dendrimers have been known to be prepared as carriers of drugs or bioactive molecules for controlled release,<sup>14–16</sup> or as carriers of metal ions for clinic diagnosis or for catalysis,<sup>17,18</sup> the immobilization of dendrimers onto chromatographic supports to be used as HPLC stationary phase selectors has not been reported until the publication of Fréchet and coworkers' work on preparation of dendritic CSPs containing L-proline indanilide chiral selectors through two different approaches, i.e. the convergent, and the divergent ways.<sup>19</sup> In these CSPs, macroporous poly(2-hydroxyethyl methacrylate-co-ethylene dimethacrylate) beads were used as the supports. The CSP prepared in the convergent manner had relatively low loading, whereas the CSP prepared by divergent manner had comparatively higher loading. These CSPs had excellent enantioseparation capabilities in separating racemic mixture of *N*-(3,5-dinitrobenzoyl)-*R*-

amino acid alkyl amides. Mitchell et al. reported a dendrimer-based CSP by immobilizing a dendrimer derived from L-glutamic acid derivatives onto silica gel, but no enantioseparation evaluation was given.<sup>20</sup> In our recent work, we have also synthesized three generations of CSPs based on silica gel using (1*R*,2*R*)-(+)-1,2-diphenylethylenediamine and tricarbonylbenzene trichloride as building blocks by divergent approach.<sup>21</sup> The one-generation dendritic CSP exhibited the best enantioseparation ability, while the three-generation dendritic CSP showed the worst separation capability, which is probably caused by the congestion of chiral selectors. It is essential for chiral recognition that analytes access the chiral centers of the selectors immobilized on support.

Continuing our investigation on enantioseparation ability of dendrimer-type CSPs based on silica gel, we used ethylene diamine (EDA) and methyl acrylate (MA) as building blocks to construct dendrimers of different generations on aminated silica gel. And L-phenylalanine derivative was immobilized on the dendrimers to afford dendritic CSPs. Different from the CSPs reported in our previous work, where dendrimers were constructed through chiral

Contract grant sponsor: National Natural Science Foundation of China (NSFC); Contract grant number: 20371037

\*Correspondence to: Zao-Ying Li, College of Chemistry and Molecular Sciences, Wuhan University, Wuhan, Hubei Province 430072, China.

E-mail: zyliwuc@whu.edu.cn

Received for publication 28 October 2007; Accepted 1 February 2008

DOI: 10.1002/chir.20555

Published online 1 April 2008 in Wiley InterScience (www.interscience.wiley.com).

molecules directly,<sup>21</sup> L-phenylalanine derivative as the selector was located on the surface of the newly constructed dendrimers. This work aims at finding out the difference in chiral separation of these two types of CSPs. The enantioseparation of these newly synthesized CSPs was evaluated.

## MATERIALS AND METHODS

### Materials and Chemicals

Silica gel (LiChrosorb Si100) was purchased from Merck (Darmstadt, Germany) with a particle size of 5  $\mu\text{m}$ , a pore size of 100 Å, and a surface area of 300  $\text{m}^2 \text{g}^{-1}$ . L-phenylalanine was purchased from Hongyuan Co. Ltd. of Wuhan University (China). Trichloroacetic acid (TCA) was purchased from Aldrich (St. Louis, MO). All other reagents were obtained from commercial suppliers and used as received. MA and  $\text{SOCl}_2$  were freshly distilled before used. Triethylamine (TEA) was dried over phosphorous pentoxide and redistilled. Solvents were distilled with appropriate drying agents (solvents/drying agents):  $\text{CHCl}_3/\text{CaCl}_2$ , toluene/Na, tetrahydrofuran/Na-benzophenone, pyridine/ $\text{CaH}_2$ . All mobile phases were freshly prepared, filtered, and degassed.

### Instruments and Measurements

IR spectra were recorded on a Nicolet FT-IR instrument with KBr pellets. Elemental analysis (EA) was carried out on an Elemental VarioEL III CHNOS apparatus (Germany).  $^1\text{H}$  NMR spectra were obtained from a Varian INOVA 500 spectrometer (USA), operating at 500 MHz. Chemical shifts were reported relative to residual protons of the deuterated solvents. Solid-state  $^1\text{H}$  NMR spectra were recorded on a Varian Infinity Plus 300 spectrometer (USA), operating at 300 MHz. The CSPs were packed into stainless steel columns ( $250 \times 4.6 \text{ mm}$ ) with a model 1666 Alltech slurry packer. Enantioseparation was performed on an Agilent 1100 chromatographic apparatus consisted of an Agilent G1365B DAD, an Agilent G1311A Quat Pump, an Agilent G1379A degasser, and an Agilent G1313A ALS autosampler.

### Preparation of Chiral Selector

**L-2-(*p*-toluenesulfonamido)-3-phenylpropionic acid (2).** To a solution of L-phenylalanine **1** (16.50 g, 0.10 mol) dissolved in 1 mol/L NaOH (200 mL), *p*-toluenesulfonyl chloride (19.00 g, 0.10 mol) in  $\text{CHCl}_3$  (100 mL) was added dropwise. The reaction mixture was stirred at room temperature for 2 h and then warmed to  $40^\circ\text{C}$  for 0.5 h. After cooled to room temperature, the organic phase was separated. The aqueous phase was neutralized with concentrated hydrochloric acid to result in a white precipitate. The solid was collected by filtration and then recrystallized in  $\text{EtOH}/\text{H}_2\text{O}$  (2:1) to give **2** (27.10 g, 85%) as a white powder. Mp:  $159\text{--}161^\circ\text{C}$ .  $[\alpha]_D^{20}$ :  $-2.6^\circ$  (C 4.5, acetone). FT-IR (KBr,  $\text{cm}^{-1}$ ): 3536, 3370 ( $-\text{CO}_2\text{H}$ ), 1374 ( $-\text{SO}_2-\text{NH}-$ ). EA found C 59.45, H 5.66, N 4.50, S 10.15,  $\text{C}_{16}\text{H}_{17}\text{NO}_4\text{S}$  requires C 60.18, H 5.33, N 4.39, S 10.03.  $^1\text{H}$  NMR ( $\text{CDCl}_3$ )  $\delta$ : 2.14 (1H, s,  $\text{ArSO}_2-\text{NH}$ ), 2.40

(3H, s,  $\text{Ar}-\text{CH}_3$ ), 3.01 (1H, m,  $\text{Ar}-\text{CH}_2$ ), 3.12 (1H, m,  $\text{Ar}-\text{CH}_2$ ), 4.22 (1H, m,  $\text{ArCH}_2-\text{CH}$ ), 7.09–7.61 (9H, m,  $\text{Ar}-\text{H}$ ).

**L-2-(*p*-toluenesulfonamido)-3-phenylpropionyl chloride (3).**  $\text{SOCl}_2$  (10 mL, 0.15 mol) was added dropwise to a solution of **2** (21.21 g, 0.07 mol) in  $\text{CHCl}_3$  (100 mL). The reaction mixture was stirred at room temperature for 1 h, followed by continuously stirring for 3 h at  $65^\circ\text{C}$ . Upon removal of the solvent under vacuum, the residue was recrystallized in toluene/cyclohexane (2:1) yielding chiral selector **3** (19.40 g, 82%) as a pale yellow solid. Mp:  $124\text{--}126^\circ\text{C}$ .  $[\alpha]_D^{20}$ :  $-7.5^\circ$  (C 4.5,  $\text{CHCl}_3$ ). FT-IR (KBr,  $\text{cm}^{-1}$ ): 1801 ( $-\text{COCl}$ ), 1372 ( $-\text{SO}_2-\text{NH}-$ ). EA found C 56.45, H 4.95, N 4.39, S 9.50,  $\text{C}_{16}\text{H}_{16}\text{ClNO}_3\text{S}$  requires C 56.89, H 4.74, N 4.15, S 9.48.  $^1\text{H}$  NMR ( $\text{CDCl}_3$ )  $\delta$ : 2.15 (1H, s,  $\text{ArSO}_2-\text{NH}$ ), 2.40 (3H, s,  $\text{Ar}-\text{CH}_3$ ), 3.03 (1H, m,  $\text{Ar}-\text{CH}_2$ ), 3.17 (1H, m,  $\text{Ar}-\text{CH}_2$ ), 4.22 (1H, m,  $\text{ArCH}_2-\text{CH}$ ), 7.08–7.61 (9H, m,  $\text{Ar}-\text{H}$ ).

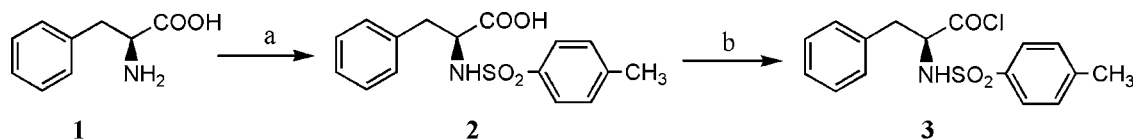
### Preparation of Dendritic Stationary Phases

Aminopropylsilica **4** was prepared by the well-known method refluxing the mixture of 3-aminopropyltriethoxysilane and dried silica gel in toluene.<sup>22</sup> The capacity of amine was estimated as 1.38 mmol/g, calculated from the nitrogen content of Aminopropylsilica which was available from EA. FT-IR (KBr,  $\text{cm}^{-1}$ ): 3444 (N—H, st), 1635 (N—H, m), 1113 (Si—O, st). EA: C 5.39, N 1.94, H 1.56.

Above obtained **4** (20.84 g) was dispersed in toluene (60 mL) and MA (55 mL, 0.61 mol) was added. After being vibrated at a rate of 120 times per minute in a temperature-constant environment of  $37^\circ\text{C}$  for 24 h, the mixture was filtered. The collected solid was extracted with THF and dried under vacuum to give **G1a** as a yellow powder (22.45 g). FT-IR (KBr,  $\text{cm}^{-1}$ ): 1735 ( $-\text{CO}_2-$ , m), 1103 (Si—O, st). EA: C 11.95, H 2.48, N 1.64.

To a suspension of above obtained **G1a** (22.28 g) in toluene (75 mL) was added EDA (90 mL, 1.35 mol). After vibrated in a temperature-constant environment of  $37^\circ\text{C}$  for 24 h at a rate of 120 times per min, the mixture was filtered. The collected solid was extracted with THF and dried under vacuum to give **G1b** (22.32 g). FT-IR (KBr,  $\text{cm}^{-1}$ ): 3444 (N—H, st), 1650 ( $-\text{NH}-\text{CO}-$ , m), 1100 (Si—O, st). EA: C 13.55, H 2.95, N 4.60.

The preparation of **G2a**, **G2b**, **G3a**, **G3b**, **G4a**, and **G4b** was carried out by recursively repeating the above two procedures, and the same reagents were used in the similar proportions, respectively. For **G2a**: FT-IR (KBr,  $\text{cm}^{-1}$ ): 1739 ( $-\text{CO}_2-$ , m), 1697 ( $-\text{NH}-\text{CO}-$ , m), 1104 (Si—O, st). EA: C 16.98, H 3.39, N 3.80. For **G2b**: FT-IR (KBr,  $\text{cm}^{-1}$ ): 3444 (N—H, st), 1653 ( $-\text{NH}-\text{CO}-$ , m), 1101 (Si—O, st). EA: C 18.19, H 3.94, N 6.97. For **G3a**: FT-IR (KBr,  $\text{cm}^{-1}$ ): 1736 ( $-\text{CO}_2-$ , m), 1653 ( $-\text{NH}-\text{CO}-$ , st), 1101 (Si—O, st). EA: C 23.10, H 4.17, N 5.93. For **G3b**: FT-IR (KBr,  $\text{cm}^{-1}$ ): 3444 (N—H, st), 1643 ( $-\text{NH}-\text{CO}-$ , m), 1101 (Si—O, st). EA: C 23.16, H 4.72, N 8.54. For **G4a**: FT-IR (KBr,  $\text{cm}^{-1}$ ): 1737 ( $-\text{CO}_2-$ , m), 1655 ( $-\text{NH}-\text{CO}-$ , st), 1101 (Si—O, st). EA: C 25.99, H 4.31, N 7.65. For **G4b**: FT-IR (KBr,  $\text{cm}^{-1}$ ): 3444



a: *p*-toluenesulfonyl chloride, 1 mol/L NaOH; b:  $\text{SOCl}_2$ ,  $\text{CHCl}_3$

**Scheme 1.** Synthesis of chiral selector.

(N—H, st), 1653 (—NH—CO—, m), 1101 (Si—O, st). EA: C 26.63, H 5.06, N 10.86.

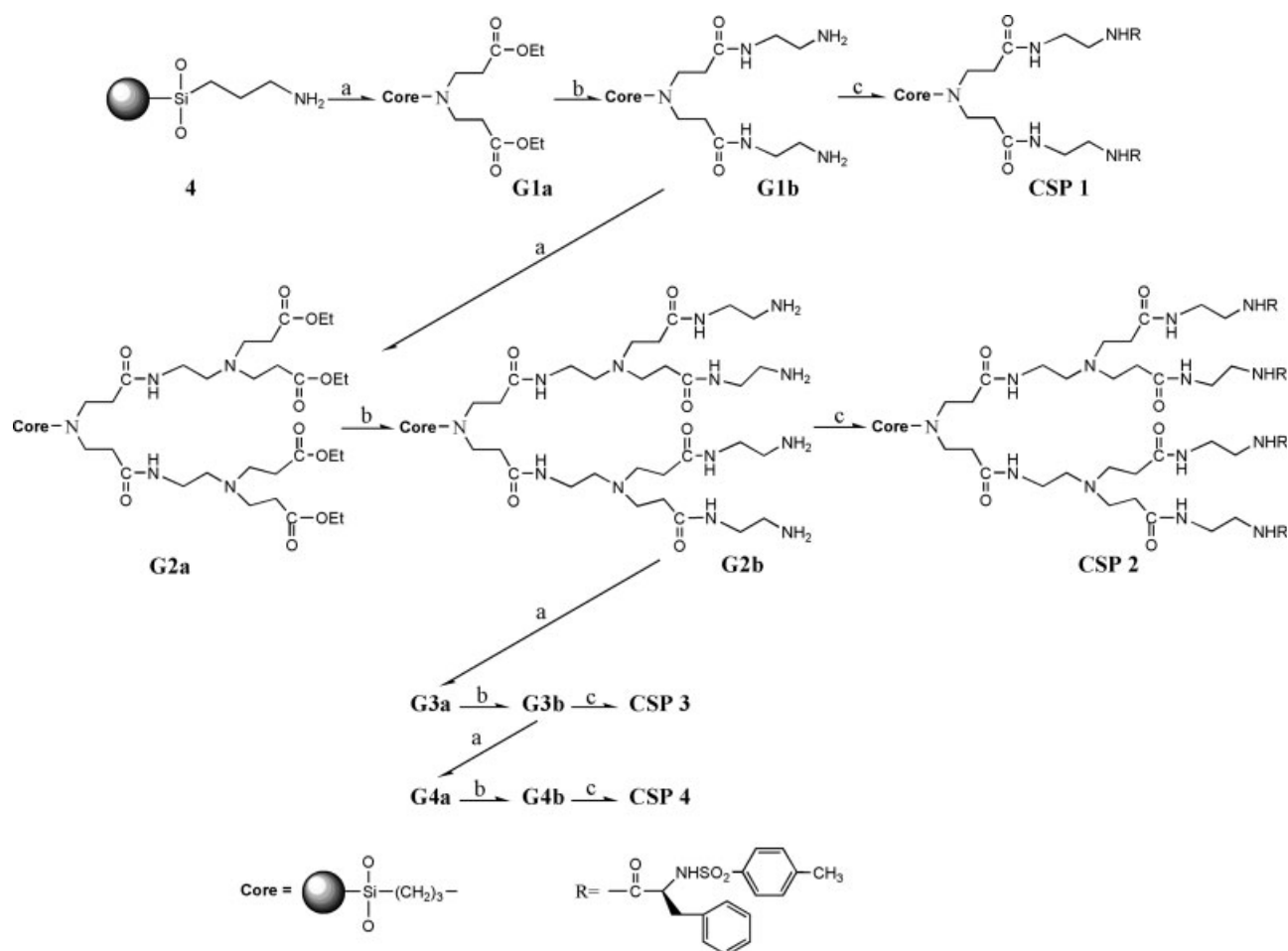
### Preparation of Dendritic Chiral Stationary Phases

To a suspension of **G1b** (3.70 g) in pyridine (16 ml) was added **3** (3.0 g, 8.90 mmol) and TEA (3 ml). After stirred at 60°C for 24 h, the mixture was filtered. The collected solid was extracted with THF and dried under vacuum to afford **CSP 1** as a yellow powder (4.62 g). FT-IR (KBr,  $\text{cm}^{-1}$ ): 1649 (—CO—NH—), 1398 (—SO<sub>2</sub>—NH—), 1102

(Si—O, st). EA: C 20.56, H 3.96, N 4.63, S 1.02. Solid-state  $^1\text{H}$  NMR (25°C)  $\delta$ : 0.9 (s, Si—CH<sub>2</sub>), 1.4 (s, SiCH<sub>2</sub>—CH<sub>2</sub>), 2.1 (s, ArSO<sub>2</sub>—NH), 2.3 (s, Ar—CH<sub>3</sub>), 2.7 (m, N—CH<sub>2</sub>), 3.2 (m, Ar—CH<sub>2</sub>), 3.9 (m, CONH—CH<sub>2</sub>), 4.9 (m, ArCH<sub>2</sub>—CH), 6.5 (s, CO—NH), 6.9–7.6 (m, Ar—H).

Identical coupling procedures were applied to **G2b**, **G3b**, and **G4b** to prepare **CSP 2**, **3**, and **4**, respectively.

For **CSP 2**: FT-IR (KBr,  $\text{cm}^{-1}$ ): 1650 (—NH—CO—), 1400 (—SO<sub>2</sub>—NH—), 1101 (Si—O, st). EA: C 21.33, H 4.42, N 6.05, S 0.96. Solid-state  $^1\text{H}$  NMR (25°C)  $\delta$ : 0.9 (s,



a: MA, Toluene, 37°C, 24h; b: EDA, Toluene, 37°C, 24h; c: **3**, pyridine, TEA, 60°C, 24h

**Scheme 2.** Synthesis of CSPs with dendritic linkers.

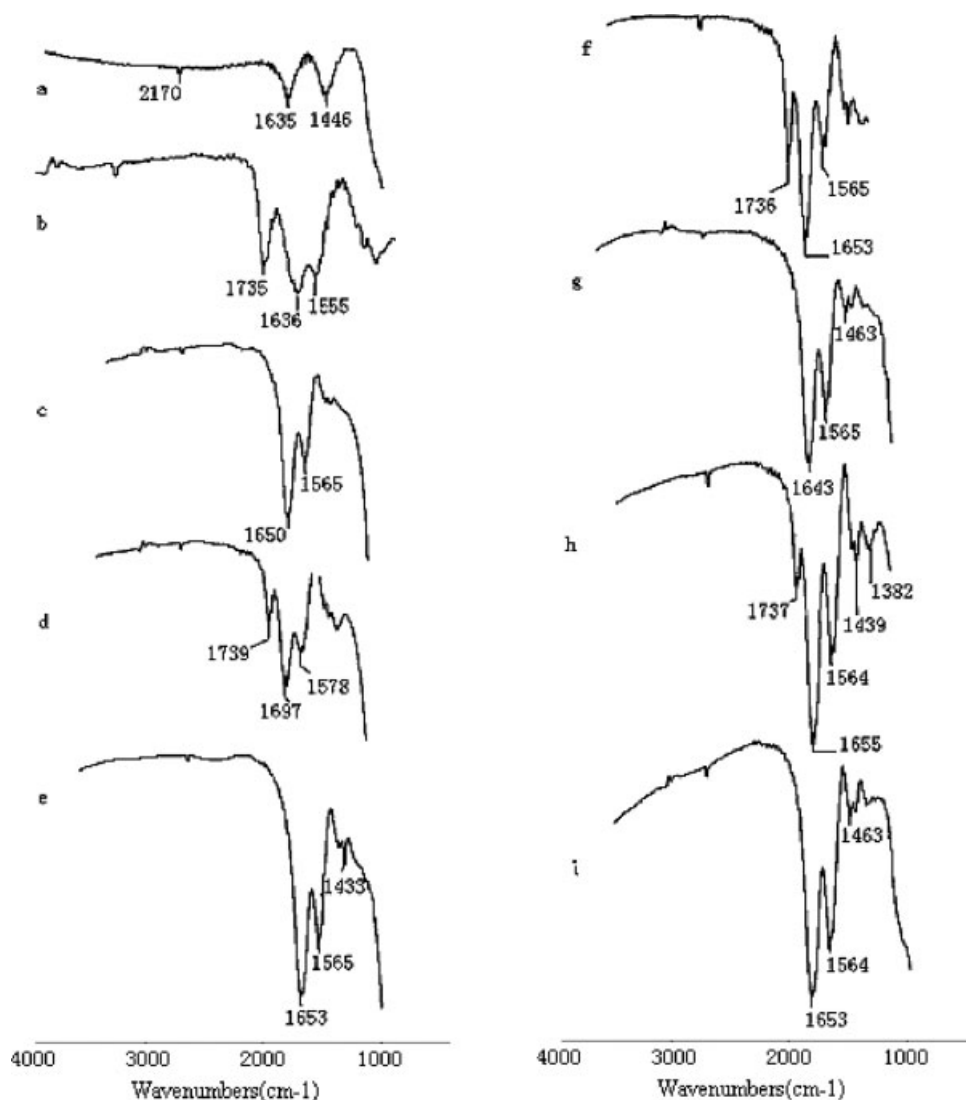


Fig. 1. The FT-IR spectra of 4 (a), G1a (b), G1b (c), G2a (d), G2b (e), G3a (f), G3b (g), G4a (h), G4b (i).

Si—CH<sub>2</sub>), 1.4 (s, SiCH<sub>2</sub>—CH<sub>2</sub>), 2.1 (s, ArSO<sub>2</sub>—NH), 2.3 (s, Ar—CH<sub>3</sub>), 2.7 (m, N—CH<sub>2</sub>), 3.2 (m, Ar—CH<sub>2</sub>), 3.9 (m, CONH—CH<sub>2</sub>), 4.9 (m, ArCH<sub>2</sub>—CH), 6.8 (s, CO—NH),

7.2–7.6 (m, Ar—H). For **CSP 3**: FT-IR (KBr, cm<sup>-1</sup>): 1651 (—NH—CO—), 1400 (—SO<sub>2</sub>—NH—), 1100 (Si—O, st). EA: C 25.01, H 4.99, N 9.27, S 0.38. Solid-state <sup>1</sup>H NMR (25°C) δ: 0.9 (s, Si—CH<sub>2</sub>), 1.4 (s, SiCH<sub>2</sub>—CH<sub>2</sub>), 2.1 (s, ArSO<sub>2</sub>—NH), 2.3 (s, Ar—CH<sub>3</sub>), 2.7 (m, N—CH<sub>2</sub>), 3.1 (m, Ar—CH<sub>2</sub>), 3.9 (m, CONH—CH<sub>2</sub>), 4.3 (m, ArCH<sub>2</sub>—CH),

TABLE 1. Elemental analysis data of the generation-various dendrimers

Dendrimer	Elemental analysis		
	C (%)	H (%)	N (%)
G1a	11.95	2.48	1.64
G1b	13.55	2.95	4.60
G2a	16.98	3.39	3.80
G2b	18.19	3.94	6.97
G3a	23.10	4.17	5.93
G3b	23.16	4.72	8.54
G4a	25.99	4.31	7.65
G4b	26.63	5.06	10.86

TABLE 2. Elemental analysis data and chiral selector loadings for CSPs

Elemental analysis	CSP 1	CSP 2	CSP 3	CSP 4
C%	20.56	21.33	25.01	27.48
H%	3.96	4.42	4.99	4.94
N%	4.63	6.05	9.27	10.47
S%	1.02	0.96	0.38	0.20
Selector Loading, μmol/g	318	300	118	62

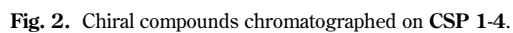




TABLE 3. Chromatographic resolution of racemates on CSP 1<sup>a</sup>

Compounds	Mobile phase composition (v/v)	Chromatographic results		
		$k_1$	$\alpha$	$R_s$
<b>5</b>	<i>n</i> -Hexane/ethanol (60/40)	1.09	1.48	1.41
<b>7</b>	<i>n</i> -Hexane/ethanol (60/40)	0.29	1.47	0.86
<b>8</b>	<i>n</i> -Hexane/ethanol (60/40)	0.05	1.47	3.67
<b>10</b>	ACN /buffer (70/30, pH5.94)	0.17	1.06	0.76
<b>11</b>	<i>n</i> -Hexane/iso-propanol (70/30)	0.06	1.92	0.44
<b>15</b>	<i>n</i> -Hexane/ethanol (60/40)	0.73	1.62	1.64
<b>18</b>	ACN/water (75/25)	0.36	1.18	0.53
<b>19</b>	Methanol/ACN (65/35)	0.15	1.45	2.48
<b>23</b>	ACN/water/TCA (60/40)	0.10	1.89	0.61
<b>24</b>	ACN/water (70/30)	0.37	1.05	0.48
<b>26</b>	Methanol/water/TCA (60/40) <sup>b</sup>	1.45	1.26	1.60
<b>30</b>	<i>n</i> -Hexane/iso-propanol (70/30)	0.34	2.02	1.10

<sup>a</sup>Retention factor ( $k_1$ ):  $(t_1 - t_0)/t_0$ , where  $t_1$  is the retention time of the first-eluted enantiomer, and  $t_0$  is determined by measuring the retention time of the solvent, which is used to prepare samples. Separation factor ( $\alpha$ ):  $k_1/k_2$ ; retention ( $R_s$ ):  $2(t_2 - t_1)/(w_1 + w_2)$ , where  $w_1$  is the bandwidth of the first-eluted enantiomer, and  $t_2$  and  $w_2$  are the retention time and bandwidth of the second-eluted enantiomer, respectively. The same parameter definitions are for other cases hereafter. Chromatographic conditions: column temperature: 25°C; UV detection: 225 nm (compounds **5** and **8**), 245 nm (compounds **7**, **19**, and **30**), 265 nm (compounds **10**, **11**, **18**, **23**, and **26**), 285 nm (compounds **15** and **24**); flow-rate: 1.0 ml/min.

<sup>b</sup>TCA/water: 1 g/100 ml.

6.0 (s, CO—NH), 7.2–7.8 (m, Ar—H). For **CSP 4**: FT-IR (KBr,  $\text{cm}^{-1}$ ): 1652 (—NH—CO—), 1399 (—SO<sub>2</sub>—NH—), 1103 (Si—O, st). EA: C 27.48, H 4.94, N 10.47, S 0.20. Solid-state <sup>1</sup>H NMR (25°C)  $\delta$ : 0.9 (s, Si—CH<sub>2</sub>), 1.4 (s, SiCH<sub>2</sub>—CH<sub>2</sub>), 2.1 (s, ArSO<sub>2</sub>—NH), 2.3 (s, Ar—CH<sub>3</sub>), 2.6 (m, N—CH<sub>2</sub>), 3.2 (m, Ar—CH<sub>2</sub>), 4.0–4.3 (m, CONH—CH<sub>2</sub>, ArCH<sub>2</sub>—CH), 6.1 (s, CO—NH), 7.1–7.6 (m, Ar—H).

#### Column Packing and Enantioseparation Conditions

**CSP 1**, **2**, **3** and **4** were, respectively, packed into four columns through a slurry method with chloroform as solvent to form the slurries and hexane as the packing solvent. And their column efficiencies were 26,680, 27,300, 27,792, and 24,116 plates/m, respectively, which were determined using biphenyl as the probe, and *n*-hexane/IPA (90/10) as the mobile phase. The enantioseparation of chiral compounds on these four CSPs was conducted in various mobile phase conditions at 25°C. The sample solutions were prepared by dissolving the chiral solutes in acetonitrile (ACN) and were filtered before injection. Triethylammonium acetate buffer was prepared by adjusting the pH value of 1% aqueous glacial acetic acid to desired value with addition of triethylamine.

## RESULTS AND DISCUSSION

### Preparation of Chiral Selector

According to Scheme 1, chiral selector **3** was prepared by the reaction between *L*-phenylalanine and *p*-toluenesulfonyl chloride in NaOH solution, followed by reacting the resultant with SOCl<sub>2</sub>. Because of highly reactive functional group of acyl chloride, chiral selector **3** is readily coupled with amine in the dendrimers in comparison with **2**, in which carboxyl is coupling group. In addition, there are

two phenyls in the molecular structure of **3**, which show  $\pi$ -basic and might be helpful for enantioseparation of racemates on CSPs.

### Preparation of Dendritic Stationary Phases by Divergent Approach

As shown in Scheme 2, the preparation of the one-generation stationary phase was carried out in two-step procedure: (i) bonding MA onto the surface of aminated silica gel via Michael addition to give **G1a**, followed by (ii) amidation of the resulting ester of **G1a** with EDA to afford the one-generation dendrimer containing bifunctional linkers (**G1b**). In the first step reaction, an excess of MA was added and **G1a** was obtained with a weight increment of 7.7% in comparison with that of aminated silica gel **4**. To ensure that only one of the two amino groups of EDA was acylated and another one was remained as the linking group for the further reaction, a large excess of EDA was adopted to react with **G1a** to form the one-generation dendrimer **G1b**. The weight of **G1b** increased by 0.18% when compared with that of **G1a**. The preparation of two-, three-, and four-generation dendrimers was carried out by repeating this two-step procedure, i.e. Michael addition and amidation. Figure 1 shows the FT-IR spectra of the products of all reactions involving the preparation of four dendrimers. The typical ester bands of **G1a**, **G2a**, **G3a**, and **G4a** appear approximately at 1735  $\text{cm}^{-1}$ . The amide bands of dendrimers appear approximately at 1650  $\text{cm}^{-1}$  except for that of **G2a** at 1697  $\text{cm}^{-1}$ . The amidation of **G1a**, **G2a**, **G3a**, and **G4a** is accompanied by disappearance of the ester bands. EA data of the dendrimers are shown in Table 1. The carbon and nitrogen contents do not increase proportionally in comparison with the increase of generation numbers of dendrimers, meaning that the formation of dendrimers has not been controlled

**TABLE 4. Effect of mobile phase composition on the enantioseparation of compound 19 separated by CSP 1**

Mobile phase (v/v)	$k_I$	$\alpha$	$R_s$
Methanol/water		No separation	
ACN/water (65/35)	0.08	1.07	0.61
THF/water (50/50)	0.19	1.28	1.41
Methanol/ACN (50/50)	0.32	1.45	2.50

Chromatographic condition: column temperature: 25°C; UV detection: 225 nm; flow-rate: 0.5 ml/min.

precisely in architecture. It is probably due to a combination of the factors that include the intra-molecular amidation, as well as the bulkiness of dendritic linker to small molecules, such as EDA and MA.

#### Preparation of Dendritic Chiral Stationary Phases

Finally, **CSP 1**, **2**, **3**, and **4** were prepared by coupling selector **3** to the surface of corresponding dendrimers through amidation (Scheme 2). The typical sulfonamide bands appear approximately at  $1399\text{ cm}^{-1}$  from the FT-IR spectra of the four generations of CSPs. And the solid-state  $^1\text{H}$  NMR spectra of these four CSPs show the chemical shifts of the aromatic protons at the range from  $\delta$  6.9 to 7.8, and sulfonamide proton at  $\delta$  2.1. Table 2 shows the EA data and the selector loadings of **CSP 1–4**, which are calculated from the increase of sulfur content. The selector loadings of CSPs generally show a decrease tendency with the increase of the generation number of CSPs from 318 to  $62\text{ }\mu\text{mol/g}$ , although each increase in generation number of dendritic linker, theoretically, should result in doubled loading. Noteworthily, the selector loadings of **CSP 1** and **2** are almost equal, and the selector loading of **CSP 4** is one fifth of those of **CSP 1** and **2**.

#### Enantioseparation Evaluation of CSP 1

The enantioseparation evaluation of **CSP 1** was preliminarily performed with a variety of racemates or drugs shown in Figure 2, and the related enantioseparation data of 12 compounds are tabulated in Table 3. It was noticed

that several compounds, such as compounds **11** and **23**, were separated with rather small resolution factors but high separation factors. In these cases, the retention time of the first-eluted enantiomer ( $t_1$ ) is close to that of the solvent ( $t_0$ ), and two peaks of enantiomers are tailed. When  $t_1$  is close to  $t_0$ , the value of  $t_1 - t_0$  will be very small. As denominator, the small value of  $t_1 - t_0$  should lead to a high separation factor ( $\alpha = (t_2 - t_0)/(t_1 - t_0)$ ). And the broad tailed peaks always have rather big bandwidths, which lead to a small resolution factor ( $R_s = 2(t_2 - t_1)/(w_1 + w_2)$ ).

As one of the factors that influence the enantioseparation of racemates, the effect of mobile phase composition on the enantioseparation of compound **19** on **CSP 1** was investigated (Table 4). Compound **19** was not separated in the mobile phase of methanol/water, but was discriminated when the mobile phase consisted of ACN/water, THF/water and ACN/methanol, respectively. Especially in the mobile phase of ACN/methanol 50/50, compound **19** was separated with optimum resolution ( $R_s = 2.50$ ). It is obvious that the increase of the content of aprotic solvent in mobile phase results in better separation of compound **19**. In the molecular structure of compound **19**, there are a hydroxyl group and an ester group. The diastereomer is easier formed through intermolecular hydrogen bond among **19**, protic solvent and chiral selector. Therefore, the composition of mobile phase should be adjusted so that the retention factor and resolution of **19** fall into the reasonable range.

#### Enantioseparation Evaluation of CSP 2

Table 5 shows that nine compounds shown in Figure 2 were separated on **CSP 2**. In view of the number of the racemates separated, the enantioseparation ability of **CSP 2** was not as good as that of **CSP 1**. Table 6 shows the effect of the methanol contents in mobile phase of methanol/water on the enantioseparation of compounds **6** and **16** resolved by **CSP 2**. Obviously, the methanol contents differently affect the enantioseparation of compounds **6** and **16**. Compound **6** cannot be separated when the content of methanol was less than 25%, but is separated as the

**TABLE 5. Chromatographic resolution of racemates on CSP 2**

Compounds	Mobile phase composition (v/v)	Chromatographic results		
		$k_I$	$\alpha$	$R_s$
<b>5</b>	ACN/water (33/67)	0.66	3.62	1.50
<b>6</b>	ACN/water (33/67)	0.17	1.47	0.73
<b>7</b>	Methanol/water (80/20)	0.18	1.41	0.56
<b>8</b>	Methanol/water (70/30)	0.86	1.16	1.03
<b>9</b>	Methanol/water (65/35)	0.16	1.77	1.22
<b>15</b>	Methanol/water (65/35)	1.65	1.45	1.53
<b>16</b>	Methanol/water (40/60)	0.23	1.49	0.64
<b>25</b>	n-Hexane/iso-propanol (60/40)	0.15	1.39	0.55
<b>26</b>	n-Hexane/iso-propanol (70/30)	0.17	2.40	1.97

Chromatographic conditions: column temperature: 25°C; UV detection: 225 nm (compounds **5**, **6**, **8**, **9**, and **25**), 245 nm (compounds **7**, **15**, and **26**), 265 nm (compound **16**); flow-rate: 1.0 ml/min.

Chirality DOI 10.1002/chir

**TABLE 6. Effect of the methanol content in eluent on the enantioseparation of compounds **6** and **16** resolved by CSP **2****

Methanol/water (v/v)	Compound <b>6</b>			Compound <b>16</b>		
	$k_1$	$\alpha$	$R_s$	$k_1$	$\alpha$	$R_s$
15/85	No separation			0.17	1.16	0.82
25/75	No separation			0.12	1.12	0.71
30/70	0.22	1.25	1.10	0.10	1.09	0.64
35/65	0.24	1.23	0.90	0.08	1.07	0.60
40/60	0.16	1.15	0.76	0.08	1.08	0.69

Chromatographic condition: column temperature: 25°C; UV detection: 245 nm (compound **6**), 265 nm (compound **16**); flow-rate: 0.5 ml/min.

methanol content increased. Compound **16** can be separated in various proportions of methanol/water, and its enantioseparation is hardly affected by the methanol content. This difference may be caused by the different ability of these two compounds to form hydrogen bond with mobile phase. Compound **6** weakly interacts with methanol to form hydrogen bond, while compound **16** strongly interacts with methanol due to one hydroxyl and one secondary amine contained in its structure.

#### Enantioseparation Evaluation of CSP **3**

As shown in Table 7, seventeen compounds shown in Figure 2 were separated on CSP **3**. Comparing the se-

lector loadings and enantioseparation abilities of CSP **1–3**, it is apparent that the CSP with higher selector loading does not definitely have higher enantioseparation ability. Despite the lowest content of selector moieties, CSP **3** shows the better enantioseparation ability in comparison with CSP **1** or **2**. This feature is possibly contributed to the imprecision in architecture of the dendrimers. When coupling with dendrimer, not all selectors of CSP **1** and **2** are located on the surface of the dendrimer and some of them are enveloped inside the dendrimer, which results in hindrance for analyte to access the chiral center of the selector to form diastereomers. For CSP **3**, it seems that fewer selectors are enveloped inside the dendrimer, and the most selectors expose to analytes.

In this work, the incorporation of TCA or TEA as additive in mobile phase was needed for efficient enantioseparation of acidic compounds. Acidic compounds **12**, **13**, **21**, **22**, and **25** were not separated on CSP **3** in the absence of TEA or TCA, but were separated in the presence of TEA or TCA, where the mobile phase consisted of methanol and water (Table 7). It is well known that acidic compounds will react with residual free amine on CSPs to form adducts, which reduce the enantioseparation. The role of added TEA or TCA in mobile phase is believed to suppress the deleterious effect of the formation of the adducts, making the acidic compounds eluted in a reasonable range with improved peak symmetry, resolution, and selectivity.<sup>23</sup>

**TABLE 7. Chromatographic resolution of racemates on CSP **3**<sup>a</sup>**

Compounds	Mobile phase composition (v/v)	Chromatographic results		
		$k_1$	$\alpha$	$R_s$
<b>5</b>	Methanol/water (70/30)	0.33	1.53	0.70
<b>7</b>	ACN/water (50/50)	0.43	1.09	0.27
<b>8</b>	Methanol/water (70/30)	0.37	1.48	0.66
<b>10</b>	Methanol/water/TEA (60/40) <sup>b</sup>	0.95	1.46	0.67
<b>12</b>	Methanol/water/TEA (70/30) <sup>b</sup>	0.76	1.45	1.13
<b>13</b>	Methanol/water/TEA (70/30) <sup>b</sup>	1.12	1.39	0.97
<b>14</b>	ACN /water (60/40) <sup>c</sup>	2.75	1.22	0.53
<b>15</b>	Methanol/water (70/30)	0.11	1.07	0.59
	Methanol/water/TEA (70/30) <sup>b</sup>	0.23	1.10	0.81
	Methanol/water/TEA (60/40) <sup>b</sup>	0.55	1.43	1.20
<b>16</b>	ACN /water/TEA (60/40)	0.12	1.98	0.64
<b>17</b>	Methanol/water (70/30) <sup>d</sup>	0.10	5.78	2.33
<b>18</b>	Methanol/water (70/30)	0.35	1.57	1.07
<b>21</b>	Methanol/water/TCA (70/30)	0.29	1.77	0.72
<b>22</b>	Methanol/water/TEA (70/30) <sup>b</sup>	0.09	1.16	0.60
<b>25</b>	Methanol/water/TEA (50/50)	0.08	1.22	0.96
<b>27</b>	Methanol/water/TEA (70/30) <sup>b</sup>	2.02	1.37	0.89
<b>28</b>	ACN /water (50/50)	1.31	1.15	0.67
<b>29</b>	Methanol/water (70/30)	0.43	1.22	0.60

<sup>a</sup>Chromatographic conditions: column temperature: 25°C; UV detection: 225 nm (compounds **7**, **8**, **13**, **18**, **21**, and **29**), 245 nm (compounds **5**, **10**, **14**, **15**, **25**, **27** and **28**), 265 nm (compounds **12**, **16**, **17** and **22**); flow-rate: 0.5 ml/min; amount of additive: TEA/water: 1 ml/100 ml, TCA/water: 1 g/100 ml.

<sup>b</sup>flow-rate: 0.2 ml/min.

<sup>c</sup>flow-rate: 0.7 ml/min.

<sup>d</sup>flow-rate: 0.4 ml/min.

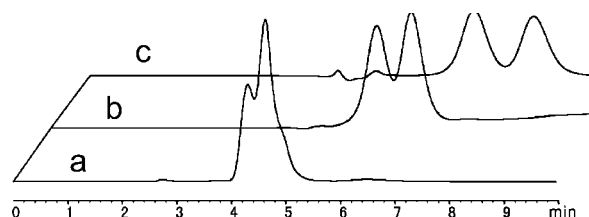


**Fig. 3.** Chromatograms of the enantioseparation of compound **15** by **CSP 3**. Chromatographic conditions: mobile phase: (a) methanol/water (70/30, v/v); (b) methanol/water (70/30, v/v) + TEA; (c) methanol/water (60/40, v/v) + TEA.

In addition to protonic acidic compounds, the enantioseparation of strong  $\pi$ -acidic compounds, such as compound **15**, can also be improved in the presence of TEA (Table 7). It is supposed that TEA decreases the interaction between nitro group and amine on the surface of **CSP 3**. Figure 3 shows the typical enantioseparation difference of compound **15** on **CSP 3** in the absence and presence of TEA. It is obvious that the resolution of compound **15** was further improved when the content of methanol in mobile phase was changed from 70 to 60% (v/v).

The influence of molecular structure on enantioseparation was assessed. In the mobile phase of methanol/water, compound **20** was not separated, whereas compounds **21** and **22** were separated in the presence of TCA and TEA, respectively. In this case, the dominant enantioselectivity is most likely through  $\pi$ - $\pi$  interaction of the phenyls in the analytes and the chiral selectors. These three compounds are similar in structural backbones with different substituents, hydroxyl, acetoxy, and acetyl, on the individual *para*-position of benzene rings (see Fig. 2). Electron-withdrawing acetyl group and electron-donating hydroxyl group lead to  $\pi$ -acidity and strong  $\pi$ -basicity of the aromatic moiety, respectively. And weak electron-donating group acetoxy leads to weak  $\pi$ -basicity of aromatic moiety. Therefore, compound **20** can not be discriminated due to lack of  $\pi$ - $\pi$  interaction with  $\pi$ -basic aromatic moiety on **CSP 3**. The similar feature on the enantioseparation of these three compounds on polymer-type CSPs was reported in our previous work.<sup>24</sup> Furthermore, because of the  $\pi$ -basicity of the aromatic moiety on **CSP 3**, the com-

pounds bearing stronger  $\pi$ -basic aromatic moiety, such as compounds **11** and **23**, were not separated on **CSP 3**. On the contrary, the compounds with stronger  $\pi$ -acidic aromatic moiety, such as compounds **5**, **15**, and **28**, were better separated.

#### Enantioseparation Evaluation of CSP 4

The enantioseparation ability of **CSP 4** was evaluated with the same racemic mixtures, but only seven compounds were separated under various conditions even at lower flow rates (Table 8). It is obvious that the chiral recognition of **CSP 4** is the poorest among these four CSPs. The possible reasons include: first, there is much less selectors loaded on **CSP 4**, and second, as the generation number of the dendrimer increases, the terminal groups became crowded, resulting in more steric hindrance of the interaction between the analytes and the chiral selectors.

Generally, the resolution values of most analytes separated by these four CSPs are comparatively low. This is probably resulted from lots of amides in dendritic linkers produced when constructing dendrimers. Interactions, such as the formation of hydrogen bonds in different sites of dendritic linkers, occur between analytes and dendrimers, leading small retention time difference of enantiomers when eluted by mobile phases. This can be exemplified that some peaks of enantiomers broaden or tail.

## CONCLUSIONS

Four generations of dendrimer-like CSPs were prepared by divergent approach; while their formation was not controlled precisely in architecture. In view of the number of racemic mixtures separated by these four CSPs, the three-generation-dendrimer selector demonstrates best separation ability, and the four-generation-dendrimer selector shows the poorest separation ability. The enantioseparation capability of these dendritic CSPs seems to be influenced by a combination of factors that include the bulkiness of dendritic linkers, amides contained in dendritic linkers and selectors loading on the surface of CSPs. In chiral recognition, the resolution of racemates is affected by the composition of mobile phase and the proportion of solvents in mobile phase. Especially, the analytes that

**TABLE 8.** Chromatographic resolution of racemates on **CSP 4**<sup>a</sup>

Compound	Mobile phase composition (v/v)	Chromatographic results		
		$k_1$	$\alpha$	$R_s$
<b>5</b>	<i>n</i> -hexane/iso-propanol (70/30)	0.46	2.27	0.33
<b>15</b>	Methanol/water/TEA (70/30) <sup>b</sup>	0.50	1.35	0.89
<b>16</b>	Methanol/water (70/30)	0.10	2.20	0.69
<b>26</b>	Methanol/water (60/40)	0.49	1.65	1.76
<b>28</b>	ACN/water (60/40)	0.14	1.43	0.54
<b>29</b>	Methanol/water/TEA (70/30) <sup>b</sup>	0.41	1.13	0.36
<b>31</b>	Methanol/water (70/30)	0.71	1.20	0.67

<sup>a</sup>Chromatographic conditions: column temperature: 25°C; UV detection: 225 nm (compounds **5** and **16**), 245 nm (compounds **26** and **29**), 265 nm (compounds **15** and **31**), 285 nm (compound **28**); flow-rate: 0.5 ml/min.

<sup>b</sup>flow-rate: 0.2 ml/min.

Chirality DOI 10.1002/chir

form stronger hydrogen bonds with selectors were separated better in the mobile phase of ACN/water than that in methanol/water. The  $\pi$ -basicity or  $\pi$ -acidity of aromatic moiety of analytes remarkably affects their chiral discrimination. The analytes bearing stronger  $\pi$ -basic aromatic moiety cannot be separated, whereas the compounds bearing  $\pi$ -acidic aromatic moiety can be separated due to the formation of comparative stable complexes with  $\pi$ -basic chiral selectors on the surface of CSPs through  $\pi$ - $\pi$  interaction. In addition, the additive of TEA or TCA in the mobile phase is helpful for the separation of racemic mixtures, especially acidic mixtures.

### LITERATURE CITED

1. Rauws AG, Groen K. Current regulatory (draft) guidance on chiral medicinal products: Canada, EEC, Japan, United States. *Chirality* 1994;6:72–75.
2. Juza M, Mazzotti M, Morbidelli M. Simulated moving-bed chromatography and its application to chirotechnology. *Trends Biotechnol* 2000; 18:108–118.
3. Francotte ER. Enantioselective chromatography as a powerful alternative for the preparation of drug enantiomers. *J Chromatogr A* 2001; 906:379–397.
4. Haginaka J. Pharmaceutical and biomedical applications of enantio-separations using liquid chromatographic techniques. *J Pharm Biomed Anal* 2002;27:357–372.
5. Zhang Y, Wu D-R, Wang-Iverson DB, Tymiak AA. Enantioselective chromatography in drug discovery. *Drug Discov Today* 2005;10:571–577.
6. Gasparrini F, Misiti D, Villani C. High-performance liquid chromatography chiral stationary phases based on low-molecular-mass selectors. *J Chromatogr A* 2001;906:35–50.
7. Aboul-Enein HY, Ali I. Optimization strategies for HPLC enantioseparation of racemic drugs using polysaccharides and macrocyclic glycopeptide antibiotic chiral stationary phases. *Farmaco* 2002;57:513–529.
8. Roussel C, Rio AD, Pierrot-Sanders J, Piras P, Vanthuyne N. Chiral liquid chromatography contribution to the determination of the absolute configuration of enantiomers. *J Chromatogr A* 2004;1037:311–328.
9. Schulte M, Strube J. Preparative enantioseparation by simulated moving bed chromatography. *J Chromatogr A* 2001;906:399–416.
10. Archut A, Vögtle F. Functional cascade molecules. *Chem Soc Rev* 1998;27:233–240.
11. Vögtle F, Gestermann S, Hesse R, Schwierz H, Windisch B. Functional dendrimers. *Prog Polym Sci* 2000;25:987–1041.
12. Frechet JM. Functional polymers and dendrimers: reactivity, molecular architecture, and interfacial energy. *Science* 1994;263:1710–1715.
13. Zeng F, Zimmerman SC. Dendrimers in supramolecular chemistry: from molecular recognition to self-assembly. *Chem Rev* 1997;97:1681–1712.
14. Kolhe P, Misra E, Kannan RM, Kannan S, Lieh-Lai M. Drug complexation, in vitro release and cellular entry of dendrimers and hyper-branched polymers. *Int J Pharm* 2003;259:143–160.
15. Beezer AE, King ASH, Martin IK, Mitchel JC, Twyman LJ, Wain CF. Dendrimers as potential drug carriers; encapsulation of acidic hydrophobes within water soluble PAMAM derivatives. *Tetrahedron* 2003;59:3873–3880.
16. Schatzlein AG, Zinselmeyer BH, Elouzi A, Dufes C, Chim YTA, Roberts CJ, Davies MC, Munro A, Gray AI, Uchegbu IF. Preferential liver gene expression with polypropylenimine dendrimers. *J Control Release* 2005;101:247–258.
17. Takahashi M, Hara Y, Aoshima K, Kurihara H, Oshikawa T, Yamashita M. Utilization of dendritic framework as a multivalent ligand: a functionalized gadolinium(III) carrier with glycoside cluster periphery. *Tetrahedron Lett* 2000;41:8485–8488.
18. Bu J, Judeh ZMA, Ching CB, Kawi S. Epoxidation of olefins catalyzed by Mn(II) salen complex anchored on PAMAM-SiO<sub>2</sub> dendrimer. *Catal Lett* 2003;85:183–187.
19. Ling FH, Lu V, Svec F, Fréchet JMJ. Effect of multivalency on the performance of enantioselective separation media for chiral HPLC prepared by linking multiple selectors to a porous polymer support via aliphatic dendrons. *J Org Chem* 2002;67:1993–2002.
20. Mathews BT, Beezer AE, Snowden MJ, Hardy MJ, Mitchell JC. The synthesis of immobilised chiral dendrimers. *New J Chem* 2001; 25:807–818.
21. Huang SH, Li SR, Bai ZW, Pan ZQ, Yin CQ. Dendrimer-like chiral stationary phases derived from (1R, 2R)-(+)-1,2-diphenylethylenediamine and 1,3,5-benzenetricarbonyl trichloride. *Chromatographia* 2006;64: 641–646.
22. Ihara T, Sugimoto Y, Asada M, Nakagama T, Hobo T. Influence of the method of preparation of chiral stationary phases on enantiomer separations in high-performance liquid chromatography. *J Chromatogr A* 1995;694:49–56.
23. Zhang T, Nguyen D, Franco P, Murakami T, Ohnishi A, Kurosawa H. Cellulose 3,5-dimethylphenylcarbamate immobilized on silica; a new chiral stationary phase for the analysis of enantiomers. *Anal Chim Acta* 2006;557:221–228.
24. Huang SH, Bai ZW, Yin CQ, Li SR, Pan ZQ. Synthesis of polymer-type chiral stationary phases and their enantioseparation evaluation by high-performance liquid chromatography. *Chirality* 2007;19:129–140.

# Highly Enantioselective Synthesis, Crystal Structure, and Circular Dichroism Spectroscopy of (*R*)-Bambuterol Hydrochloride

GAO CAO,<sup>1</sup> AI-XI HU,<sup>2\*</sup> KANG-SHENG ZOU,<sup>3</sup> LING XU,<sup>3</sup> JIAN-LONG CHEN,<sup>3</sup> AND WEN TAN<sup>3\*</sup>

<sup>1</sup>The School of Chemical and Energy Engineering, South China University of Technology, Guangzhou, Guangdong, People's Republic of China

<sup>2</sup>College of Chemistry and Chemical Engineering, Hunan University, Changsha, Hunan, People's Republic of China

<sup>3</sup>Keypharma Biomedical Inc., Songshan Lake Science & Technology Industry Park, Dongguan, Guangdong, People's Republic of China

**ABSTRACT** The present article describes the asymmetric synthesis of (*R*)-bambuterol hydrochloride based on 1-(3,5-dihydroxyphenyl)ethanone as starting material, which was esterified by dimethylcarbamic chloride, and brominated by copper (II) bromide. Then the carbonyl group was reduced efficiently using (–)-B-chlorodiisopinocampheylborane [(–)-DIP-chloride<sup>TM</sup>] as an asymmetrical reducing agent. Followed by epoxide ring closure with NaOH and ring expansion with *tert*-butylamine led to the desired product (*R*)-bambuterol with *e.e.* up to 99%. The optical properties and absolute configuration of (*R*)-bambuterol hydrochloride were further investigated using circular dichroism spectroscopy and X-ray single crystal analysis. *Chirality* 20:856–862, 2008.

© 2008 Wiley-Liss, Inc.

**KEY WORDS:** (*R*)-bambuterol; asymmetric synthesis; DIP-chloride; circular dichroism; X-ray crystallography

## INTRODUCTION

Bambuterol hydrochloride is an oral long-acting  $\beta_2$ -adrenoceptor agonist for once-daily treatment of the symptoms of asthma, bronchospasm, emphysema, and chronic obstructive pulmonary disease.<sup>1–4</sup> Bambuterol also has liquid lowering effects in certain patients.<sup>5</sup> It is a bis-dimethylcarbamate prodrug of terbutaline with a considerable presystemic and metabolic stability. The drug itself is inactive, but it is metabolized enzymatically *in vivo* by Butyryl Cholinesterase (BuChE) into the active compound terbutaline (Chart 1).<sup>6</sup> On the other hand, bambuterol with two carbamate groups in the molecule also inhibits the activity of BuChE. Hence, the metabolism of bambuterol by BuChE is slow and the duration of action of bambuterol is prolonged.<sup>7,8</sup>

It has been sufficiently demonstrated that (*R*)-bambuterol was the biological active enantiomer which was at least two times more potent than (*S*)-bambuterol in the treatment of asthma.<sup>9</sup> Furthermore, (*S*)-bambuterol was inactive in anti-asthma but has more adverse cardiac toxic effects than (*R*)-bambuterol. It is also reported that (*R*)-enantiomer of bambuterol was about five times more potent for the inhibition of BuChE than (*S*)-enantiomer.<sup>10</sup> Furthermore, in recent years, a suspicion has been raised that the (*S*)-enantiomer of  $\beta_2$ -adrenoceptor agonists may cause airway hyper-reactivity and even contribute to an increase in asthma death.<sup>11</sup>

The present study investigated the asymmetric synthesis of (*R*)-bambuterol or (*S*)-bambuterol that was achieved by the reagent-controlled reduction of the corresponding aralkyl ketone with (–)-DIP-chloride<sup>TM</sup> or (+)-DIP-chloride<sup>TM</sup>. Moreover, we are able to produce single crystals

of (*R*)-bambuterol hydrochloride and elucidate the absolute configuration of (*R*)-bambuterol hydrochloride by X-ray crystal analysis. The optical properties of (*R*)-bambuterol hydrochloride were investigated further via optical rotation and circular dichroism (CD) spectroscopy for the first time.

## EXPERIMENTAL SECTION

### Instrumentation, General Methods

All melting points were measured on an X-4 electrothermal digital melting point apparatus and were uncorrected; <sup>1</sup>H NMR spectra were recorded on a Bruker advance instrument with TMS as internal standard, at 300 or 500 MHz, chemical shifts ( $\delta$ ) are expressed in ppm.; Specific rotations were measured on a JASCO P-1010 polarimeter; The IR spectra were recorded at room temperature using Bio-Rad FTS-40 Fourier transform infrared spectrometer and analyzed with Bio-Rad Win-IR software; ESI-MS were recorded on a Finnigan LCQ LC-MS spectrometer; TLC was performed on E-Merck pre-coated 60 F254 plates and the spots were rendered visible by exposing to UV light or iodine. The IUPAC names were obtained using the soft-

Contract grant sponsor: Keypharma Biomedical Inc.

\*Correspondence to: Dr. Wen Tan, Keypharma Biomedical Inc., Songshan Lake Science & Technology Industry Park, Dongguan, Guangdong 523808, People's Republic of China. E-mail: uscnwt@yahoo.com or Prof. Ai-Xi Hu, College of Chemistry and Chemical Engineering, Hunan University, Changsha, Hunan 410082, People's Republic of China. E-mail: axhu0731@yahoo.com.cn

Received for publication 16 September 2007; Accepted 1 February 2008

DOI: 10.1002/chir.20558

Published online 1 April 2008 in Wiley InterScience (www.interscience.wiley.com).



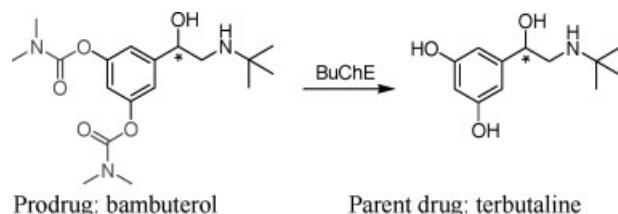


**Chart 1.** Chemical structure of bambuterol and terbutaline. \* Marks the chiral center.

ware ChemDraw Ultra<sup>®</sup>, version 9.0. Every starting material was obtained from commercial suppliers and was purified according to the literature procedures. Racemic bambuterol was prepared by the procedure as described in the literature.<sup>12</sup> (*S*)-Bambuterol hydrochloride was obtained via the same synthetic sequence by using (+)-DIP-chloride<sup>TM</sup> in the reduction step.

#### Experimental Procedure for the Preparation of (*R*)-Bambuterol Hydrochloride

**5-Acetyl-1,3-phenylene bis(dimethylcarbamate) (2).** A mixture of 1-(3,5-dihydroxy phenyl)ethanone (24 g, 0.16 mol), dimethylcarbamyl chloride (50 g, 0.46 mol), potassium carbonate 1.5 H<sub>2</sub>O (41 g, 0.25 mol), anhydrous potassium carbonate (9.4 g, 0.07 mol) and pyridine (1 g) in ethyl acetate (150 mL) was stirred at 70°C for 2 h. Water (120 mL) was added to the mixture, and the resulting mixture was stirred for further 1.5 h at 70°C. After cooling to room temperature, the reaction mixture was separated and the lower water phase was discarded. The organic phase was washed with diluted sulfuric acid (2%), dried over MgSO<sub>4</sub>, filtered, and the filtrate was concentrated in vacuo to give the product: 40 g, yield 86%. Mp: 58–60°C. <sup>1</sup>H NMR (CDCl<sub>3</sub>, 300 MHz)  $\delta$ : 2.58 (s, 3H, COCH<sub>3</sub>), 2.90, 3.10 (s, 12H, 2 $\times$ N(CH<sub>3</sub>)<sub>2</sub>), 7.20 (s, 1H, benzene ring 4-H), 7.55 (s, 2H, benzene ring 2,6-H).

**5-(2-Bromoacetyl)-1,3-phenylene bis(dimethylcarbamate) (3).** 5-Acetyl-1,3-phenylene bis(dimethylcarbamate) (38 g, 0.13 mol) was dissolved in ethyl acetate (100 mL) and chloroform (100 mL), and the mixture was stirred and heated to reflux. Copper (II) bromide (57.7 g, 0.26 mol) was added to the reaction mixture in batches and the course of the reaction was followed by TLC analysis. After the reaction finished (about 5 h), the mixture was filtered to remove the white solid CuBr, and the filtrate was washed with 10% hydrochloric acid, and then washed with water till neutral, dried over MgSO<sub>4</sub>, and filtered. The filtrate was concentrated and the crystals were collected on a filter: 44.1 g, yield 91%. Mp: 103–105°C. <sup>1</sup>H NMR (CDCl<sub>3</sub>, 300 MHz)  $\delta$ : 3.04, 3.12 (s, 12H, 2 $\times$ N(CH<sub>3</sub>)<sub>2</sub>), 4.40 (s, 2H, CH<sub>2</sub>), 7.25 (s, 1H, benzene ring 4-H), 7.58 (s, 2H, benzene ring 2,6-H).

**(*R*)-5-(2-Bromo-1-hydroxyethyl)-1,3-phenylene bis(dimethylcarbamate) (4).** A solution of 5-(2-bromoacetyl)-1,3-phenylene bis(dimethylcarbamate) (11 g, 30 mmol) in anhydrous tetrahydrofuran (100 mL) (distilled from sodium benzophenone ketyl) was added to a solution

of (–)-DIP-chloride<sup>TM</sup> (10.6 g, 33 mmol) in anhydrous tetrahydrofuran (60 mL) at –25°C under nitrogen. The resulting solution was stirred at –25°C for 60 h, and then warmed to 0°C, and diethanolamine (7 g, 66 mmol) was added dropwise. The mixture was warmed to room temperature and stirred for further 2 h, whereupon the boranes precipitated as a complex which was filtered and washed with pentane. The combined solvents were removed by distillation, and the residue was purified by silicagel column chromatography to give the product as an oil: 8.4 g, yield 75%.

**(*R*)-5-(Oxiran-2-yl)-1,3-phenylene bis(dimethylcarbamate) (5).** A 15% solution of NaOH in water (100 mL) was added to a solution of (*R*)-5-(2-bromo-1-hydroxyethyl)-1,3-phenylene bis(dimethylcarbamate) (7.0 g, 18.7 mmol) in ethanol (100 mL). The mixture was stirred at room temperature for 2 h. The reaction mixture was concentrated, treated with water, and extracted with ethyl acetate. The organic layer was washed with brine and water, and dried over MgSO<sub>4</sub>. The filtrate was evaporated and the residue dried under vacuum to give the product: 5.5 g, yield 100%. The product was used in the next step without further purification. <sup>1</sup>H NMR (CDCl<sub>3</sub>, 300 MHz)  $\delta$ : 2.56 (dd, *J* = 5.3, 2.4 Hz, 1H, epoxide CH<sub>2</sub>), 3.15 (dd, *J* = 5.1, 4.2 Hz, 1H, epoxide CH<sub>2</sub>), 4.20 (dd, *J* = 3.8 Hz, 2.6 Hz, 1H, epoxide CH), 3.0, 3.10 (s, 12H, 2 $\times$ N(CH<sub>3</sub>)<sub>2</sub>), 7.22 (s, 1H, benzene ring 4-H), 7.56 (s, 2H, benzene ring 2,6-H).

**(*R*)-Bambuterol hydrochloride (6).** A mixture of (*R*)-5-(oxiran-2-yl)-1,3-phenylene bis(dimethylcarbamate) (5.5 g, 18.7 mmol) in *tert*-butylamine (80 mL) was stirred at reflux for 3 days. The mixture was concentrated to dryness, treated with water, and extracted with ethyl acetate. The organic layer was washed with water and dried over MgSO<sub>4</sub>. The filtrate was concentrated and the residue was treated with a solution of hydrogen chloride in diethyl ether to give (*R*)-bambuterol hydrochloride as white solid. Recrystallization from ethanol gave 5.2 g product, yield 69%. Mp: 224–226°C. IR (KBr)  $\nu$ : 3220, 3047, 2877, 2846, 2801, 2451, 1716, 1691, 1612, 1561, 1494, 1447, 1417, 1400, 1388, 1360, 1326, 1293, 1270, 1182, 1141, 1102 cm<sup>–1</sup>. <sup>1</sup>H NMR (DMSO, 500 MHz)  $\delta$ : 1.30 (s, 9H, NC(CH<sub>3</sub>)<sub>3</sub>), 2.90, 3.03 (s, 14H, CH<sub>2</sub>, 2 $\times$ N(CH<sub>3</sub>)<sub>2</sub>), 5.02 (d, *J* = 9.5 Hz, 1H, CH), 6.31 (bs, 1H, OH), 6.88 (s, 1H, benzene ring 4-H), 7.06 (s, 2H, benzene ring 2,6-H), 8.54, 9.57 (2 $\times$ bs, 2H, NH, HCl). <sup>13</sup>C NMR (Pyridine, 125MHz)  $\delta$ : 24.96, 36.15, 39.50, 48.12, 56.30, 68.06, 115.08, 116.07, 143.84, 151.52, 153.58 ppm. Anal. Calcd for C<sub>18</sub>H<sub>29</sub>N<sub>3</sub>O<sub>5</sub>·HCl (403.19): C, 53.53; H, 7.49; N, 10.40; Cl, 8.78. Found: C, 53.58; H, 7.47; N, 10.42; Cl, 8.72. ESI-MS *m/z*: 367.2 (M<sup>+</sup>–HCl), 293.4, 86.2, 72.1.  $[\alpha]_D^{20}$  = –26.1 (c 2, H<sub>2</sub>O). Chiral high-performance liquid chromatography (HPLC), 99.9% *e.e.* (*R*, 99.95%, *S*, 0.05%).

#### Chiral HPLC Analysis

The HPLC used was a CLASS-VP Ver. 6.1 system (Shimadzu, Japan) comprised of a Shimadzu SPD10Avp UV detector, a Shimadzu LC-10ATvp multisolvent delivery system, a Shimadzu SCL-10Avp controller, a Shimadzu LC pump, and a Shimadzu CLASS-VP Ver. 6.1 workstation.

**TABLE 1.** Crystallographic data and structure refinement for (*R*)-bambuterol hydrochloride

CCDC No.	655621
Empirical formula	C <sub>18</sub> H <sub>30</sub> N <sub>3</sub> O <sub>5</sub> Cl
Mol. Weight	403.90
Color, habit	Colorless, block
Crystal dimensions (mm <sup>3</sup> )	0.40 × 0.24 × 0.20
Crystal system	Monoclinic
Space group	<i>P</i> 2 <sub>1</sub>
<i>Z</i>	2
Lattice parameters (Å)	<i>a</i> = 8.3028(7) <i>b</i> = 14.5439(11) <i>c</i> = 8.8130(7)
β (°)	105.9310(10)
Volume (Å <sup>3</sup> )	1023.34(14)
Calculated density (g/cm <sup>3</sup> )	1.311
<i>F</i> (000)	432
θ Range for data collection (°)	2.40–26.92
Measured reflections	5485
Independent reflections	3519
Goodness-of-fit on <i>F</i> <sup>2</sup>	1.110
Final <i>R</i> indices [ <i>I</i> > 2σ( <i>I</i> )]	<i>R</i> <sub>1</sub> = 0.0457, <i>wR</i> <sub>2</sub> = 0.1072
<i>R</i> Indices (all data)	<i>R</i> <sub>1</sub> = 0.0684, <i>wR</i> <sub>2</sub> = 0.1199
Absolute structure parameter <i>γ</i>	0.05(9)
Largest diff. peak and hole (e Å <sup>−3</sup> )	0.323, −0.238

The Chiralcel-OJ column packed with the polysaccharide derivative coated on 10 μm silica particles was obtained from Daicel Chemical Industries (Tokyo, Japan). The column dimensions were 250 mm × 4.6 mm. Mobile phase of following composition was used: hexanes/ethanol/diethylamine = 230:20:0.75 (v/v). The flow rate was 1.0 mL/min.

#### Circular Dichroism Spectrum

The CD spectrum of racemic bambuterol hydrochloride and its enantiomers were measured on a JASCO J-715

spectropolarimeter, equipped with a Hamamatsu R376 photomultiplier (185–850 nm) using a bandwidth of 1 nm. The test was taken at 25°C and in 0.1 mol/L diluted hydrochloric acid solution at the concentration of 1 mmol/L. Scans were obtained in a range from 230 to 350 nm by taking points every 1 nm.

#### X-ray Crystallography

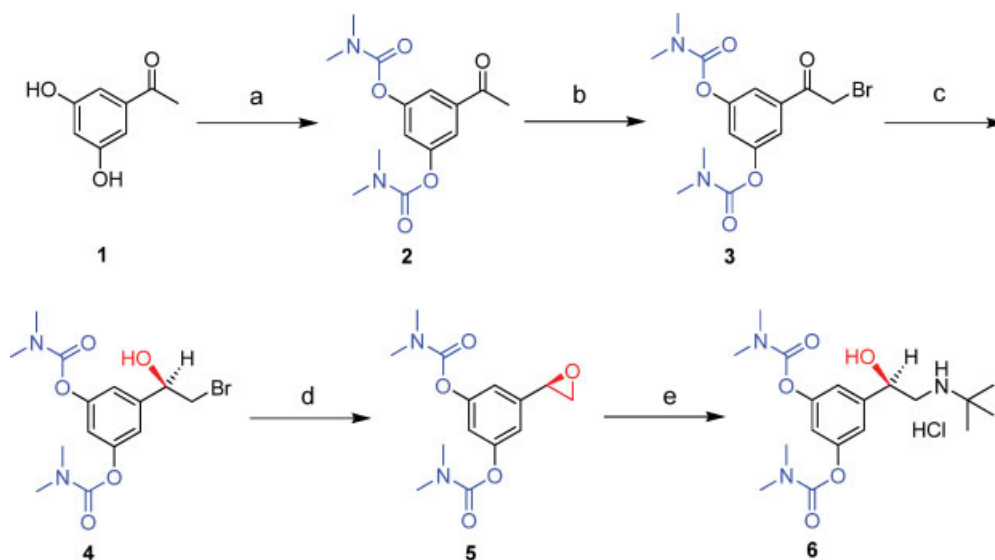
Single-crystal X-ray diffraction experiment for (*R*)-bambuterol hydrochloride was performed on a Bruker AXS SMART 1000 CCD diffractometer equipped with graphite-mono chromated Mo-*K*<sub>α</sub> radiation (λ = 0.71073 Å). Colorless crystals suitable for X-ray diffraction analysis were grown by slow evaporation of ethanol. The data set was recorded at 173(2) K in an ω-φ scan mode. Preliminary orientation matrices were obtained from the first frames using SMART. The data were empirically corrected for absorption and other effects using SADABS. The structure was solved by direct methods and refined by the full-matrix least-squares methods on *F*<sup>2</sup> with the program SHELXTL-97. H atoms were positioned at geometrically possible positions and refined using the riding model with *U*<sub>eq</sub> set equal to 1.2 (or to 1.5 for the methyl groups and hydroxy H atom) times the *U*<sub>eq</sub> of the parent atom. Further details of data collection and structure refinement were given in Table 1.

## RESULTS AND DISCUSSION

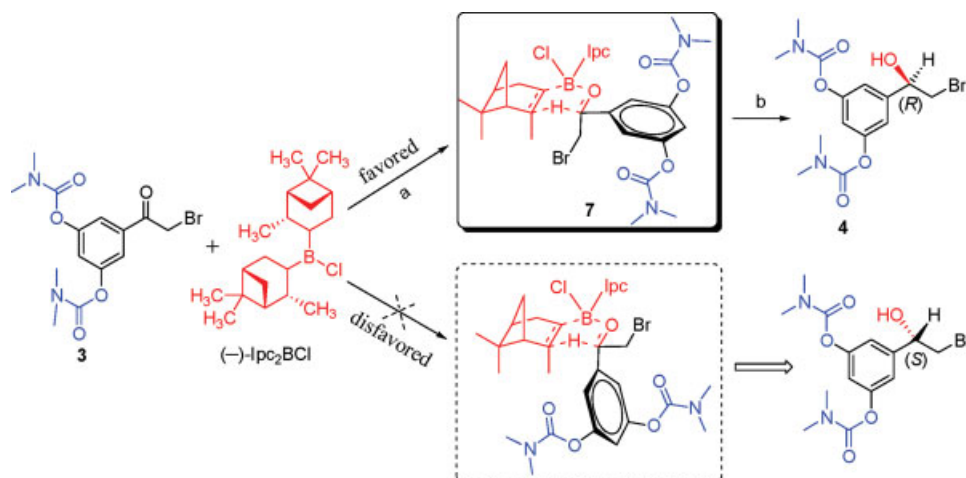
### Synthesis of Optically Active (*R*)-Bambuterol Hydrochloride

The chemistry to prepare (*R*)-bambuterol hydrochloride is depicted in Scheme 1.

Reagents and Conditions: (a) K<sub>2</sub>CO<sub>3</sub>, pyridine, Me<sub>2</sub>N-COCl, 86%; (b) CuBr<sub>2</sub>, CHCl<sub>3</sub>-AcOEt, 91%; (c) (−)-DIP-chloride<sup>TM</sup>, THF, diethanolamine, 75%; (d) aq. NaOH,



**Scheme 1.** Asymmetric synthesis of (*R*)-bambuterol hydrochloride. [Color figure can be viewed in the online issue, which is available at [www.interscience.wiley.com](http://www.interscience.wiley.com).]



**Scheme 2.** Proposed transition states for the reagent-controlled reduction of (3). (a) THF,  $-25^{\circ}\text{C}$ , 60 h, Ipc = Isopinocampheyl; (b) Diethanolamine, room temperature  $0^{\circ}\text{C}$  for 2 h. [Color figure can be viewed in the online issue, which is available at [www.interscience.wiley.com](http://www.interscience.wiley.com).]

ethanol, 100%; (e) *tert*-butylamine, diethyl ether, HCl, 69%,  $[\alpha]_D^{20} = -26.1$  (c 2,  $\text{H}_2\text{O}$ ), 99.9% *e.e.*

1-(3,5-Dihydroxyphenyl)ethanone (1) was used as a starting precursor for the preparation of (*R*)-bambuterol. The key asymmetric step in this synthesis was the carbonyl reduction of bromoketone that produces the product of (*R*)-configuration. The reduction was performed with commercially available reagent (-)-DIP-chloride<sup>TM</sup>.<sup>13,14</sup> Initially, (1) reacted with dimethylcarbamic chloride in the presence of potassium carbonate and pyridine as catalyst to produce the ester (2). Herein the use of the hydrate form of potassium carbonate is essential for a successful reaction. Then we used copper (II) bromide as bromination reagent. The bromination proceeds to take place at the carbon atom activated by the  $>\text{C}=\text{O}$  group. Via the Lewis acid ( $\text{CuBr}_2$ ) catalyzed formation of the metal enolate and the vinyloxy radical intermediates, the aralkyl ketone was brominated to give the  $\alpha$ -bromoketone (3).<sup>15</sup>

As indicated in Scheme 2, intermediate (3) then underwent a reagent-controlled reduction by (-)-DIP-chloride<sup>TM</sup> in THF at  $-25^{\circ}\text{C}$  under nitrogen protection. Followed by the usual diethanolamine workup provided a 75% yield of (4). It is believed that (-)-DIP-chloride<sup>TM</sup> effects its asymmetric reduction via a six-membered, cyclic, "boat-like" transition state (7).<sup>16,17</sup> The substituted aryl group

flanking the carbonyl moiety of the ketone prefers to sit in the equatorial-like orientation and the  $-\text{CH}_2\text{Br}$  group has to face the interaction of the axial methyl group in (-)-DIP-chloride<sup>TM</sup>. Hence, the hydride of the borane attacks the carbonyl carbon from its *re*-face. The boron moiety is eliminated by diethanolamine, followed by the transfer of the  $\beta$ -hydrogen to give the (*R*)-configuration of (4) with excellent enantioselectivity.

Compared with the chiral 2-bromoethanol straightforward nucleophilic attack by the amine, the epoxide route can inhibit the amount of the kinetically less favored isomer giving the  $\beta$ -amino alcohol in better enantiomeric excess.<sup>18,19</sup> Consequently, the resulting chiral 2-bromoethanol (4) was transformed to the corresponding epoxide (5) via intramolecular  $\text{S}_{\text{N}}2$  substitution without any loss of enantiomeric purity under basic condition.

Afterwards, the reaction between epoxide (5) and *tert*-butylamine resulted in the opening of the epoxide ring by a preferential attack on the terminal carbon atom. The bond between the chiral carbon atom and the oxygen atom did not break up during the two  $\text{S}_{\text{N}}2$  reactions, the (*R*)-conformation was reserved to give the title optical purity compound (*R*)-bambuterol. Finally, since (*R*)-bambu-

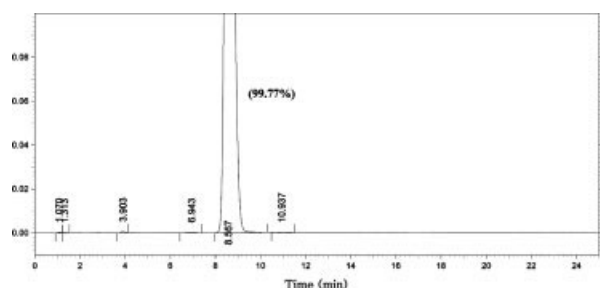


**Fig. 1.** The result of HPLC analyses of the (*R*)-bambuterol hydrochloride. Column: Shim-Pack CLC-ODS  $\text{C}_{18}$  column (250 mm  $\times$  4.6 mm), UV detection was performed at 220 nm.

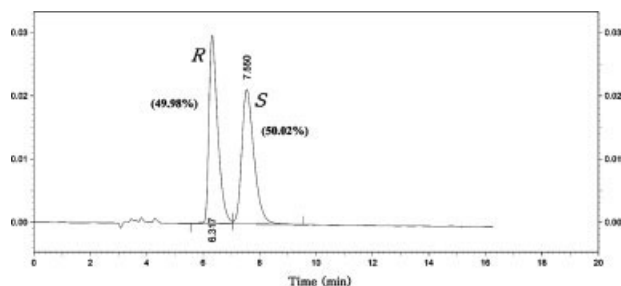


**Fig. 2.** Chiral separation of racemic bambuterol hydrochloride on Chiralcel-OJ column under optimal conditions. Addition of small amounts of amine is necessary for separation of enantiomers of compounds with basic amino group. UV detector: 263 nm. For other conditions, see the experimental section.

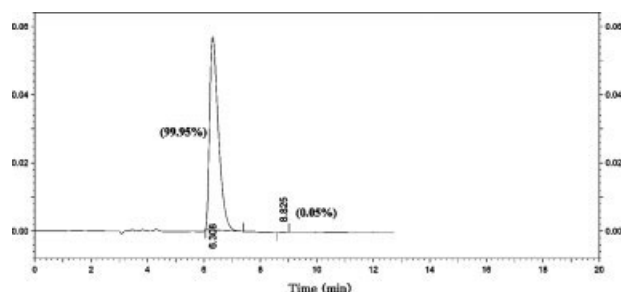


Fig. 3. Chromatogram of analysis of the (*R*)-bambuterol hydrochloride on Chiralcel-OJ. UV detector: 263 nm.

terol in the form of free amino base is readily polymerizable, the obtained products were quickly converted to its hydrochloride salts in diethyl ether solution of hydrochloric acid.

### HPLC Analysis

The chemical purity of (*R*)-bambuterol hydrochloride was investigated using the HPLC (Fig. 1). The scale in UV absorption was expanded for better illustration of the related substances. The results show that the chemical purity is higher than 99%.

The optical purity of (*R*)-bambuterol hydrochloride was analyzed with Chiral HPLC using a Chiralcel-OJ column. Analysis was performed under optimal conditions and its chromatograms are shown in Figures 2 and 3. In the enantioselective separations of racemic bambuterol hydrochloride, the (*R*)-enantiomer and (*S*)-enantiomer were well separated. The (*R*)-enantiomer was eluted before than (*S*)-enantiomer with the retention time of 6.3 and 7.6 min,

respectively. The separation of peaks was satisfied with the theoretical plates 1614.50 for (*R*)-enantiomer and 1363.23 for (*S*)-enantiomer. The value of resolution factor ( $R_s$ ) was 1.7. In the HPLC analysis of the pure (*R*)-bambuterol hydrochloride, the relative amount of (*S*)-bambuterol hydrochloride was less than 0.05% as shown in Figure 3. The calculated *e.e.* value is greater than 99%.

### Optical Rotation of (*R*)-Bambuterol Hydrochloride

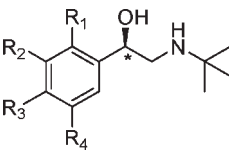
To the best of our knowledge, most aryethanolamines stayed with the (–)-(*R*)-enantiomer with few exceptions (Table 2). (*R*)-Bambuterol hydrochloride is levorotatory, with the specific rotation  $[\alpha]_D^{20}$  value of  $-26.1^\circ$  (*c* 2, H<sub>2</sub>O).

### Experimental CD Spectrum

In studying conformational properties, CD spectroscopy has great importance. Analysis of experimental CD spectrum with known absolute configuration is important for the development of CD theory. A common drawback encountered with a majority of optical active compounds is that, because of their conformational mobility, the weakly absorbing chromophores yield CD spectrum that are difficult to interpret. Consequently, many studies have focused on the CD in situ complexation method as a tool to enhance the sign of the Cotton effects (CEs).<sup>31</sup>

The CD spectrum of racemic bambuterol hydrochloride and its enantiomers were measured straightforward in acidic solutions. Figure 4 shows the strong CD absorption of (*R*) and (*S*)-bambuterol hydrochloride. The sign of the characteristic intense CE band occurring around 240–275 nm make it clear that the test compound was an optical active compound. (*R*)-configuration displayed a positive

TABLE 2. The specific rotations of some (*R*)- $\beta_2$ -adrenoceptor agonists with a *tert*-butyl group attached to the nitrogen atom<sup>20–30</sup>

					
Compound	R <sub>1</sub>	R <sub>2</sub>	R <sub>3</sub>	R <sub>4</sub>	Optical rotation
Colterol	H	HO	HO	H	$[\alpha]_D^{18}:-39.0^\circ$ ( <i>c</i> 2.2, 0.5N HCl)
Terbutaline	H	HO	H	HO	$[\alpha]_D^{20}:-32.5^\circ$ ( <i>c</i> 0.76, MeOH) <sup>a</sup>
Albuterol	H	HOCH <sub>2</sub>	HO	H	$[\alpha]_D^{20}:-36.5^\circ$ ( <i>c</i> 1, MeOH) <sup>b</sup>
Carbuterol	H	H <sub>2</sub> NCONH	HO	H	$[\alpha]_D^{25}:-43.0^\circ$ ( <i>c</i> 1, MeOH) <sup>a</sup>
Sulfoneterol	H	CH <sub>3</sub> SO <sub>2</sub> CH <sub>2</sub>	HO	H	$[\alpha]_D^{25}:-38.7^\circ$ ( <i>c</i> 1, MeOH) <sup>a</sup>
Ephedrine	H	H	H	H	$[\alpha]_D^{23}:-78.8^\circ$ ( <i>c</i> 1, CHCl <sub>3</sub> )
Clenbuterol	H	Cl	H <sub>2</sub> N	Cl	$[\alpha]_{364}^{20}:-192^\circ$ ( <i>c</i> 2.42, DMF) <sup>a</sup>
Meludrine	Cl	H	HO	H	$[\alpha]_D^{20}:-20.3^\circ$ ( <i>c</i> 1, MeOH)
Mabuterol	H	Cl	H <sub>2</sub> N	CF <sub>3</sub>	$[\alpha]_{364}^{20}:154.8^\circ$ ( <i>c</i> 1.0, MeOH)
–	H	CH <sub>3</sub> CH=CH	H	CH <sub>3</sub> CH=CH	$[\alpha]_D^{20}:-25.4^\circ$ ( <i>c</i> 0.5, MeOH) <sup>a</sup>
–	H	CH <sub>3</sub> OC=O	HO	H	$[\alpha]_D^{20}:-49.1^\circ$ ( <i>c</i> 0.97, CHCl <sub>3</sub> )
–	H	Cl	H <sub>2</sub> N	F	$[\alpha]_{364}^{20}:-139.2^\circ$ ( <i>c</i> 2.0, MeOH) <sup>a</sup>
–	H	F	H <sub>2</sub> N	H	$[\alpha]_{364}^{20}:-123.3^\circ$ ( <i>c</i> 1.0, MeOH) <sup>a</sup>

<sup>a</sup>Hydrochloride salts.

<sup>b</sup>Albuterol sulfate; (*R*)-Albuterol acetate monomethanolate  $[\alpha]_D^{20} = -37.9^\circ$  (*c*0.5, MeOH).



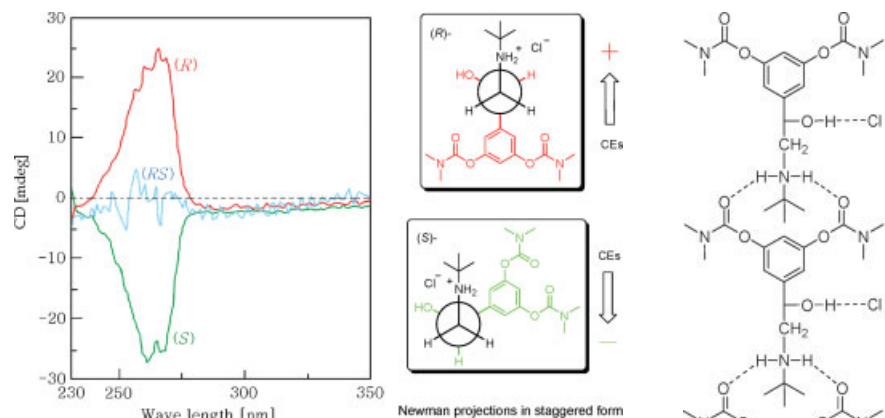


**Fig. 4.** CD spectra of racemic bambuterol hydrochloride and its enantiomers in acidic solutions. Conditions: Cell length: 0.2 cm; Data pitch: 1 nm; Data point: 121; Band width: 1.0 nm; Response: 0.5 sec; Measurement range: 350–230 nm; Scanning speed: 200 nm/min. [Color figure can be viewed in the online issue, which is available at [www.interscience.wiley.com](http://www.interscience.wiley.com).]

band in the CD spectrum. In contrast, while it was negative for the respective (*S*)-enantiomer. At lower wavelengths, the curves tended toward a contrary CEs although this is somewhat masked by the high aromatic absorption. The CD and absorption spectra of the text compound did not change after the samples had been allowed to stand at room temperature for one day.

#### Single Crystal Investigation of (*R*)-Bambuterol Hydrochloride

The X-ray structure was determined in order to establish unambiguously the absolute configuration at the asymmetric carbon center. The molecular structure of (*R*)-bambuterol hydrochloride is illustrated in Figure 5, showing the configuration at C7 to be (*R*). The absolute configuration was assigned by using Flack parameter<sup>32,33</sup> from the X-ray diffraction data. The final value of the freely refined Flack parameter  $\chi$  was 0.05(9), which confirm the correctness of the assigned handedness of the structure.

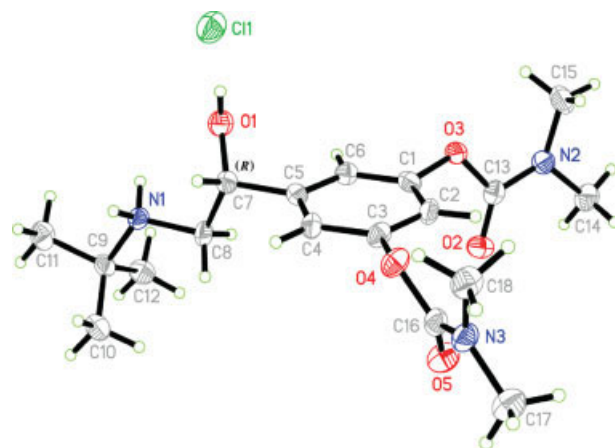


**Fig. 5.** X-ray structure for (*R*)-bambuterol hydrochloride, with displacement ellipsoids drawn at the 50% probability level. Created by XP, a subprogram of shelxtl (Bruker AXS, Madison, WI). [Color figure can be viewed in the online issue, which is available at [www.interscience.wiley.com](http://www.interscience.wiley.com).]

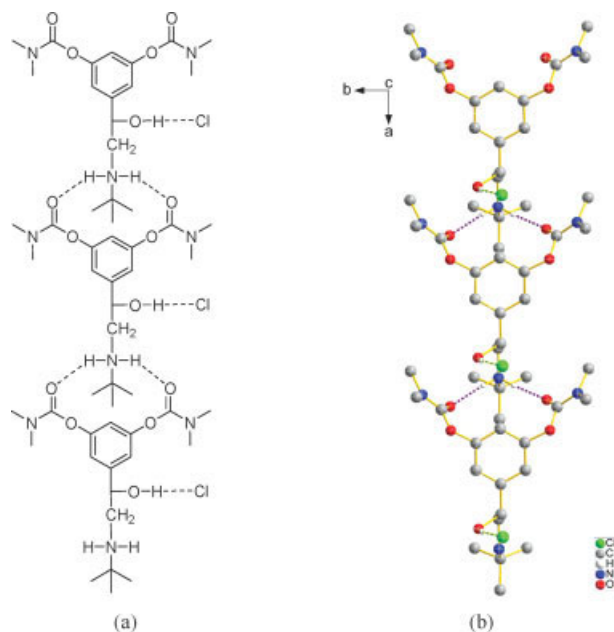


**Fig. 6.** (a) The two types of hydrogen bonds ribbon-like structure in the supramolecular assembly; (b) A perspective view of the crystal packing in (*R*)-bambuterol hydrochloride along the *c* axis. H atoms bonded to C atoms have been omitted for clarity. Dashed lines indicate hydrogen bonds. [Color figure can be viewed in the online issue, which is available at [www.interscience.wiley.com](http://www.interscience.wiley.com).]

In the crystal lattice, the molecules are connected in a head-to-tail fashion. The chlorine atom is closer to the hydroxyl oxygen atom and form an intramolecular hydrogen bond of type O—H...Cl. In addition, the structure exhibits intermolecular hydrogen bonds of type N—H...O (Fig. 6). The hydrogen bonds are O—H...Cl (2.96 Å, 163.5°), N—H<sub>A</sub>...O1<sup>i</sup> (2.78 Å, 171.3°), and N—H<sub>B</sub>...O2<sup>i</sup> (2.83 Å, 166.8°) with symmetry codes  $x+1, y, z$ . The molecular structure in crystal is further stabilized by the intermolecular electrostatic interactions between the positively charged atom N<sup>+</sup> and Cl<sup>−</sup>.

#### CONCLUSIONS

In conclusion, the highly enantioselective synthesis of (*R*)-bambuterol hydrochloride by the reduction of aralkyl ketone with (−)-DIP-chloride<sup>TM</sup> has been accomplished. Results from HPLC studies indicate that this method yields high optical pure (*R*)-bambuterol hydrochloride with excellent e.e. value (up to 99%). In addition, systematic studies of the stereochemical properties of (*R*)-bambuterol hydrochloride using specific rotations, CD spectroscopy and X-ray single crystal analysis were performed; the (*R*) configuration of the target product was established unambiguously. This approach can be applied to asymmetric synthesis of other classical phenylethanolamine  $\beta_2$ -adrenoceptor agonists in an enantiomerically pure form.

#### ACKNOWLEDGMENTS

The authors gratefully thank the Keypharma Biomedical Inc. for the financial support for this project. The authors are also grateful to the Sun Yat-Sen University Analytical

and Testing Center for single-crystal X-ray diffraction analysis.

### LITERATURE CITED

1. Olsson OAT, Svensson LA. New lipophilic terbutaline ester prodrugs with long effect duration. *Pharm Res* 1984;1:19–23.
2. D'Alonzo GE, Smolensky MH, Feldman S, Gnosspelius Y, Karlsson K. Bambuterol in the treatment of asthma. A placebo-controlled comparison of once daily morning vs evening administration. *Chest* 1995;107:406–412.
3. Persson G, Baas A, Knight A, Larsen B, Olsson H. One month treatment with the once daily oral  $\beta_2$ -agonist bambuterol in asthmatic patients. *Eur Respir J* 1995;8:34–39.
4. Petrie GR, Chookang JY, Hassan WU, Morrison JF, O'Reilly JF, Pearson SB, Shneerson JM, Tang OT, Ning AC, Turbitt ML. Bambuterol: effective in nocturnal asthma. *Respir Med* 1993;87:581–585.
5. Ostergaard D, Rasmussen SN, Viby-Mogensen J, Pedersen NA, Boysen R. The influence of drug-induced low plasma cholinesterase activity on the pharmacokinetics and pharmacodynamics of mivacurium. *Anesthesiol* 2000;92:1581–1587.
6. Svensson LA. Bambuterol-a prodrug with built-in hydrolysis brake. *Acta Pharm Suec* 1987;24:333–341.
7. Svensson LA, Tunek A. The design and bioactivation of presystemically stable prodrugs. *Drug Metab Rev* 1988;19:165–194.
8. Bang U, Nyberg L, Rosenborg J, Viby-Mogensen J. Pharmacokinetics of bambuterol in subjects homozygous for the atypical gene for plasma cholinesterase. *Br J Pharmacol* 1998;45:479–484.
9. Tan W, Cheng JL. *R*-Bambuterol, its preparation and therapeutic uses. *US Pat Appl Publ US20050171197*. 2005;08-04.
10. Gazic I, Bosak A, Sinko G, Vinkovic V, Kovarik Z. Preparative HPLC separation of bambuterol enantiomers and stereoselective inhibition of human cholinesterases. *Anal Bioanal Chem* 2006;385:1513–1519.
11. Handley DA, McCullough JR, Crowther SD, Morley J. Sympathomimetic enantiomers and asthma. *Chirality* 1998;10:262–272.
12. Wu HH, Zhang XL, Zhu XY, Yang LP. Study on synthesis of bambuterol. *Hecheng Huaxue* 2000;8:146–150.
13. Brown HC, Chandrasekharan J, Ramachandran PV. Diisopinocampheylchloroborane, an exceptionally efficient chiral reducing agent. *J Am Chem Soc* 1988;110:1539–1546.
14. Moeder CW, Whitener MA, Sowa JR Jr. Quantitative stereochemical analysis of a reagent that exhibits asymmetric amplification, B-chlorodiisopinocampheylborane (Dip-Cl). *J Am Chem Soc* 2000;122:7218–7225.
15. Hu AX, Chen P, Yang Z, Wu XY, Chen K. Bromination of alkylaryl ketone with cupric bromide. *Chin J Med Chem* 2002;12:340–343.
16. Brown HC, Chandrasekharan J, Ramachandran PV. Asymmetric reduction of  $\alpha$ -keto esters with potassium 9-O-(1,2,5,6-di-O-isopropylidene- $\alpha$ -D-glucopyranose)-9-boratabicyclo[3.3.1]nonane. Chiral synthesis of  $\alpha$ -hydroxy esters with optical purity approaching 100% ee. *J Org Chem* 1986;51:3396–3398.
17. Kim J, Suri JT, Cordes DB, Singaram B. Asymmetric reductions involving borohydrides: a practical asymmetric reduction of ketones mediated by (1*L*)-TarB-NO<sub>2</sub>: a chiral lewis acid. *Org Process Res Dev* 2006;10:949–958.
18. Hu B, Ellingboe J, Gunawan I, Han S, Largis E, Li Z, Malamas M, Mulvey R, Oliphant A, Sum FW, Tillett J, Wong V. 2,4-Thiazolidinediones as potent and selective human  $\beta_3$  agonists. *Bioorg Med Chem Lett* 2001;11:757–760.
19. Guy A, Doussot J, Ferroud C, Garreau R, Godefroy-Falguieres A. Regioselective ring opening of epoxides with lithium azide. *Synthesis* 1992;9:821–822.
20. Pratesi P, La Manna A, Pagani G, Grana E. Optical resolution of *N*-*tert*-butylnoradrenaline and biological activity of the optical antipodes. *Farmaco Edizione Scientifica* 1963;18:950–956.
21. Effenberger F, Jager J. Synthesis of the adrenergic bronchodilators (*R*)-terbutaline and (*R*)-salbutamol from (*R*)-cyanohydrins. *J Org Chem* 1997;62:3867–3873.
22. Caira MR, Hunter R, Nassimbeni LR, Stevens AT. Resolution of albuterol acetone. *Tetrahedron: Asymmetry* 1999;10:2175–2189.
23. Palacios SM, Palacio MA. Enantiomeric resolution of albuterol sulfate by preferential crystallization. *Tetrahedron: Asymmetry* 2007;18:1170–1175.
24. Kaiser C, Schwartz MS, Colella DF, Wardell JR Jr. Adrenergic agents. III. Synthesis and adrenergic activity of some catecholamine analogs bearing a substituted sulfonyl or sulfonylalkyl group in the meta position. *J Med Chem* 1975;18:674–683.
25. Guenther E, Johannes K, Gerd K, Klaus-reinhold N. Neue optisch active verbindungen. *Ger Offen DE2212600* 1973;09–27.
26. Guenther E, Johannes K, Gerd K, Klaus-reinhold N, Helmut P. Neue optisch active verbindungen. *Ger Offen DE2345442* 1975;03–20.
27. Yasuo I, Hideo K, Eiichi K, Sakae K, Koji M. Optically active benzyl alcohol compound and pharmaceutical composition. *Eur Pat Appl EP0420120* 1991;04–03.
28. Kaiser C, Colella DF, Schwartz MS, Garvey E, Wardell JR Jr. Adrenergic agents. I. Synthesis and potential  $\beta$ -adrenergic agonist activity of some catechol amine analogs bearing a substituted amino functionality in the meta position. *J Med Chem* 1974;17:49–57.
29. Xiao YJ, Yang SN, Shi W, Yang LP. Synthesis of (*R*)-salbutamol via asymmetric transfer hydrogenation of  $\alpha$ -iminoketone. *Chin J Org Chem* 2006;26:1103–1105.
30. Calet S, Urso F, Alper H. Enantiospecific and stereospecific rhodium(I)-catalyzed carbonylation and ring expansion of aziridines. Asymmetric synthesis of  $\beta$ -lactams and the kinetic resolution of aziridines. *J Am Chem Soc* 1989;111:931–934.
31. Ahmad H, Atta-ur-Rahman SG. The CD in situ complexation method as a tool for determination of absolute configurations of cottonogenic derivatives. *J Am Chem Soc* 1993;115:12533–12544.
32. Flack HD. On enantiomorph-polarity estimation. *Acta Crystallogr* 1983;A39:876–881.
33. Flack HD, Bernardinelli G. Reporting and evaluating absolute-structure and absolute-configuration determinations. *J Appl Crystallogr* 2000;33:1143–1148.



# Discrimination of Chiral Guests by Chiral Channels: Variable Temperature Studies by SXRD and Solid State $^{13}\text{C}$ NMR of the Deoxycholic Acid Complexes of Camphorquinone and *Endo*-3-Bromocamphor

MOHAMED I. M. TAHIR, NICHOLAS H. REES,\* STEPHEN J. HEYES, ANDREW R. COWLEY, AND KEITH PROUT  
*Department of Chemistry, University of Oxford, Chemistry Research Laboratory, Mansfield Road, Oxford OX1 3TA, UK*

**ABSTRACT**  $3\alpha,12\alpha$ -Dihydroxy- $5\beta$ -cholan-24-oic acid (deoxycholic acid DCA) is able to discriminate between the *R*- and *S*-enantiomers of camphorquinone and *endo*-(+)-3-bromocamphor and select only the *S*-enantiomers from a racemic mixture. DCA forms novel well ordered 1:1 adducts with (1*S*)-(+)-camphorquinone and (1*S*)-*endo*-(+)-3-bromocamphor, both of which have been characterized by single crystal X-ray diffraction (SXRD). When DCA is cocrystallized with (*RS*)-camphorquinone and (*RS*)-*endo*-3-bromocamphor, 1:1 adducts of the *S*-enantiomers are produced together with crystals of the free racemic guest. In contrast, in the absence of (1*S*)-(+)-camphorquinone, DCA forms a 2:1 adduct with (1*R*)-(–)-camphorquinone. In this 2:1 adduct the guest is disordered at ambient temperature and undergoes a phase change in the region 160–130 K similar to that observed for the ferrocene adduct, but with only partial ordering of the guest. The SXRD structure of the low temperature form and the variable temperature  $^{13}\text{C}$  CP/MAS NMR are reported. Cocrystallizing DCA with (1*R*)-*endo*-(+)-3-bromocamphor gives the free guest and a glassy solid. *Chirality* 20:863–870, 2008. © 2008 Wiley-Liss, Inc.

**KEY WORDS:** molecular complexes; chiral discrimination; chiral selection

## INTRODUCTION

For chiral molecules, about 10% of racemic mixtures crystallize as conglomerates<sup>1</sup> analogous to Pasteur's sodium ammonium tartrate in which the crystal class requires that individual crystals contain a single enantiomer. This gives spontaneous chiral discrimination and (occasionally) enables enantiomeric separation by hand picking. However, the vast majority of crystals grown from solutions of *RS*-mixtures lead to the formation of structures with pairs of enantiomers related by improper symmetry operators (e.g., centers of symmetry, mirror planes, glide planes etc). Very rarely, randomized solid solutions of one enantiomer in the other are formed. In neither case is there any chiral discrimination.

Diastereomers (obtained when an enantiomerically pure reagent combines with a racemic mixture to form two isomers unrelated by mirror symmetry), are used to discriminate between enantiomers and to effect chiral resolution. According to Craig<sup>2</sup> "chiral discrimination" occurs, where the pair-interaction energy of two molecules or ions is different for the two enantiomers of the one, acting on the same enantiomer of the other. Thus, diastereomers are usually immiscible in the solid state and form two distinct solids separable by fractional crystallization, to effect chiral resolution. Rarely, a 50–50 mixture of two diastereomers will form a distinct compound as observed in the *l*-menthyl-*dl*-mandelate<sup>3</sup> system and various organometallic compounds or a solid solution.<sup>4</sup> In these cases chiral resolution cannot be achieved.

Just as diastereomers may be used to discriminate between enantiomers, so chiral hydrogen-bonding environments and chiral crystal cavities may lead to the formation of inclusion compounds that discriminate between chiral guests. These inclusion compounds are ideal candidates for the investigation of the structure and dynamics of intermolecular interactions in chiral environments. In 1952, Powell proposed that if a host substance (tri-*o*-thymotide, TOT) with chiral cavities is crystallized from a solvent which itself is a *dl*-mixture and forms a molecular compound with the solvent, then the cavities of any one crystal will enclose preferentially the *d'*- or *l'*- forms of the solvent. Using this method he then partially resolved 2-bromobutane.<sup>5</sup> Subsequently, from SXRD and polarimetry it was shown that TOT forms two different classes of complex. These are channel-type complexes, which give a low degree of chiral separation, and cage-like complexes which give a much higher degree of discrimination and a variable but potentially large excess of the preferred enan-

Dedicated to the memory of Prof. Keith Prout.

Contract grant sponsor: EPSRC, HFCE Joint Research Equipment Initiative, Universiti Putra Malaysia.

M. I. Mohamed Tahir is currently at Department of Chemistry, Faculty of Science, Universiti Putra Malaysia, 43400 UPM Serdang, Selangor, Malaysia.

\*Correspondence to: Nicholas H. Rees, Inorganic Chemistry, University of Oxford, South Parks Road, Oxford OX1 3QR, UK.

E-mail: nick.rees@chem.ox.ac.uk

Received for publication 24 August 2007; Accepted 7 February 2008

DOI: 10.1002/chir.20561

Published online 1 April 2008 in Wiley InterScience (www.interscience.wiley.com).

tiomer (up to 80%).<sup>6</sup> Fortuitously, Powell's 2-bromobutane complex is of the latter type. Using solid-state  $^2\text{H}$  and  $^{13}\text{C}$  NMR, Ripmeester demonstrated that the conversion of *cis*-2,3-epoxybutane to but-3-en-2-ol in the TOT:*cis*-2,3-epoxybutane complex takes place within the chiral cavities of the adduct and is stereoselective. Thus, the chirality of a cavity can dictate the preferred stereochemical pathway.<sup>7</sup> Further, he found two optically-distinct diastereomorphs for TOT:2-bromobutane.<sup>8</sup> These diastereomorphs were also characterized by their distinct dynamic behavior. We regard the level of discrimination shown by Ripmeester's diastereomorphs<sup>8</sup> as "chemical discrimination" and is analogous to diastereomers A and B being immiscible.

Enantioselective enclathration in bile acid complexes where there is host-guest or guest-guest hydrogen bonding, has been extensively reviewed recently.<sup>9–12</sup> Like TOT, the bile acids form clathrate complexes with a wide range of organic and organometallic compounds without host-guest hydrogen bonding. However, in contrast to TOT (which is a racemate and is only resolved on crystallization) the bile acids are themselves optically pure. Therefore, in the crystals, there are only two host-guest combinations for a racemic guest. This is in contrast to the four possible host-guest combinations for TOT complexes, thus eliminating one degree of complexity from the system.

Previously, it has been shown that the DCA (3 $\alpha$ ,12 $\alpha$ -dihydroxy-5 $\beta$ -cholan-24-oic acid [deoxycholic acid]) (Fig. 1a) complexes of (+)(1*R*)camphor<sup>13</sup> and –(1*S*)camphor<sup>14</sup> at ambient temperature have a 2:1 stoichiometry and are isomorphous with each other and with the high temperature form of DCA<sub>2</sub>:ferrocene.<sup>15</sup> There is the implication that the DCA does not discriminate between the camphor enantiomers. In this work we present the DCA complexes of *R*- and *S*-camphorquinone, (*R*-1, *S*-1, 1,7,7-trimethylbicyclo[2.2.1]heptan-2,3-dione) (Fig. 1b), and *R*- and *S*-endo-3-bromocamphor (*R*-2, *S*-2) (3-bromo-1,7,7-trimethylbicyclo[2.2.1]heptan-2-one) (Fig. 1c). These provide an opportunity to investigate the effects of increased polarity and size, and changes in pseudo-symmetry, on the chiral selectivity and solid state properties in this series of complexes. Camphorquinone is a conformationally-rigid, fused ring, chiral, cisoid,  $\alpha$ -diketone, which is similar to camphor, but differs from camphor by the presence of an additional carbonyl (which replaces a methylene group at C2). Although this substitution has little effect on the molecular volume, it greatly increases the polarity of the molecule and changes the pseudo-symmetry so that there is a pseudo-mirror plane in both the shape and electrostatic potential surface, which is at right angles to that in camphor. In *endo*-3-bromocamphor, one of the hydrogen atoms of the methylene C2 group is replaced with bromine. This increases the molecular volume of the guest, while maintaining the increase in polarity and ensures that neither the shape nor the electrostatic surface potential have any pseudosymmetry. Enantiomerically pure *endo*-3-bromocamphor<sup>16</sup> also has a well-ordered crystal structure at ambient temperature. In the Cambridge Crystallographic Database<sup>17</sup> there are no examples of camphorquinone or *endo*-3-bromocamphor as a guest in DCA or any other host systems.

Chirality DOI 10.1002/chir

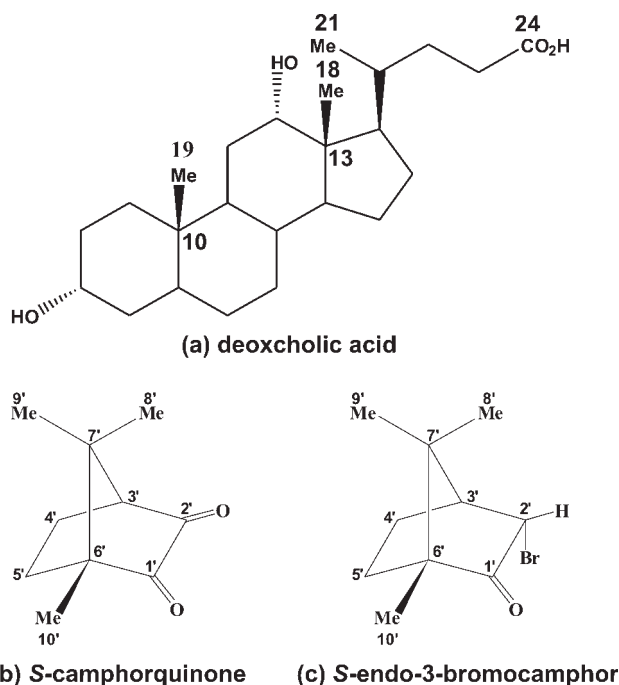


Fig. 1. Structures of (a) deoxycholic acid, (b) S-Camphorquinone and (c) S-endo-3-bromocamphor.

## MATERIALS AND METHODS

### Preparation and Characterization

*R*-, *S*- and *RS*-camphorquinone and *R*- and *S*-endo-3-bromocamphor were purchased from Sigma-Aldrich and were used without further purification. DCA free from any included guest was made using the method previously described.<sup>15</sup> The inclusion compounds were formed by recrystallisation of the purified DCA with the specific enantiomeric guest molecule from a solution containing methanol and ethanol 3:1 (v/v).

For DCA with (1*R*)-(–)-camphorquinone (*R*-camphorquinone), various different ratios of the host and guest were tried in the crystallization procedure, but always resulted in the same product. Elemental analysis after recrystallization: Found C 72.53, H 9.67; the 2:1 complex, C<sub>48</sub>H<sub>80</sub>O<sub>8</sub>·2C<sub>10</sub>H<sub>14</sub>O<sub>2</sub>, requires C 73.08, H 9.74, O 17.18. Determination of the unit cell parameters and space group by SXRD showed this was the 2:1 inclusion compound of DCA<sub>2</sub>:*R*-camphorquinone. When DCA and (1*S*)-(+)-camphorquinone (*S*-camphorquinone) were recrystallized from an alcoholic solution, different ratios of the host and guest gave a crystalline product. From SXRD the crystals were monoclinic with unit cell parameters, *a* = 7.2234(4), *b* = 13.6511(9), *c* = 16.5199(7) Å,  $\beta$  = 99.556(4)° and space group P2<sub>1</sub>. Subsequently, a full structure analysis showed the compound to be the 1:1 complex of DCA:*S*-camphorquinone. Elemental analysis after recrystallization did not distinguish the 1:1 and 2:1 products: Found C 72.63, H 9.73; for a 1:1 complex, C<sub>24</sub>H<sub>40</sub>O<sub>4</sub>·C<sub>10</sub>H<sub>14</sub>O<sub>2</sub>, requires C 73.22, H 9.96, O 16.82. Crystallization of DCA with *RS*-camphorquinone produced crystals of two different morphologies: intense yellow plates and yellow needles.

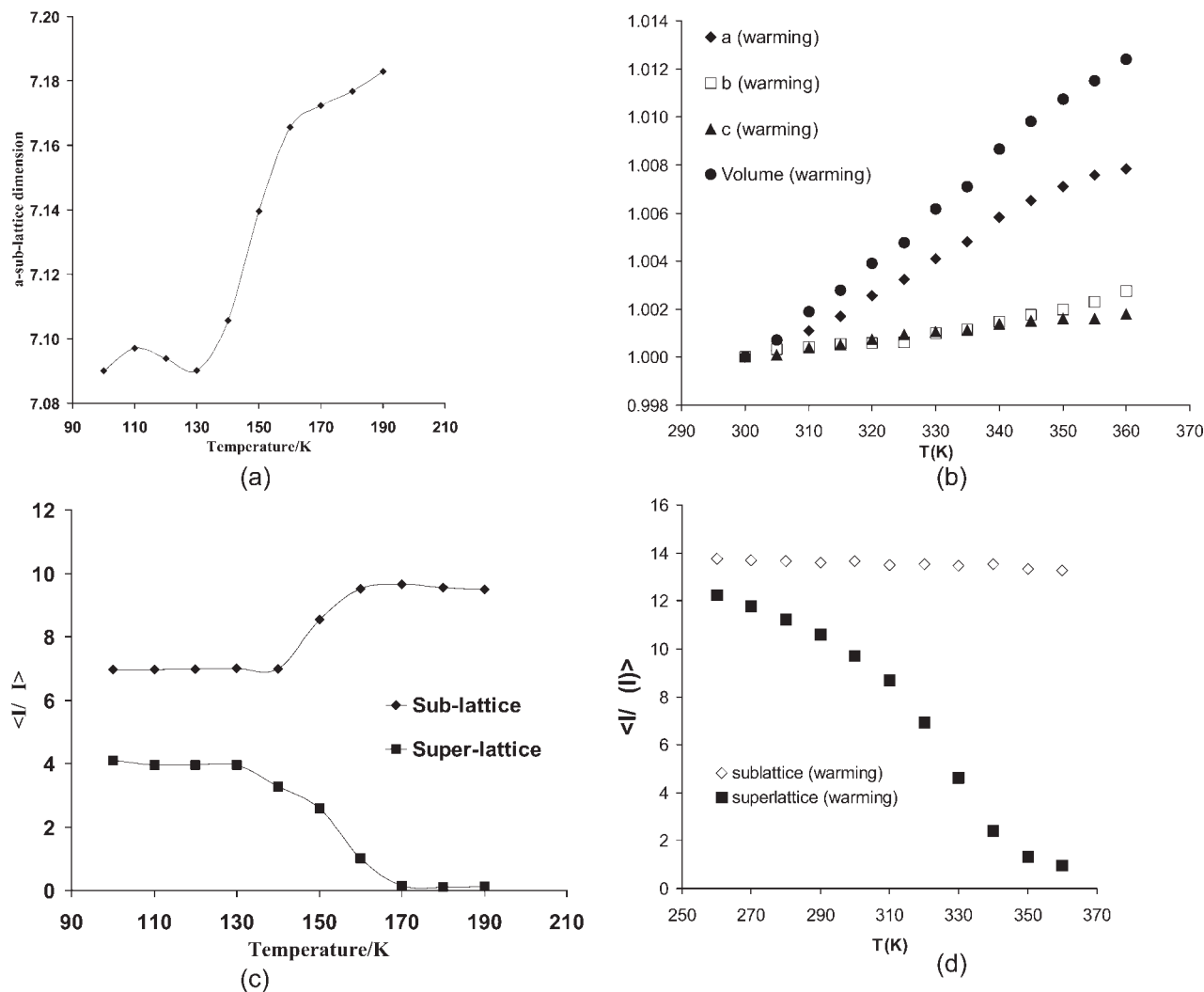


**Fig. 2.** The variation with temperature of (a) the a-sub-lattice unit cell dimension for DCA<sub>2</sub>:R-camphorquinone and (b) the dimensions and volume of the sub-lattice unit cell referred to unity values at 300 K DCA<sub>2</sub>:ferrocene (c) the mean values of I/s(I) for the sub-lattice and super-lattice reflections DCA<sub>2</sub>:R-camphorquinone (d) the mean values of I/σ(I) for the sub-lattice and super-lattice reflections DCA<sub>2</sub>:ferrocene.

dles. The needle crystals had the same unit cell parameters as DCA:S-camphorquinone whereas those of the plate-like crystals resembled neither DCA<sub>2</sub>:R-camphorquinone nor DCA:S-camphorquinone. The plate-like crystals were shown to be *RS*-camphorquinone by SXRD at 100 K ( $a = 6.13(1)$  Å,  $b = 11.503(1)$  Å,  $c = 11.995(3)$  Å and  $\beta = 91.450(18)^\circ$  space group  $P2_1/n$ , cf. Bright et al.<sup>18</sup>).

Attempts to prepare *R*- and *S-endo*-3-bromocamphor DCA complexes followed the procedures described earlier. Large crystals were obtained when DCA and *S-endo*-3-bromocamphor were present in the molecular ratio 2:1 and were shown by SXRD to be the 1:1 inclusion compound. However, no inclusion compounds of DCA with *R-endo*-3-bromocamphor were formed; the products of the crystallisation were the free guest and a glassy solid.

#### Single crystal X-ray Diffraction

CCDC holds the crystallographic data for this article; 649762, DCA<sub>2</sub>:R-camphorquinone at 100 K; 649764,

DCA:S-camphorquinone at 295 K; 649765, *RS*-camphorquinone at 100 K; 649763, DCA:*S-endo*-3-bromocamphor at 295 K. These data can be obtained free of charge from The Cambridge Crystallographic Data Centre via [www.ccdc.cam.ac.uk/data\\_request/cif](http://www.ccdc.cam.ac.uk/data_request/cif).

#### Solid State <sup>13</sup>C CP/MAS NMR

The variable temperature <sup>13</sup>C CP/MAS NMR spectra were obtained on a Varian/Chemagnetics Infinity spectrometer at 50.32 MHz using 7.5 mm O.D. rotors containing 300 mg of sample and a MAS rate of 4 kHz, utilizing dry nitrogen for all gas requirements. For variable temperature measurements, the heater gas was passed through a heat exchanger immersed in liquid nitrogen prior to passing over a heater element and finally the sample rotor. The sample was allowed to equilibrate for 20 min once the required temperature had been reached. The actual sample temperature was calculated from the indicated temperature by observing certain distinct phase changes in



known compounds (camphor, DABCO)<sup>19</sup> and using a chemical shift thermometer ( $\text{PbNO}_3$ )<sup>20</sup> to interpolate between these temperatures. A cross-polarization sequence with a variable X-amplitude spin-lock pulse<sup>21</sup> and phase modulated proton decoupling was used. Typically 800 transients were acquired using a contact time of 2.5 ms, an acquisition time of 125 ms (2500 data points zero filled to 16 K) and a recycle delay of 5 s. All  $^{13}\text{C}$  spectra were referenced to adamantane (the up field methine resonance was taken to be at  $\delta = 29.5$  ppm<sup>22</sup> on a scale where  $\delta(\text{TMS}) = 0$ ) as a secondary reference.  $^{13}\text{C}$  dipolar dephasing spectra<sup>23</sup> were run using a sequence similar to that for CP/MAS with the addition of a delay (set to 40  $\mu\text{s}$ ) between the end of the spin-lock pulse and the start of the  $^{13}\text{C}$  acquisition/proton decoupling.

## RESULTS

At ambient temperature the crystals of the  $\text{DCA}_2$ :*R*-camphorquinone inclusion compound were orthorhombic, space group  $P2_21_21$  with  $a = 7.234(1)$ ,  $b = 13.894(1)$ ,  $c = 27.319(1)$  Å. At 100 K super-lattice reflections corresponding to a doubling of the  $a$ -axis appear and the space group changes to  $P2_12_12_1$ . This phase change is very similar to that observed for  $\text{DCA}_2$ :ferrocene<sup>15</sup> at 325 K. By analogy with a similar plot for  $\text{DCA}_2$ :ferrocene (Fig. 2b), a plot of the  $a$ -sub-cell axis against temperature (Fig. 2a), suggests that the phase change takes place between 160 and 130 K. This corresponds to the onset and development of the super-lattice reflections (Fig. 2c). However, below 130 K (after the phase change may be complete) the unit cell parameters still fluctuate and, most probably, have not reached a stable value at 100 K (the low temperature limit of our Cryostream). At 100 K the reflections are less sharp than at ambient temperature and have unsymmetrical peak profiles. In contrast to  $\text{DCA}_2$ :ferrocene (Fig. 2d), the intensities of the super-lattice reflections decrease with temperature as the intensities of the sub-lattice increase. On warming, the change in cell parameters was reversed through the phase change with no significant hysteresis. However, the profile of many peaks remained irregular and examination of the crystal showed it to be slightly cracked and the sub- and super-lattice intensities did not fully recover. Repetition of the experiment with other crystals led to similar crystal damage.

The best model for the structure of  $\text{DCA}_2$ :*R*-camphorquinone at 100 K had the *R*-camphorquinone molecule disordered over two locations related by the pseudo-symmetry operator  $x, 0.5 - y, -z$ , with site occupancies 0.681(5) and 0.319(5). This residual disorder together with the apparent instability of the unit cell parameters below 130 K, may indicate that the phase change was not complete at 100 K. The packing diagrams of the  $\text{DCA}_2$ :*R*-camphorquinone modeled with two guests are shown in Figure 3. Attempts to obtain a full solution of the  $\text{DCA}_2$ :*R*-camphorquinone structure at 295 K were unsuccessful, but indicated that the structure was very similar to those of the high temperature forms of  $\text{DCA}_2$ :ferrocene<sup>15</sup> and  $\text{DCA}_2$ :camphor.<sup>13,14</sup>

For  $\text{DCA}$ :*S*-camphorquinone and  $\text{DCA}$ :*S*-endo-3-bromocamphor complexes (Figs. 3 and 4), the DCA bilayers are

still present as in the 2:1 complexes, and are virtually indistinguishable from those found in the high temperature forms of the ferrocene,<sup>15</sup> and camphor<sup>13,14</sup> complexes. Of those DCA inclusion compounds that have been reported in the Cambridge structural database,<sup>17</sup> only  $\text{DCA}$ :salicylic acid<sup>24</sup> (a hydrogen bonded adduct that does not have the bilayer structure), and  $\text{DCA}$ :acetic acid<sup>25</sup> have a 1:1 stoichiometry. In  $\text{DCA}$ :acetic acid the neighboring bilayers slide  $a/2$  with respect to each other to create two smaller cavities to every two DCA molecules rather than one larger one.<sup>25</sup> The two small acetic acid

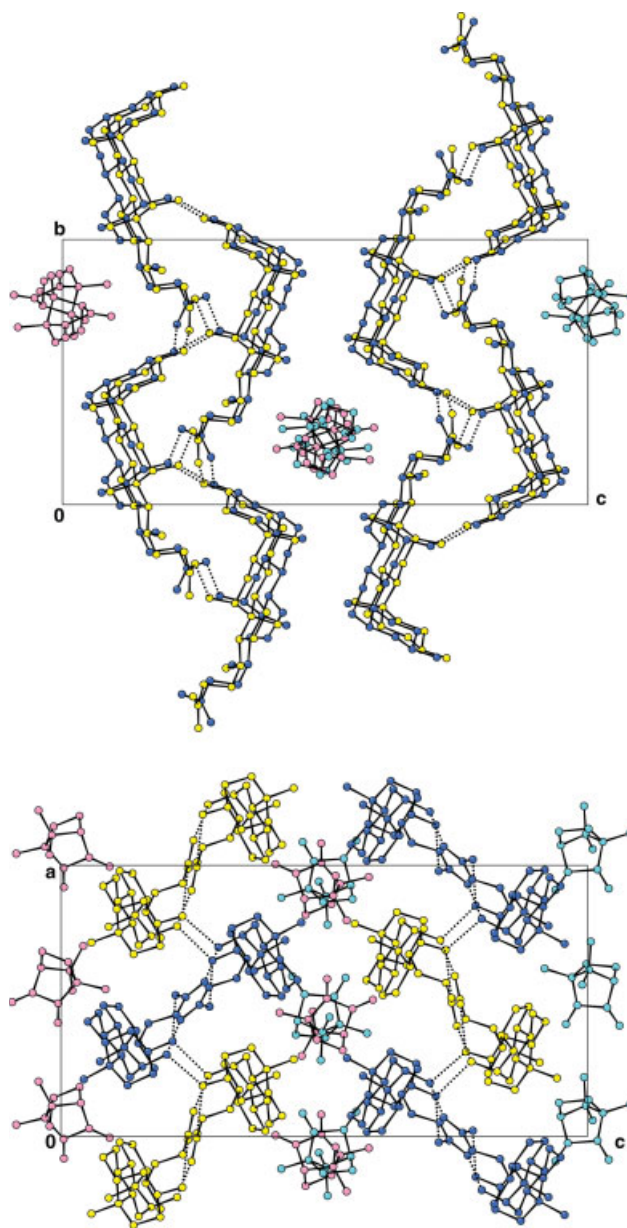


**Fig. 3.** Crystal packing at 100 K for  $\text{DCA}_2$ :*R*-camphorquinone projected along the  $a$ -axis (top) and  $b$ -axis (bottom). Channels on the right and left are represented with only one of the two guest molecule orientations. Hydrogens bonds are represented by dotted lines. [Color figure can be viewed in the online issue, which is available at [www.interscience.wiley.com](http://www.interscience.wiley.com).]

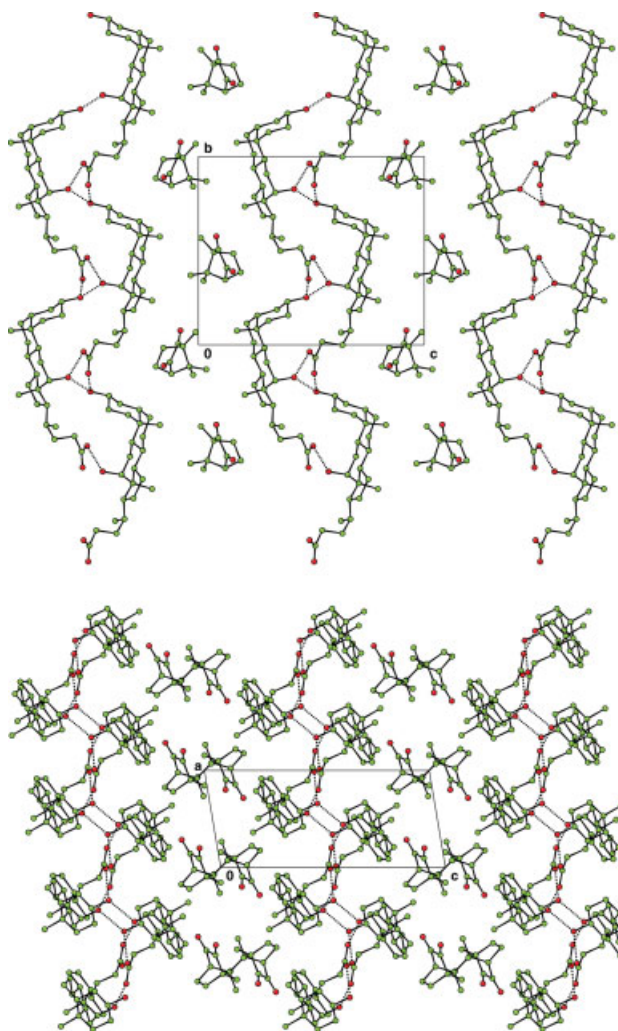


**Fig. 4.** Crystal packing at 295 K in the DCA:S-camphorquinone inclusion compound projected along the *a*-axis (top) and *b*-axis (bottom) with hydrogen bonds represented as dotted lines. [Color figure can be viewed in the online issue, which is available at [www.interscience.wiley.com](http://www.interscience.wiley.com).]

molecules then fit into these cavities. In contrast, DCA:S-camphorquinone has a unit cell which is very different from either of these two and appears to be a new type of packing arrangement, while retaining the bilayer motif. In the group of complexes typified by DCA<sub>2</sub>:*R*-ferrocene, adjacent layers are related by a twofold axis along *a* and are anti-parallel, whereas in the DCA:S-camphorquinone the layers are related by a simple translation along *c* and are parallel (see Fig. 4). The 16.5 Å separation between the bilayers in this complex (i.e., the *c*-axis dimension), is substantially greater than the range of values, found in the DCA<sub>2</sub>:*R*-ferrocene and other 2:1 complexes (typically 12.5–13.5 Å). This greater separation allows the accommodation of twice the number of guest molecules between the layers. The relative positions of the bilayers along the *a*-axis is intermediate between that found for 2:1 complexes with a 7 Å *a*-axis and space group *P*2<sub>2</sub>1<sub>2</sub>1, and those with a similar *a*-axis dimension and space group *P*<sub>2</sub>1<sub>2</sub>1<sub>2</sub>1.

The separation between the bilayers is increased to accommodate the extra guest molecules present. The guest molecules are well ordered and there is no evidence for any order/disorder phase change. The DCA:S-*endo*-3-bromocamphor complex (see Fig. 5) adopts a similar packing arrangement to DCA:S-camphorquinone. However the orientations of the *S*-*endo*-3-bromocamphor and *S*-camphorquinone molecules in the channels of their respective complexes are different. The *S*-camphorquinone molecules have the methyl groups (C8' and C9') pointing away from the groove created by the formation of the bilayers, whereas those of the *S*-*endo*-3-bromocamphor point towards it. When the two structures are superimposed on each other the two chiral molecules are related by a rotation of ~180° around an axis parallel to the *c*-axis.

The ambient temperature <sup>13</sup>C CP/MAS NMR spectra of crystalline DCA<sub>2</sub>:*R*-camphorquinone and DCA:S-camphorquinone inclusion compounds are shown in Figures 6a and 6b. Assignments of the DCA carbon peaks were made

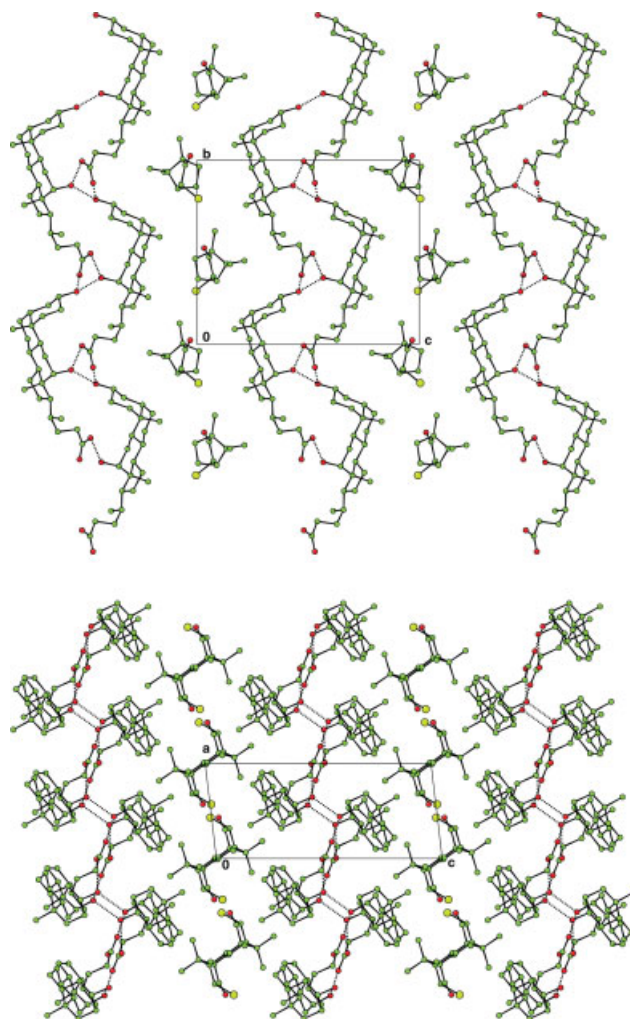


**Fig. 5.** Crystal packing at 295 K in the DCA:S-3-bromocamphor projected along the *a*-axis (top) and *b*-axis (bottom) with hydrogen bonds represented as dotted lines. [Color figure can be viewed in the online issue, which is available at [www.interscience.wiley.com](http://www.interscience.wiley.com).]



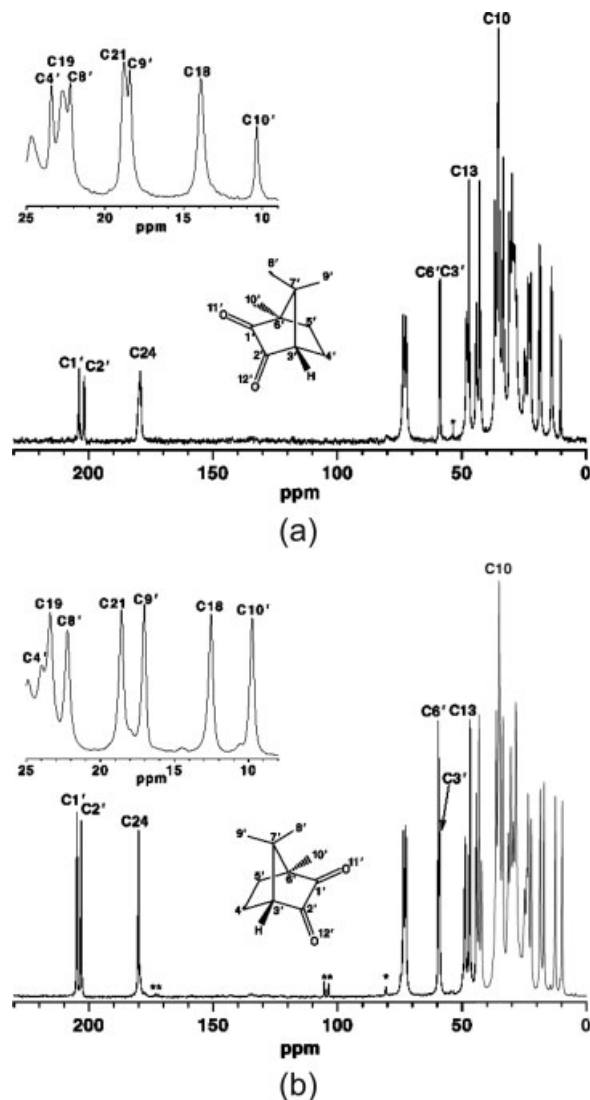


Fig. 6. RT  $^{13}\text{C}$  CP/MAS NMR spectra of (a)  $\text{DCA}_2$ :*R*-camphorquinone and (b)  $\text{DCA}$ :*S*-camphorquinone inclusion compounds showing partial assignments of the resonances. Asterisks denote spinning sidebands.

by comparison with the  $\text{DCA}_2$ :ferrocene complex<sup>15</sup> and those of the camphorquinone molecules were assigned by comparison with the solution  $^{13}\text{C}$  NMR spectra previously reported.<sup>26,27</sup> The assignment is consistent with the ambient temperature SXRD studies.

For the  $\text{DCA}_2$ :*R*-camphorquinone the peaks due to all the carbon nuclei of the camphorquinone survive in the dipolar dephased spectrum (NQS) and were assigned as in Figure 7. This implies that the whole camphorquinone molecule is undergoing relatively rapid ( $k > 10^6 \text{ s}^{-1}$ ) reorientation, in addition to any independent methyl group dynamics.<sup>23</sup> As the chemical shifts of the resonances  $\text{C4'}$ ,  $\text{C19}$ ,  $\text{C8'}$ , and  $\text{C21}$ ,  $\text{C9'}$  are very close, there is some ambiguity over the assignments for these peaks. However, the line-widths of the peaks show that three of the dipolar dephased peaks (in the region 8–24 ppm), have significantly greater line-widths ( $\Delta\nu_{1/2} \approx 12 \text{ Hz}$ ) than the other

four ( $\Delta\nu_{1/2} \approx 7 \text{ Hz}$ ) suggesting that the narrower peaks<sup>23</sup> are those of the camphorquinone molecule (i.e., in the fast motional regime), whereas the broader peaks are those of the  $\text{DCA}$  methyl carbons. Assignment of the peaks at 13.8 ppm ( $\text{C18}$ ), 18.8 ppm ( $\text{C21}$ ) and 22.8 ppm ( $\text{C19}$ ) to the  $\text{DCA}$  methyl carbons is therefore reasonably secure.

A variable temperature  $^{13}\text{C}$  CP/MAS NMR experiment was performed only on  $\text{DCA}_2$ :*R*-camphorquinone. The methyl regions of a selection of  $^{13}\text{C}$  CP/MAS NMR spectra of  $\text{DCA}_2$ :*R*-camphorquinone acquired between 293 and 133 K are shown in Figure 8. In the temperature range studied, the  $\text{DCA}$  (and camphorquinone) peaks are observed to broaden very slowly as the temperature was decreased, but they do not split.

## CONCLUSIONS

### Chiral Selection and Discrimination

On recrystallization of  $\text{DCA}$  with racemic camphorquinone, the *S*-camphorquinone molecules are selected from the mixture to form the 1:1  $\text{DCA}$ :*S*-camphorquinone complex. SXRD studies show that *RS*-camphorquinone also crystallizes from the same solution. In the experiments performed there was no evidence to suggest that either the  $\text{DCA}_2$ :*RS*-camphorquinone or the  $\text{DCA}$ :*RS*-camphorquinone adducts could be obtained for any guest enantiomeric composition. Attempts to obtain an *RS* adduct always produced crystals of  $\text{DCA}$ :*S*-camphorquinone. This also suggests that the  $\text{DCA}$ :*S*-camphorquinone complex is much more stable (much less soluble) at ambient temperature than  $\text{DCA}_2$ :*R*-camphorquinone. This is an example of what we define as “chemical discrimination,” where separation of the enantiomers is readily achieved. However it appears that such complete enantiomeric selection by inclusion in bile acid clathrates is exceedingly rare.<sup>28,29</sup>  $\text{DCA}$ :*S*-endo-3-bromocamphor is a similar case, except that so far it has not been possible to isolate any *R*-endo-3-bromocamphor complex. These examples contrast with  $\text{DCA}$  inclusion compounds of camphor that form complexes of

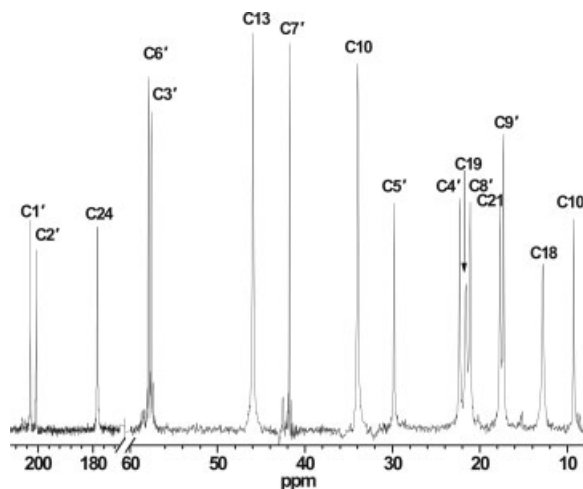


Fig. 7. Dipolar dephased NMR (dephasing period of 60  $\mu\text{s}$ ) spectrum of  $\text{DCA}_2$ :*R*-camphorquinone at 295 K showing assignments of all the resonances of the *R*-camphorquinone molecule.



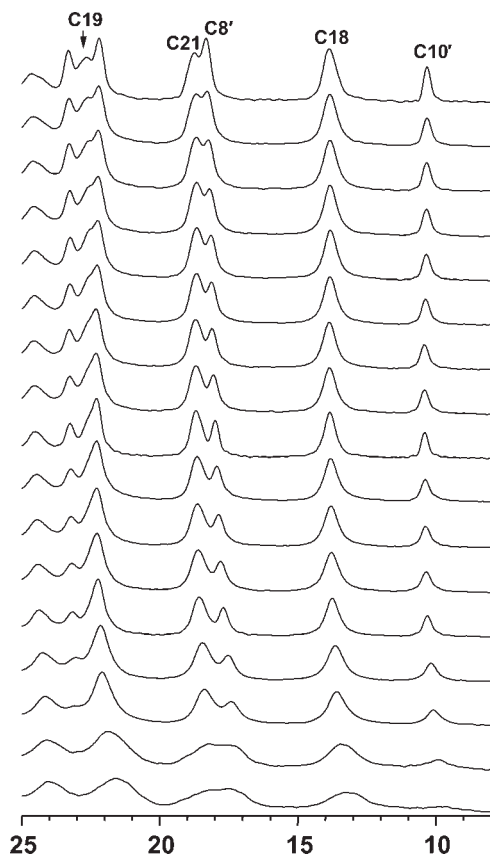


Fig. 8. VT  $^{13}\text{C}$  CP/MAS NMR spectra of the  $\text{DCA}_2$ :*R*-camphorquinone inclusion compound on cooling from 293 to 133 K in the selected region 8–25 ppm.

the same stoichiometry independent of the enantiomeric guest composition.<sup>13,14</sup>

#### Motion and Order/Disorder Phase Changes

For the ferrocene complex, the  $^{13}\text{C}$  CP/MAS NMR spectra show clear “splitting” of the DCA methyl carbon resonances C18, C19, and C21 on cooling through the phase change from the high to the low temperature form. For  $\text{DCA}_2$ :*R*-camphorquinone, the variable temperature  $^{13}\text{C}$  CP/MAS NMR does not show this splitting. The presence in the ambient temperature  $^{13}\text{C}$  dipolar dephased spectra of all the carbon resonances of *R*-camphorquinone and their intensities relative to those of the host, show qualitatively that the guest molecules in  $\text{DCA}_2$ :*R*-camphorquinone are highly mobile compared with the ferrocene guest in  $\text{DCA}_2$ :ferrocene. However, the onset temperature, at which the transition occurs, is lower in the  $\text{DCA}_2$ :*R*-camphorquinone complex than in the isomorphous high temperature phase of  $\text{DCA}_2$ :*R*-ferrocene. This also suggests that the *R*-camphorquinone molecules have enhanced dynamic behavior at any given temperature. The broadening of the  $^{13}\text{C}$  CP/MAS NMR resonances on cooling without the splitting of the C18 C19 and C21 resonances of the DCA, may reflect a slowing down of the camphorquinone

molecular re-orientational motion to a rate comparable with the decoupling frequency. This is consistent with the proposal that cooling through the region of the SXRD observed phase transition represents a repositioning of the DCA molecules. If this repositioning were to take place without an ordering of the guest molecules, it would explain the failure to find an ordered guest structure by SXRD. This is further supported by the failure to model the ambient temperature guest structure as a twofold disorder. The electron density where the guest should reside in  $\text{DCA}_2$ :*R*-camphorquinone complex was too diffuse to fit a simple twofold disorder and strongly suggestive of more extensive dynamic disorder which NMR supports.

#### LITERATURE CITED

- Jacques J, Collet A, Willen SH. Enantiomers, racemates, and resolutions. New York: Wiley; 1981 and references therein.
- Craig DP. Chiral discrimination. In: Mason SF, editor. Optical activity and chiral discrimination. Dordrecht: D. Reidel; 1979. p 293–318.
- Findlay A, Hickmans EM. Freezing point curves of the menthyl mandelates, *J Chem Soc* 1907;91:905–911.
- Brunner H. Diastereomers do, what they should not do. In: Palyi G, Zucchi C, Caglioti L, editors. Progress in biological chirality. Oxford: Elsevier; 2004. p 39–47.
- Powell HM. New procedures for resolution of racemic substances. *Nature* 1952;170:155.
- Edge SJ, Ollis WD, Stephanatou JS, Stoddart JF. Synthesis and conformational behaviour of tri-3-methyltrianthranilides. A new example of spontaneous resolution and inclusion compound formation on crystallization. *Tetrahedron Lett* 1981;22:2229.
- Facey GA, Ripmeester JA. Probing molecular motion and chemical reactions inside the chiral tri-*o*-thymotide clathrate cavity by solid state NMR techniques. *J Chem Soc Chem Commun* 1990;22:1585–1587.
- Ripmeester JA, Burlinson NE. Chiral discrimination and solid-state carbon-13 NMR. Application to tri-*o*-thymotide clathrates. *J Am Chem Soc* 1985;107:3713–3714.
- Bortolini O, Fantin G, Fogagnolo M. Bile acid derivatives as enantio-differentiating host molecules in inclusion processes. *Chirality* 2005; 17:121–130.
- Coiro VM, Giglio E, Mazza F, Pavel NV. Crystal structure of the 2:1 inclusion compound between deoxycholic acid and quadricyclane. *J Includ Phenom* 1984;1:329–337.
- Giglio E. Inclusion compounds of deoxycholic acid. In: Atwood JL, Davies JED, MacNicol DD, editors. Inclusion compounds, Vol 2. London: Academic Press; 1984. p 207–229.
- Miyata M, Sada K. Deoxycholic acid and related hosts. In: MacNicol DD, Toda F, Bishop R, editors. Comprehensive supramolecular chemistry, Vol 6. New York: Pergamon; 1996. p 147–176.
- Jones JG, Schwarzbaum S, Lessinger L, Low BW. The structure of the 2:1 complex between the bile acid deoxycholic acid and (+)-camphor. *Acta Crystallogr B* 1982;38:1207–1215.
- Candellero De Santis S, Coiro VM, Mazza F, Pochetti G. The inclusion compound of deoxycholic acid with (–)-camphor: a structural and energetic study. *Acta Crystallogr B* 1995;51:81–89.
- Muller M, Edwards AJ, Prout K, Simpson WM, Heyes SJ. (Deoxycholic acid)<sub>2</sub>:Ferrocene: a phase transition determined by the dynamic behavior of the included guest molecules. *Chem Mater* 2000;12:1314–1322.
- Allen FH, Rogers DJ. X-ray studies of terpenoids. III. A redetermination of the crystal structure of (+)-3-bromocamphor: the absolute configuration of (+)-camphor. *J Chem Soc B* 1971;632–636.
- Allen FH. The Cambridge structural database: a quarter of a million crystal structures and rising. *Acta Crystallogr B* 2002;58:380–388.

18. Bright WM, Cannon JF, Langa DA, Silverton JV. 1,7,7-Trimethylbicyclo[2.2.1]hepta-2,3-dione, C<sub>10</sub>H<sub>14</sub>O<sub>2</sub>. *Cryst Struct Commun* 1980;9: 251–256.
19. Riddell FG, Spark RA, Gunther GV. Measurement of temperature in <sup>13</sup>C CP/MAS NMR. *Magn Reson Chem* 1996;34:824–828.
20. Dybowski C, Neue G. Solid state <sup>207</sup>Pb NMR spectroscopy. *Prog Nucl Magn Reson Spec* 2002;41:153–170.
21. Peersen OB, Wu X, Kustanovich I, Smith SO. Variable-amplitude cross-polarization MAS NMR. *J Magn Reson A* 1993;104:334–339.
22. Earl WL, VanderHart DL. Measurement of <sup>13</sup>C chemical shifts in solids. *J Magn Reson* 1982;48:35–54.
23. Opella SJ, Frey MH. Selection of nonprotonated carbon resonances in solid-state nuclear magnetic resonance. *J Am Chem Soc* 1979;101: 5854–5856.
24. Limmatvapirat S, Yamaguchi K, Yonemochi E, Oguchi T, Yamamoto K. A 1:1 deoxycholic acid-salicylic acid complex. *Acta Cryst C* 1997; 53:803–805.
25. Craven BM, DeTitta GT. Crystal structure determination of the 1:1 complex of deoxycholic acid and acetic acid. *Chem Commun* 1972;530–531.
26. Brown FC, Morris DG, Murray AM. Influence of substituents on carbonyl carbon chemical shifts in 4-substituted bornane-2,3-diones and the preparation of bornane-2,3-dione. *Tetrahedron* 1978;34:1845–1847.
27. Rodina LL, Kurucz J, Korobitsyna IK. Synthesis and structure of E, Z-isomeric 5-membered cyclic α-keto-N-methyl nitrons. *Zhurnal Organicheskoi Khimii* 1981;17:1916–1929.
28. Muller S, Afras MC, de Gelder R, Ariaans GJA, Kaptein B, Broxterman QB, Bruggink A. Design and evaluation of inclusion resolutions, based on readily available host compounds. *Eur J Org Chem* 2005; 1082–1096.
29. Yoswathananont N, Miyata M, Nakano K, Sada K. Separation of isomers and enantiomers by bile acid derivatives. In: Toda F, Bishop R. editors. *Perspectives in supramolecular chemistry*, Vol. 8. Chichester: Wiley; 2004. p 87–122.